Supplementary Materials for

Multiplexed and portable nucleic acid detection platform with Cas13, Cas12a, and Csm6

Jonathan S. Gootenberg[1,2,3,4,7]*, Omar O. Abudayyeh[1,2,3,4,5]*, Max J. Kellner[1], Julia Joung[1,2,3,4], James J. Collins[1,4,5,6,8], and Feng Zhang[1,2,3,4†]

* These authors contributed equally to this work.

correspondence to: F. Z. (zhang@broadinstitute.org).

This PDF file includes:

Materials and Methods

Protein expression and purification of Cas13 and Csm6 orthologs

LwaCas13a expression and purification was carried out as described before(*3*) with minor modifications and is detailed below. LbuCas13a, LbaCas13a, Cas13b and Csm6 orthologs were expressed and purified with a modified protocol. In brief, bacterial expression vectors were transformed into Rosetta™ 2(DE3)pLysS Singles Competent Cells (Millipore). A 12.5 mL starter culture was grown overnight in Terrific Broth 4 growth media (Sigma) (TB), which was used to inoculate 4 L of TB for growth at 37°C and 300 RPM until an OD600 of 0.5. At this time, protein expression was induced by supplementation with IPTG (Sigma) to a final concentration of 500 μM, and cells were cooled to 18°C for 16 h for protein expression. Cells were then centrifuged at 5000 g for 15 min at 4°C. Cell pellet was harvested and stored at -80°C for later purification.

All subsequent steps of the protein purification were performed at 4°C. Cell pellet was crushed and resuspended in lysis buffer (20 mM Tris-HCl, 500 mM NaCl, 1 mM DTT, pH 8.0) supplemented with protease inhibitors (Complete Ultra EDTA-free tablets), lysozyme (500μg/1ml), and benzonase followed by high-pressure cell disruption using the LM20 Microfluidizer system at 27,000 PSI. Lysate was cleared by centrifugation for 1 hr at 4°C at 10,000 g. The supernatant was applied to 5mL of StrepTactin Sepharose (GE) and incubated with rotation for 1 hr followed by washing of the protein-bound StrepTactin resin three times in lysis buffer. The resin was resuspended in SUMO digest buffer (30 mM Tris-HCl, 500 mM NaCl 1 mM DTT, 0.15% Igepal (NP-40), pH 8.0) along with 250 Units of SUMO protease (250mg/ml) and incubated overnight at 4°C with rotation. The suspension was applied to a column for elution and separation from resin by gravity flow. The resin was washed two times with 1 column volume of Lysis buffer to maximize protein elution. The elute was diluted in cation exchange buffer (20 mM HEPES, 1 mM DTT, 5% glycerol, pH 7.0; pH 7.5 for LbuCas13a, LbaCas13a, EiCsm6, LsCsm6, TtCsm6) to lower the salt concentration in preparation for cation exchange chromatography to 250mM.

For cation exchange and gel filtration purification, protein was loaded onto a 5 mL HiTrap SP HP cation exchange column (GE Healthcare Life Sciences) via FPLC (AKTA PURE,

GE Healthcare Life Sciences) and eluted over a salt gradient from 250 mM to 2M NaCl in elution buffer (20 mM HEPES, 1 mM DTT, 5% glycerol, pH 7.0; pH 7.5 for LbuCas13a, LbaCas13a). The resulting fractions were tested for presence of recombinant protein by SDS-PAGE, and fractions containing the protein were pooled and concentrated via a Centrifugal Filter Unit (Millipore 50MWCO) to 1 mL in S200 buffer (10 mM HEPES, 1 M NaCl, 5 mM MgCl2, 2 mM DTT, pH 7.0). The concentrated protein was loaded onto a gel filtration column (Superdex® 200 Increase 10/300 GL, GE Healthcare Life Sciences) via FPLC. The resulting fractions from gel filtration were analyzed by SDS-PAGE and fractions containing protein were pooled and buffer exchanged into Storage Buffer (600 mM NaCl, 50 mM Tris-HCl pH 7.5, 5% glycerol, 2mM DTT) and frozen at -80°C for storage.

Accession numbers and plasmid maps for all proteins purified in this study are available in Table S1.

Nucleic acid target and crRNA preparation

Nucleic acid targets for Cas12a and genomic DNA detection were PCR amplified with NEBNext PCR master mix, gel extracted, and purified using MinElute gel extraction kit (Qiagen). For RNA based detection, purified dsDNA was incubated with T7 polymerase overnight at 30°C using the HiScribe T7 Quick High Yield RNA Synthesis kit (New England Biolabs) and RNA was purified with the MEGAclear Transcription Clean-up kit (Thermo Fisher)

crRNA preparation was carried out as described before(*3*) with minor modifications and is detailed below. For preparation of crRNAs, constructs were ordered as ultramer DNA (Integrated DNA Technologies) with an appended T7 promoter sequence. crRNA DNA was annealed to a short T7 primer (final concentrations 10 uM) and incubated with T7 polymerase overnight at 37°C using the HiScribe T7 Quick High Yield RNA Synthesis kit (New England Biolabs). crRNAs were purified using RNAXP clean beads (Beckman

Coulter) at 2x ratio of beads to reaction volume, with an additional 1.8x supplementation of isopropanol (Sigma).

All crRNA sequences used in this study are available in Table S2. All DNA and RNA target sequences used in this study are available in Table S3.

e

Primers for RPA were designed using NCBI Primer-BLAST(*27*) using default parameters, with the exception of amplicon size (between 100 and 140 nt), primer melting temperatures (between 54°C and 67°C), and primer size (between 30 and 35 nt). Primers were then ordered as DNA (Integrated DNA Technologies).

RPA and RT-RPA reactions run were as instructed with TwistAmp® Basic or TwistAmp® Basic RT (TwistDx), respectively, with the exception that 280 mM MgAc was added prior to the input template. Reactions were run with 1 µL of input for 1 hr at 37°C, unless otherwise described.

For SHERLOCK quantification of nucleic acid, RPA primer concentration tested at standard concentration (480nM final) and lower (240nM, 120nM,60nM, 24nM) to find the optimum concentration. RPA reactions were further run for 20 minutes.

When multiple targets were amplified with RPA, primer concentration was adjusted to a final concentration of 480nM. That is, 120nM of each primer for two primer pairs were added for duplex detection.

All RPA primers used in this study are available in Table S4.

Fluorescent cleavage assay

Detection assays were carried out as described before(*3*) with minor modifications and the procedure is detailed below. Detection assays were performed with 45 nM purified Cas13, 22.5 nM crRNA, quenched fluorescent RNA reporter (125nM RNAse Alert v2, Thermo

Scientific, homopolymer and di-nucleotide reporters (IDT); 250nM for polyA Trilink reporter), 0.5 μL murine RNase inhibitor (New England Biolabs), 25 ng of background total human RNA (purified from HEK293FT culture), and varying amounts of input nucleic acid target, unless otherwise indicated, in nuclease assay buffer (20 mM HEPES, 60 mM NaCl, 6 mM $MgCl_2$, pH 6.8). For Csm6 fluorescent cleavage reactions, protein was used at 10nM final concentration along with 500nM of 2', 3' cyclic phosphate oligoadenylate, 250nM of fluorescent reporter, and 0.5 μL murine RNase inhibitor in nuclease assay buffer (20 mM HEPES, 60 mM NaCl, 6 mM $MgCl_2$, pH 6.8). Reactions were allowed to proceed for 1-3 hr at 37°C (unless otherwise indicated) on a fluorescent plate reader (BioTek) with fluorescent kinetics measured every 5 min. In reactions involving AsCas12a, 45nM AsCas12a was included using recombinant protein from IDT. In the case of multiplexed reactions, 45nM of each protein and 22.5nM of each crRNA was used in the reaction.

All cleavage reporters used in this study are available in Table S5.

SHERLOCK nucleic acid detection

Detection assays were performed with 45 nM purified Cas13, 22.5 nM crRNA, quenched fluorescent RNA reporter (125nM RNAse Alert v2, Thermo Scientific, homopolymer and di-nucleotide reporters (IDT), 250nM for polyA Trilink reporter), 0.5 μL murine RNase inhibitor (New England Biolabs), 25 ng of background total human RNA (purified from HEK293FT culture), and 1uL of RPA reaction in nuclease assay buffer (20 mM HEPES, 60 mM NaCl, 6 mM $MgCl_2$, pH 6.8), rNTP mix (1mM final, NEB), 0.6 μL T7 polymerase (Lucigen) and 3mM $MgCl_2$. Reactions were allowed to proceed for 1-3 hr at 37°C (unless otherwise indicated) on a fluorescent plate reader (BioTek) with fluorescent kinetics measured every 5 min.

For one-pot nucleic acid detection, the detection assay was carried out as described before (*3*) with minor modifications. A single 100 μL combined reaction assay consisted of 0.48 μM forward primer, 0.48 μM reverse primer, 1x RPA rehydration buffer, varying amounts

of DNA input, 45 nM LwCas13a recombinant protein, 22.5 nM crRNA, 125 ng background total human RNA, 125 nM substrate reporter (RNase alert v2), 2.5 µL murine RNase inhibitor (New England Biolabs), 2 mM ATP, 2 mM GTP, 2 mM UTP, 2 mM CTP, 1 µL T7 polymerase mix (Lucigen), 5 mM MgCl2, and 14 mM MgAc. Reactions were allowed to proceed for 1-3 hr at 37°C (unless otherwise indicated) on a fluorescent plate reader (BioTek) with fluorescent kinetics measured every 5 min. For lateral flow readout, 20 uL of the combined reaction was added to 100uL of HybriDetect 1 assay buffer (Milenia) and run on HybriDetect 1 lateral flow strips (Milenia).

Nucleic acid labeling for cleavage fragment analysis

Target RNA was *in vitro* transcribed from a dsDNA template and purified as described above. The *in vitro* cleavage reaction was performed as described above for fluorescence cleavage reaction with the following modifications. Fluorescence reporter was substituted for 1µg RNA target and no background RNA was used. Cleavage reaction was carried out for 5 minutes (LwaCas13a) or 1 hour (PsmCas13b) at 37°C. The cleavage reaction was purified using the RNA clean & concentrator-5 kit (Zymo Research) and eluted in 10 uL UltraPure water (Gibco). Cleavage reaction was further labeled with a 10µg of maleimide IRDye 800CW (Licor) following the 5'EndTag labeling Reaction (Vector Laboratories) kit protocol. To determine the 5' end produced by Cas13 cleavage, the protocol was modified to either perform an Alkaline Phosphatase (AP) treatment or substitute with UltraPure water to only label 5'-OH containing RNA species, while undigested triphosphorylated (PPP) RNA species are only labeled when AP treatment is performed.

Mass Spectrometry for high resolution cleavage fragment analysis

For determining the cleavage ends produced by Cas13 collateral RNase activity by Mass Spectrometry, an *in vitro* cleavage reaction was performed as described above with the following modifications. Cas13 RNA target was used at 1 nM final concentration, Csm6 activator at 3µM final concentration and no background RNA was used. For control

reactions, either Cas13 target was substituted by UltraPure water, or standard *in vitro* cleavage reaction was incubated with hexaadenylate containing a 2',3'cyclic phosphate activator in the absence of Cas13 target, Cas13 protein and Cas13 crRNA. The cleavage reactions were carried out for 1h at 37°C and purified using an New England Biolabs siRNA purification protocol. In brief, one-tenth volume of 3 M NaOAc, 2 µL of RNase-free Glycoblue (Thermofisher) and three volumes of cold 95% ethanol was added, placed at -20°C for 2 hours, and centrifuged for 15 minutes at 14,000g. The supernatant was removed and two volumes of 80% EtOH was added and incubated for 10 minutes at room temperature. The supernatant was decanted and samples centrifuged for 5 minutes at 14,000g. After air-drying the pellet, 50 µL of UltraGrade water added and sent on dry ice for Mass spectrometry analysis.

For mass spectrometry analysis, samples were diluted 1:1 with UltraGrade water and analyzed on Bruker Impact II q-TOF mass spectrometer in negative ion mode coupled to an Agilent 1290 HPLC. 10 µL were injected onto a PLRP-S column (50 mm, 5 um particle size, 1000 angstrom pore size PLRP-S column, 2.1 mm ID) using 0.1% ammonium hydroxide v/v in water as mobile phase A and acetonitrile as mobile phase B. The flow rate was kept constant throughout at 0.3 ml/minute. The mobile phase composition started at 0%B and was maintained for the first 2 minutes. After this point, the composition was changed to 100% B over the next 8 minutes and maintained for one minute. The composition was then returned to 0% B over 0.1 minute and then maintained for the following 4.9 minutes to allow the column to re-equilibrate to starting conditions. The mass spectrometer was tuned for large MW ions, and data was acquired between m/z 400-5000. The entire dataset from the mass spectrometer was calibrated by m/z using an injection of sodium formate. Data was analyzed using Bruker Compass Data Analysis 4.3 with a license for MaxEnt deconvolution algorithm to generate a calculated neutral mass spectrum from the negatively charged ion data.

Genomic DNA extraction from human saliva

Saliva DNA extraction was carried out as described before(*3*) with minor modifications and is detailed below. 2 mL of saliva was collected from volunteers, who were restricted from consuming food or drink 30 min prior to collection. Samples were then processed using QIAamp® DNA Blood Mini Kit (Qiagen) as recommended by the kit protocol. For boiled saliva samples, 400 µL of phosphate buffered saline (Sigma) was added to 100 µL of volunteer saliva and centrifuged for 5 min at 1800 g. The supernatant was decanted and the pellet was resuspended in phosphate buffered saline with 0.2% Triton X-100 (Sigma) before incubation at 95°C for 5 min. 1 µL of sample was used as direct input into RPA reactions.

Digital droplet PCR quantification

ddPCR quantification was carried out as described before(*3*) with minor modifications and is detailed below. To confirm the concentration of target dilutions, we performed digital-droplet PCR (ddPCR). For DNA quantification, droplets were made using the ddPCR Supermix for Probes (no dUTP) (BioRad) with PrimeTime qPCR probes/primer assays (IDT) designed for the target sequence. For RNA quantification, droplets were made using the one-step RT-ddPCR kit for probes with PrimeTime qPCR probes/primer assays designed for the target sequence. Droplets were generated in either case using the QX200 droplet generator (BioRad) and transferred to a PCR plate. Droplet-based amplification was performed on a thermocycler as described in the kit protocol and nucleic acid concentrations were subsequently determined via measurement on a QX200 droplet reader.

Cas13-Csm6 fluorescent cleavage assay

Cas13-Csm6 combined fluorescent cleavage assays were performed as described for standard Cas13 fluorescent cleavage reactions with the following modifications. Csm6 protein was added to 10 nM final concentration, 400 nM of Csm6 fluorescent reporter and 500 nM Csm6 activator unless otherwise indicated. For distinguishing Cas13 from Csm6 collateral RNase activity, two distinct fluorophores were used for fluorescence detection (FAM and HEX). Because of the interference of rNTPs with Csm6 activity, the IVT was

performed in the RPA pre-amplification step and then 1μL of this reaction was added as input to the Cas13-Csm6 cleavage assay.

In the case where we tested a three-step Cas13-Csm6 cleavage assay, the RPA was performed normally as discussed above for varying times and then used as input to a normal IVT reaction for varying times. Then 1μL of the IVT was used as input to the Cas13-Csm6 reaction described in the previous paragraph.

All Csm6 activators used in this study are available in Table S6.

Motif discovery screen with library

To screen for Cas13 cleavage preference, an *in vitro* RNA cleavage reaction was set up as described above with the following modifications. Cas13 target was used at 20nM, fluorescent reporter was substituted for 1 μM of DNA-RNA oligonucleotide (IDT) that contains a 6-mer stretch of randomized ribonucleotides flanked by DNA handles for NGS library preparation. Reactions were carried out for 60 minutes (unless otherwise indicated) at 37°C. The reactions were purified using the Zymo oligo-clean and concentrator-5 kit (Zymo research) and 15μL of UltraPure water was used for elution. 10μL of purified reaction was used for reverse transcription using a gene-specific primer that binds to the DNA handle.

Reverse transcription (RT) was carried out for 45 minutes at 42°C according to the qScript Flex cDNA-kit (quantabio) protocol. To assess cleavage efficiency and product purity, RT-reactions were diluted 1:10 in water and loaded on a Small RNA kit and run on a Bioanalyzer 2100 (Agilent). Four microliters of RT-reaction was used for the first-round of NGS library preparation. NEBNext (NEB) was used to amplify first strand cDNA with a mix of forward primers at 625 nM final and a reverse primer at 625 nM for 15 cycles with 3 minute initial denaturation at 98°C, 10s cycle denaturation at 98°C, 10s annealing at 63°C, 20s 72°C extension and 2 minute final extension extension at 72°C.

Two microliters of first round PCR reaction was used for second round PCR amplification to attach Illumina-compatible indices (NEB) for NGS sequencing. The same NEBNext PCR protocol was used for amplification. PCR product were analysed by agarose gel-electrophoresis (2% Sybr Gold E-Gel Invitrogen system) and 5µL of each reaction was pooled. The pooled samples was gel extracted, quantified with Qubit DNA 2.0 DNA High sensitivity kit and normalized to 4 nM final concentration. The final library was diluted to 2 pM and sequenced on a NextSeq 500 Illumina system using a 75-cycle kit.

Motif Screen Analysis

To analyze depletion of preferred motifs from the random motif library screen, 6-mer regions were extracted from sequence data and normalized to overall read count for each sample. Normalized read counts were then used to generated log ratios, with psuedocount adjustment, between experimental conditions and matched controls. For Cas13 experiments, matched controls did not have target RNA added; for Csm6 and RNase A experiments, matched controls did not have enzyme. Log ratio distribution shape was used to determine cut-offs for enriched motifs. Enriched motifs were then used to determine occurrence of 1-, 2-, or 3- nucleotide combinations. Motif logos were generated using Weblogo3(*26*).

Phylogenetic analysis of Cas13 protein and crRNA direct repeats

To study ortholog clustering, multiple sequence alignments were generated with Cas13a and Cas13b protein sequences in Geneious with MUSCLE and then clustered using Euclidean distance in R with the heatmap.2 function. To study direct repeat clustering, multiple sequence alignments were generated with Cas13a and Cas13b direct repeat sequences in Geneious using the Geneious algorithm and then clustered using Euclidean distance in R with the heatmap.2 function. To study clustering of orthologs based on di-nucleotide motif preference, the cleavage activity matrix was clustered using Euclidean distance in R using the heatmap.2 function.

Gold nanoparticle colorimetric

An RNA oligo was synthesized from IDT with thiols at the 5' and 3' ends (Table S5 for sequence). In order to deprotect the thiol groups, the oligo at a final concentration of 20mM was reduced in 150mM sodium phosphate buffer containing 100mM DTT for 2 hours at room temperature. The oligo were then purified using sephadex NAP-5 columns (GE Healthcare) into a final volume of 700µL water. As previously described(*20*), the reduced oligo at 10µM was added at a volume of 280µL to 600µL of 2.32nM 15nm-gold nanoparticles (Ted Pella), which is a 2000:1 ratio of oligo to nanoparticles. Subsequently, 10µL of 1M Tris-HCl at pH8.3 and 90µL of 1M NaCl were added to the oligo-nanoparticle mixture and incubated for 18 hours at room temperature with rotation. After 18 hours, additional 1M Tris-HCl (5µL at pH8.3) was added with 5M NaCl (50µL) and this was incubated for an additional 15 hours at room temperature with rotation. Following incubation, the final solution was centrifuged for 25 min at 22,000g. The supernatant was discarded and the conjugated nanoparticles were resuspended in 50µL of 200mM NaCl.

The nanoparticles were tested for RNase sensitivity using an RNase A assay. Varying amounts of RNase A (Thermo Fischer) were added to 1x RNase A buffer and 6µL of conjugated nanoparticles in a total reaction volume of 20µL. Absorbance at 520nm was monitored every 5 minutes for 3 hours using a plate spectrophotometer.

Lateral flow readout of Cas13 activity using FAM-biotin reporters

For lateral flow based on cleavage of a FAM-RNA-biotin reporter, non-RPA LwaCas13a reactions or SHERLOCK-LwaCas13a reactions were run for 1 hour, unless otherwise indicated, with 1uM final concentration of FAM-RNA-biotin reporter. After incubation, 20uL LwaCas13a reactions supernatant was added to 100uL of HybriDetect 1 assay buffer (Milenia) and run on HybriDetect 1 lateral flow strips (Milenia).

Cloning of REPAIR constructs, Mammalian cell transfection, RNA isolation and NGS library preparation for REPAIR

Constructs for simulating reversion of *APC* mutations and guide constructs for REPAIR were cloned as previously described(*23*). Briefly, 96 nt sequences centered on the APC:c.1262G>A mutation were designed and golden gate cloned under an expression vector, and corresponding guide sequences were golden gate cloned into U6 expression vectors for PspCas13b guides. To simulate patient samples, 300ng of either mutant or wildtype *APC* expression vector was transfected into HEK293FT cells with Lipofectamine 2000 (Invitrogen), and two days post-transfection DNA was harvested with Qiamp DNA Blood Midi Kit (Qiagen) following manufacturer's instructions. 20ng of DNA were used as input into SHERLOCK-LwaCas13a reactions.

RNA correction using the REPAIR system was performed as previously described(*23*): 150ng of dPspCas13b-ADAR(DD)E488Q, 200 ng of guide vector, and 30ng of *APC* expression vector were co-transfected, and two-days post transfection RNA was harvested using the RNeasy Plus Mini Kit (Qiagen) following manufacturer's instructions. 30ng of RNA was used as input into SHERLOCK-LwaCas13a reactions. All plasmids used for REPAIR RNA editing in this study are available in Table S8.

RNA editing fractions were independently determined by NGS as previously described. RNA was reverse transcribed with the qScript Flex kit (Quanta Biosciences) with a sequence specific primer. First strand cDNA was amplified with NEBNext High Fidelity 2X PCR Mastermix (New England Biosciences) with a mix of forward primers at 625nM final and a reverse primer at 625nM for 15 cycles with 3 minute initial denaturation at 98°C, 10 second cycle denaturation at 98°C, 30 second annealing at 65°C, 30 second 72°C extension and 2 minute final extension extension at 72°C. Two microliters of first round PCR reaction was used for second round PCR amplification to attach Illumina-compatible indices for NGS sequencing, with NEBNext, using the same protocol with 18 cycles. PCR products were analysed by agarose gel-electrophoresis (2% Sybr Gold E-Gel Invitrogen) and 5μL of each reaction was pooled. The pooled samples was gel extracted, quantified with Qubit DNA 2.0 DNA High sensitivity kit and normalized to 4nM final concentration, and read out with a 300 cycle v2 MiSeq kit (Illumina).

Analysis of SHERLOCK fluorescence data

SHERLOCK fluorescence analysis was carried out as described before(*3*) with minor modifications and is detailed below. To calculate background subtracted fluorescence data, the initial fluorescence of samples was subtracted to allow for comparisons between different conditions. Fluorescence for background conditions (either no input or no crRNA conditions) were subtracted from samples to generate background subtracted fluorescence.

crRNA ratios for SNP discrimination were calculated to adjust for sample-to-sample overall variation as follows:

$$crRNA\ A_i\ ratio = \frac{(m+n)A_i}{\sum_{i=1}^{m} A_i + \sum_{i=1}^{n} B_i}$$

where A_i and B_i refer to the SHERLOCK intensity values for technical replicate i of the crRNAs sensing allele A or allele B, respectively, for a given individual. Since we typically have four technical replicates per crRNA, m and n are equal to 4 and the denominator is equivalent to the sum of all eight of the crRNA SHERLOCK intensity values for a given SNP locus and individual. Because there are two crRNAs, the crRNA ratio average across each of the crRNAs for an individual will always sum to two. Therefore, in the ideal case of homozygosity, the mean crRNA ratio for the positive allele crRNA will be two and the mean crRNA ratio for the negative allele crRNA will be zero. In the ideal case of heterozygosity, the mean crRNA ratio for each of the two crRNAs will be one. Because in SHERLOCKv2, we accomplish genotyping by measuring A_i and B_i in different color channels, we scaled the 530-color channel by 6 to match the intensity values in the 480-color channel.

Promiscuous cleavage of Cas13 orthologs in absence of target

Some members of the Cas13 family, such as PinCas13b and LbuCas13a, demonstrate promiscuous cleavage in the presence or absence of target, and this background activity is di-nucleotide reporter dependent (fig. S7B). This background activity was also spacer

dependent for LbuCas13a (fig. S7C-D). In some reporters, the U and A base preference clustered within protein or DR similarity. Interestingly, di-nucleotide preferences identified here did not correspond with Cas13 families clustered from either direct repeat similarity or protein similarity (fig. S8A-D).

Characterization of crRNA designs for PsmCas13b and CcaCas13b

To identify the optimal crRNA for detection with PsmCas13b and CcaCas13b, we tested crRNA spacer lengths from 34-12 nt and found that PsmCas13b had a peak sensitivity at a spacer length of 30, whereas CcaCas13b had equivalent sensitivity above spacer lengths of 28nt, justifying the use of 30nt spacers for evaluating Cas13 activity (fig. S10). To further explore the robustness of targeting of CcaCas13b and PsmCas13b compared to LwaCas13a, we designed eleven different crRNAs evenly spaced across ssRNA 1 and found that LwaCas13a collateral activity was robust to crRNA design, while CcaCas13b and PsmCas13b both showed more variability in activity across different crRNAs (fig. S11).

Random library motif screening for additional orthogonal motifs

To further explore the diversity of cleavage preferences of Cas13a and Cas13b orthologs, we developed a library-based approach for characterizing preferred motifs for collateral endonuclease activity. We used a degenerate 6-mer RNA reporter flanked by constant DNA handles, which allowed for amplification and readout of uncleaved sequences (fig. S12A). Incubating this library with Cas13 enzymes resulted in detectable cleavage patterns that depended on the addition of target RNA(fig. S12B), and sequencing of depleted motifs from these reactions revealed an increase in the skew of the library over digestion time (fig. S12C), indicative of a population of preferred motifs for cleavage. Sequence logos and pairwise base preferences from highly depleted motifs (fig. S12D) reproduced the U-preference observed for LwaCas13a and CcaCas13b and the A-preference of PsmCas13b (fig S12E and fig. S13A). We synthesized reporters from top motifs as determined from the screen to validate the findings, and found that LwaCas13a, CcaCas13a, and PsmCas13b all cleaved their most highly preferred motifs (fig. S13B,C). We also found multiple sequences that showed cleavage for only one ortholog, but not others, which could allow for an alternative orthogonal readout from di-nucleotide motifs (fig. S14). LwaCas13a

incubated with different targets produced similar cleavage motif preferences, indicating that the base preference of the collateral activity is constant regardless of target sequence (fig. S15).

Validation of activator products upon LwaCas13a cleavage

Using mass spectrometry, we verified that LwaCas13a digestion produced the expected cyclic-phosphate terminated products for Csm6 activation (Fig. S30). Activation was most effective for designs with 3' protection with poly U, as other activation designs, including 5' protection with poly-U and internal poly-U tracts, were less effective at activating Csm6 exclusively in the presence of target RNA (fig. S31A,B), likely because LwaCas13a has little activity on UA motifs (fig. S7) and 5' protection is ineffective at preventing activation of Csm6

Optimization for combining RPA and Csm6 reactions

As combining Csm6-enhancement with RPA pre-amplification would increase signal and sensitivity, we tested Csm6 for activity in the presence of *in vitro* transcription components necessary for combination with RPA. We found that both magnesium and free rNTP reduced the nuclease activity of Csm6 in the presence of a cyclic phosphate activator (fig. S33A). Reducing the amount of rNTP in solution reduced the amount of transcribed RNA, and therefore had a negative effect on Csm6 activation by Cas13a (fig. S33B-F), even in the presence of increased reporter or activator concentrations.

Figure S1

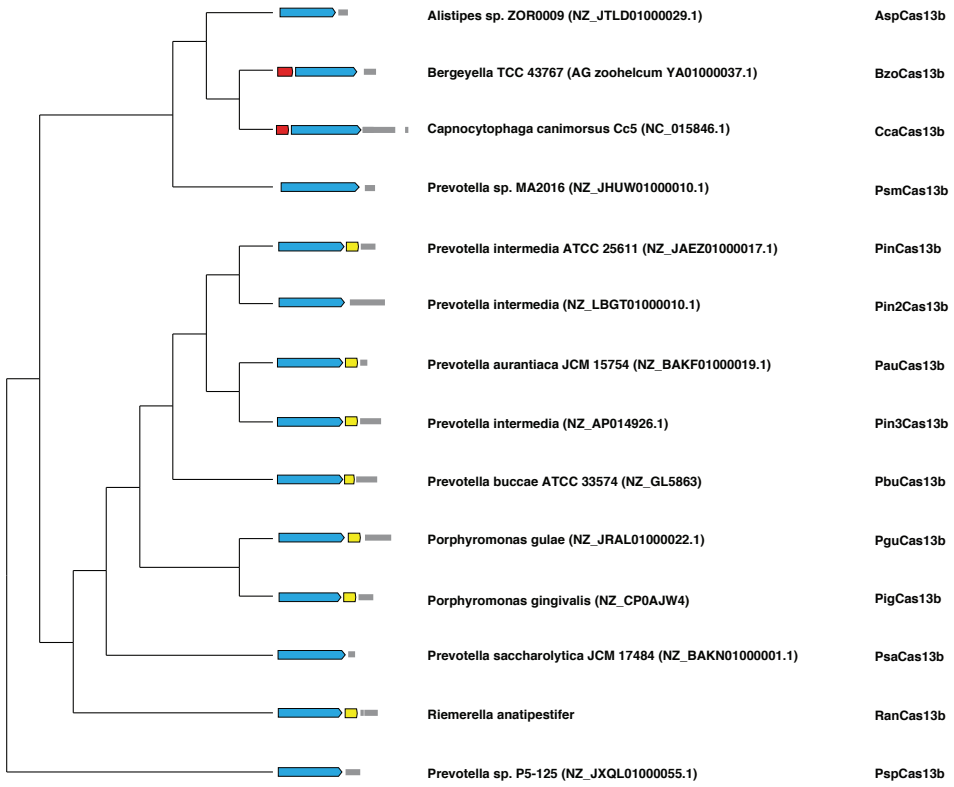

Figure S1: Cas13b orthologs evaluated for *in vitro* collateral activity.

Tree of 15 Cas13b orthologs purified and evaluated for in vitro collateral activity. Cas13b gene (blue), Csx27 gene (red), Csx28 gene (yellow), and CRISPR array (grey) are shown.

Figure S2

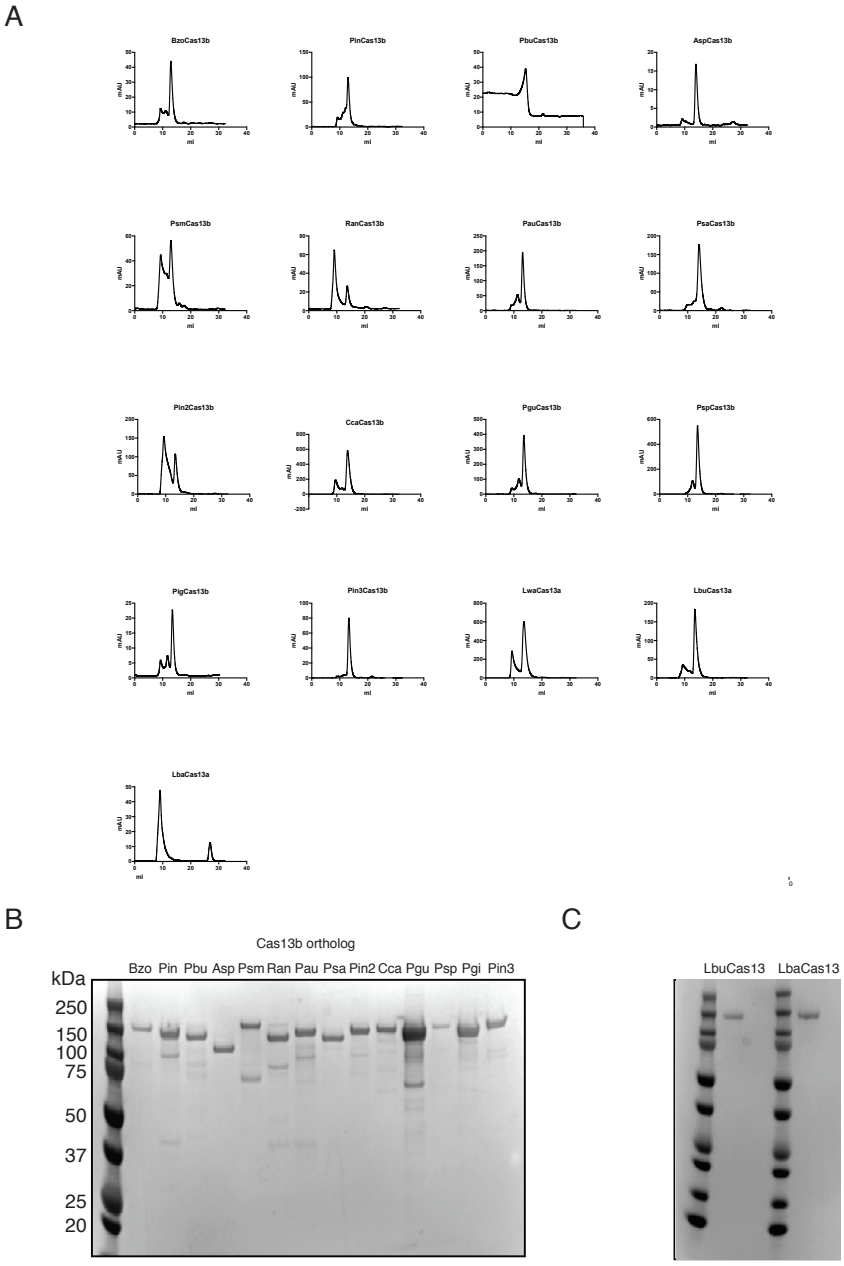

Figure S2: Protein purification of Cas13 orthologs

A) Chromatograms of size exclusion chromatography for Cas13b, LwCas13a and LbaCas13a. Measured UV absorbance (mAU) is shown against the elution volume (ml)

B) SDS-PAGE gel of purified Cas13b orthologs. Fourteen Cas13b orthologs are loaded from left to right. A protein ladder is shown to the left.

C) Final SDS-PAGE gel of LbaCas13a and LbuCas13a. Two dilutions of LbaCas13a and LbuCas13a are shown.

Figure S3

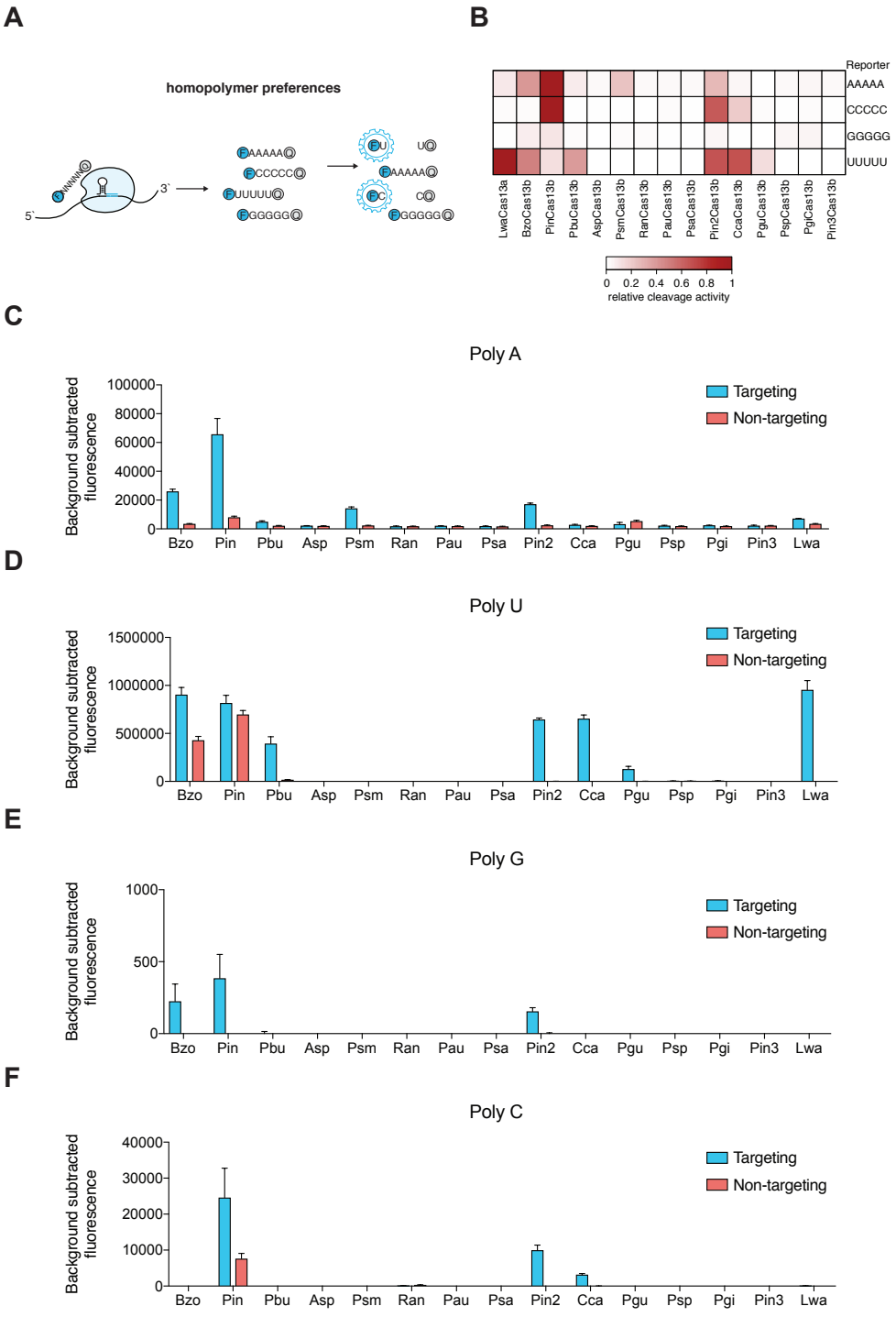

Figure S3: Base preference of Cas13b ortholog collateral cleavage.

A) Schematic of assay for determining hompolymer preferences of Cas13a/b enzymes.

B) Heatmap of the base preference of 15 Cas13b orthologs targeting ssRNA 1 with reporters consisting of a homopolymer of A, C, G, or U bases.

C) Cleavage activity of fourteen Cas13b orthologs targeting ssRNA 1 using a homopolymer adenine sensor five nucleotides long.
D) Cleavage activity of fourteen Cas13b orthologs targeting ssRNA 1 using a homopolymer uridine sensor five nucleotides long.
E) Cleavage activity of fourteen Cas13b orthologs targeting ssRNA 1 using a homopolymer guanine sensor five nucleotides long.
F) Cleavage activity of fourteen Cas13b orthologs targeting ssRNA 1 using a homopolymer cytidine sensor five nucleotides long.

Figure S4

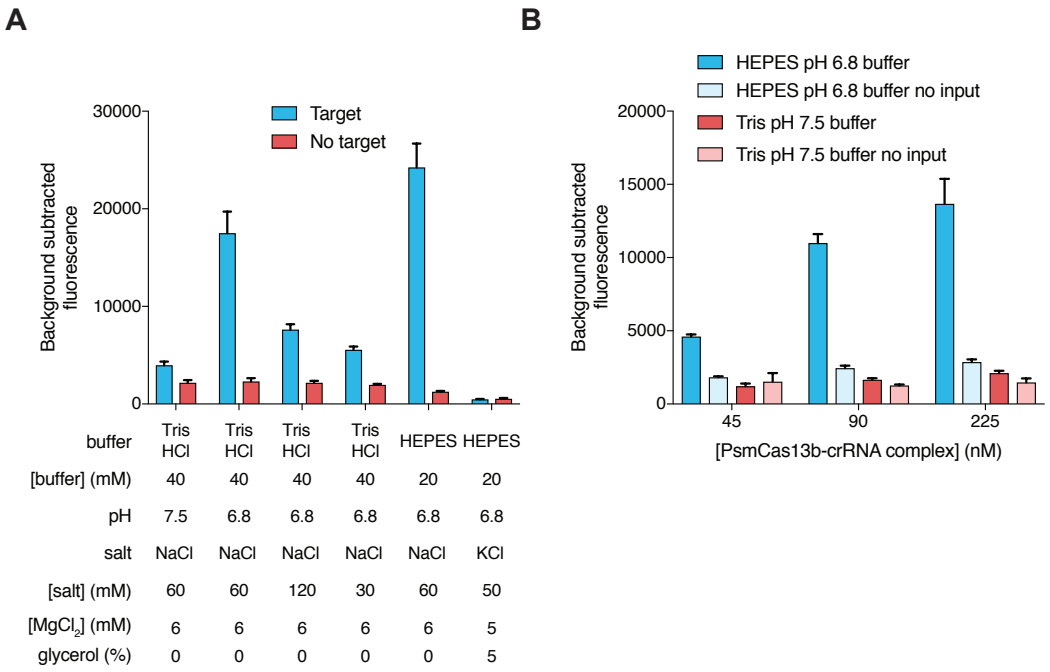

Figure S4: Buffer optimization of PsmCas13b cleavage activity.

A) A variety of buffers are tested for their effect on PsmCas13b collateral activity after targeting ssRNA 1.

B) The optimized buffer is compared to the original buffer at different PsmCas13b-crRNA complex concentrations.

Figure S5

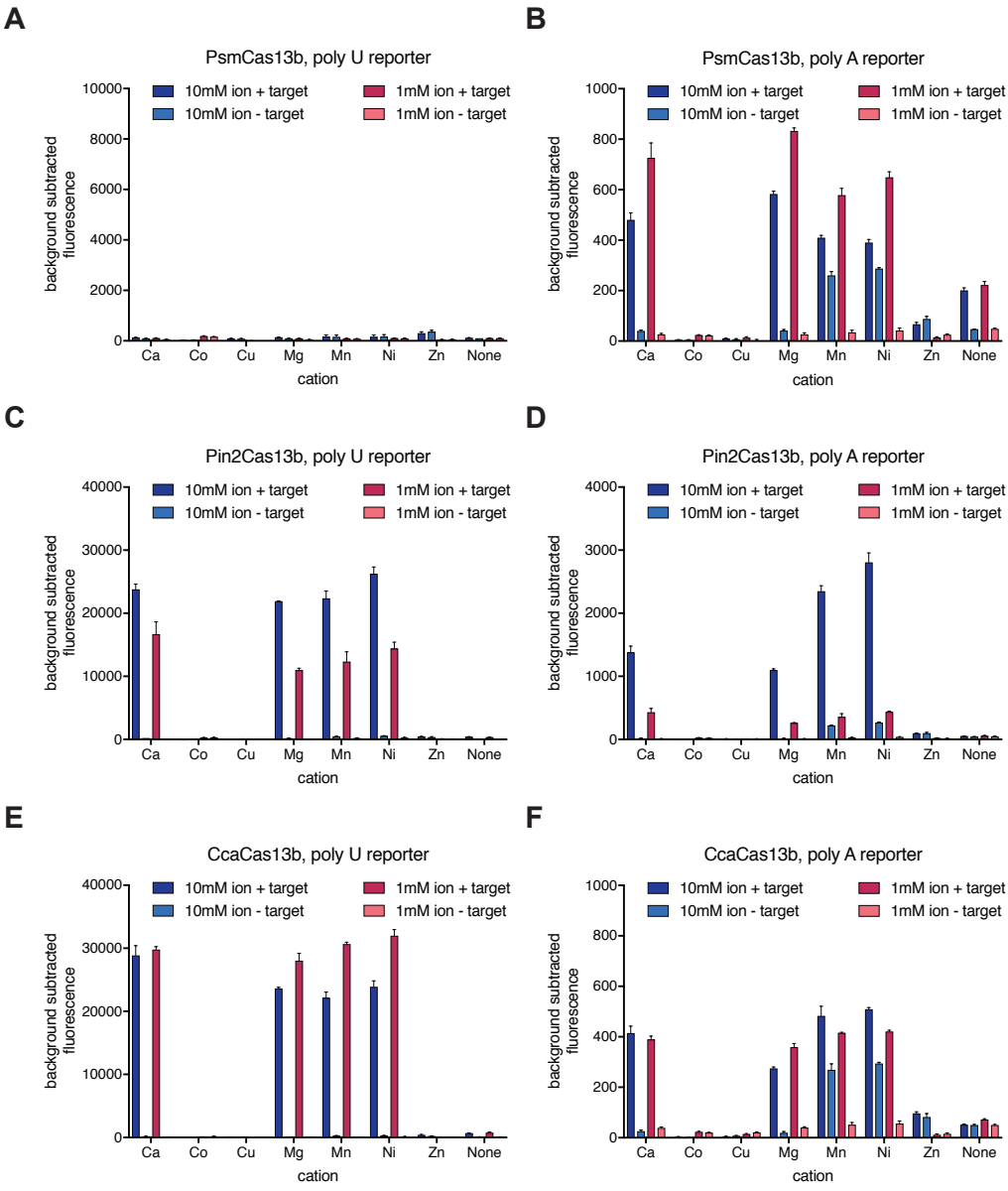

Figure S5: Ion preference of Cas13 orthologs for collateral cleavage.

A) Cleavage activity of PsmCas13b with a fluorescent poly U sensor for divalent cations Ca, Co, Cu, Mg, Mn, Ni, and Zn. PsmCas13b is incubated with a crRNA targeting a synthetic ssRNA 1.

B) Cleavage activity of PsmCas13b with a fluorescent poly A sensor for divalent cations Ca, Co, Cu, Mg, Mn, Ni, and Zn. PsmCas13b is incubated with a crRNA targeting a synthetic ssRNA 1.

C) Cleavage activity of Pin2Cas13b with a fluorescent poly U sensor for divalent cations Ca, Co, Cu, Mg, Mn, Ni, and Zn. Pin2Cas13b is incubated with a crRNA targeting a synthetic ssRNA 1.

D) Cleavage activity of Pin2Cas13b with a fluorescent poly A sensor for divalent cations Ca, Co, Cu, Mg, Mn, Ni, and Zn. Pin2Cas13b is incubated with a crRNA targeting a synthetic ssRNA 1.

E) Cleavage activity of CcaCas13b with a fluorescent poly U sensor for divalent cations Ca, Co, Cu, Mg, Mn, Ni, and Zn. CcaCas13b is incubated with a crRNA targeting a synthetic ssRNA 1.

F) Cleavage activity of CcaCas13b with a fluorescent poly A sensor for divalent cations Ca, Co, Cu, Mg, Mn, Ni, and Zn. CcaCas13b is incubated with a crRNA targeting a synthetic ssRNA 1.

Figure S7

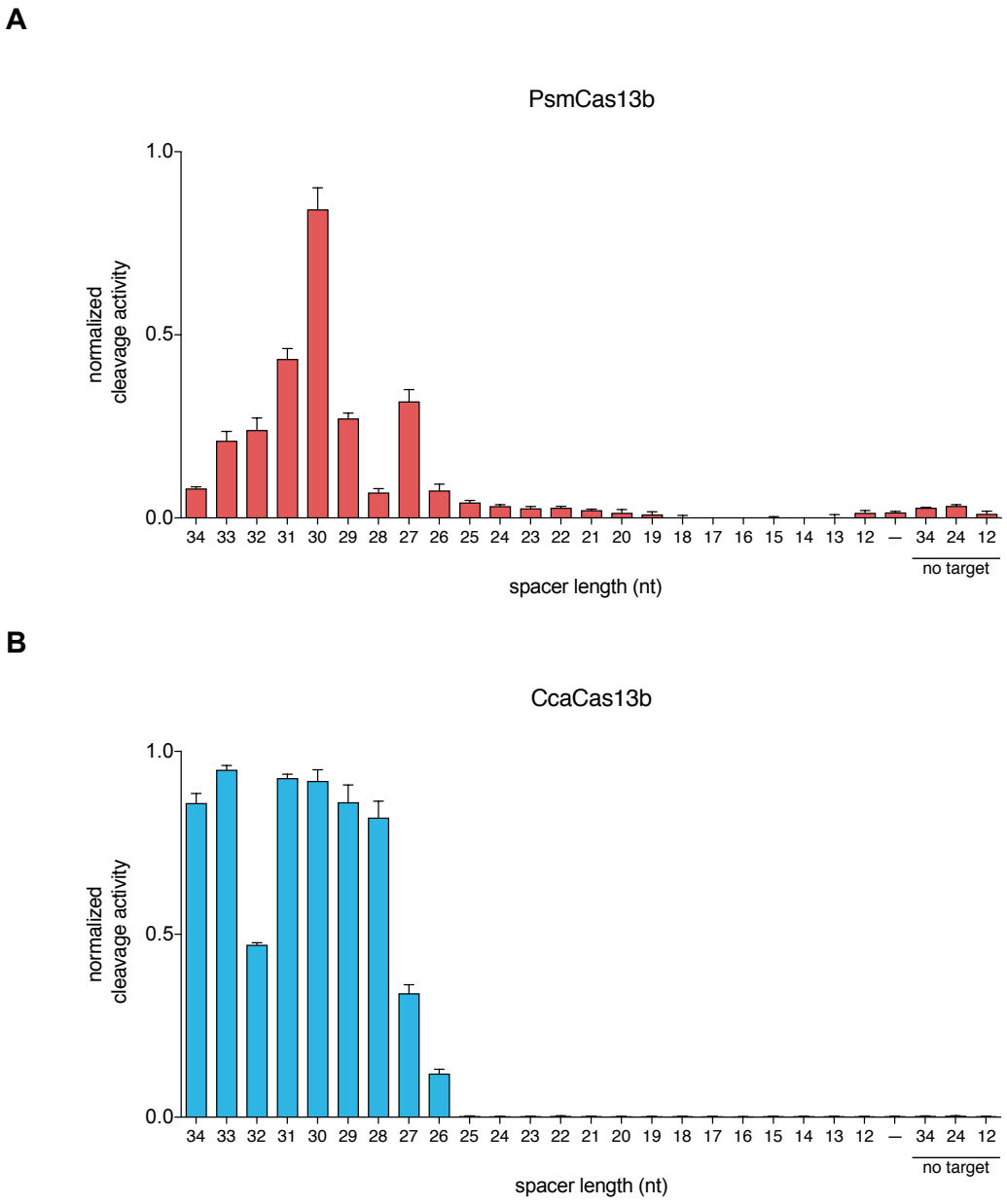

Figure S7: Effect of crRNA spacer length on Cas13 ortholog cleavage

A) Cleavage activity of PsmCas13b with ssRNA1-targeting crRNAs of varying spacer lengths.

B) Cleavage activity of CcaCas13b with ssRNA1-targeting crRNAs of varying spacer lengths.

Figure S6

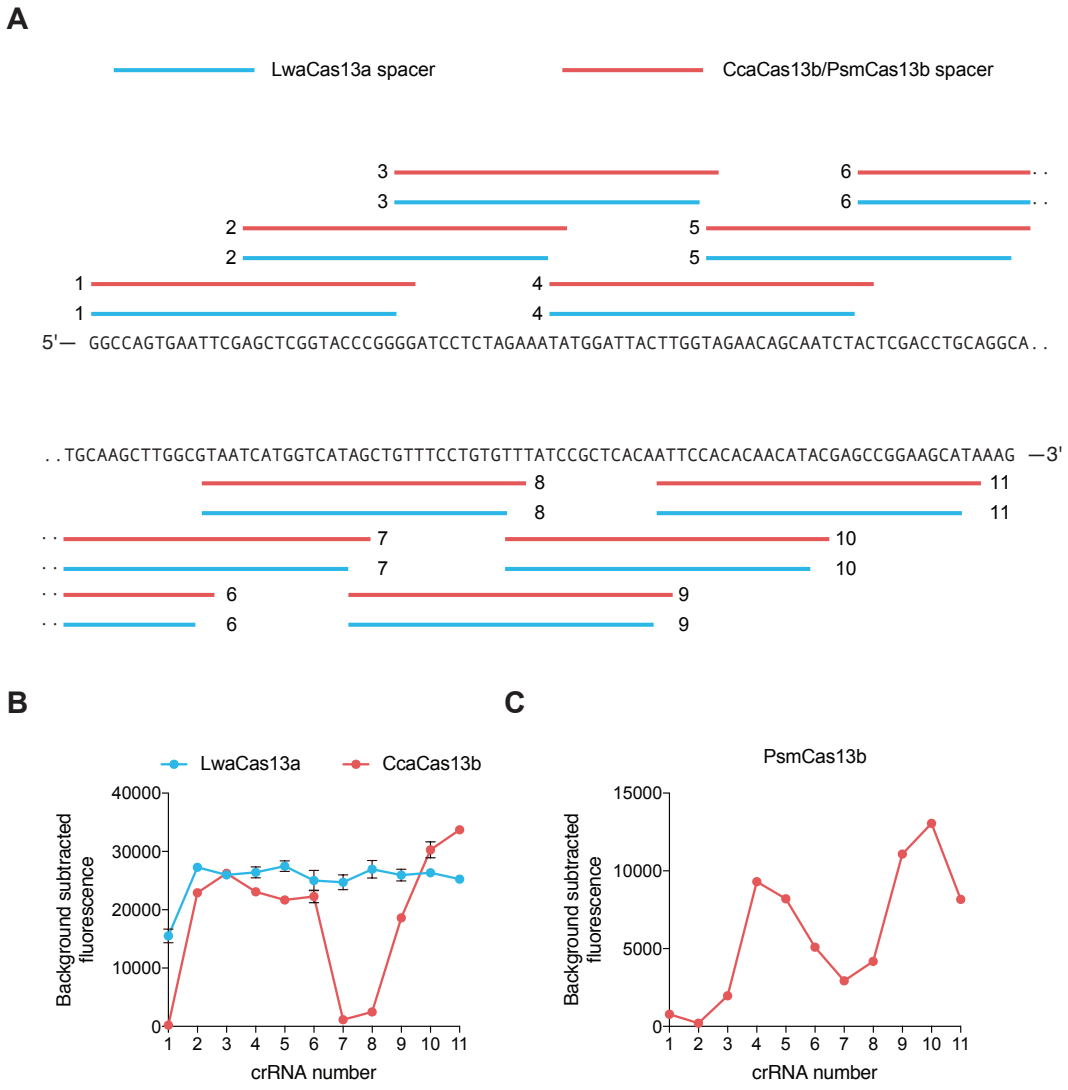

Figure S6: Testing Cas13 ortholog reprogrammability with crRNAs tiling ssRNA 1.

A) Schematic of locations tiled crRNA targeting ssRNA 1.

B) Cleavage activity of LwaCas13a and CcaCas13b with crRNAs tiled across ssRNA1.

C) Cleavage activity of PsmCas13b with crRNAs tiled across ssRNA1.

Figure S8

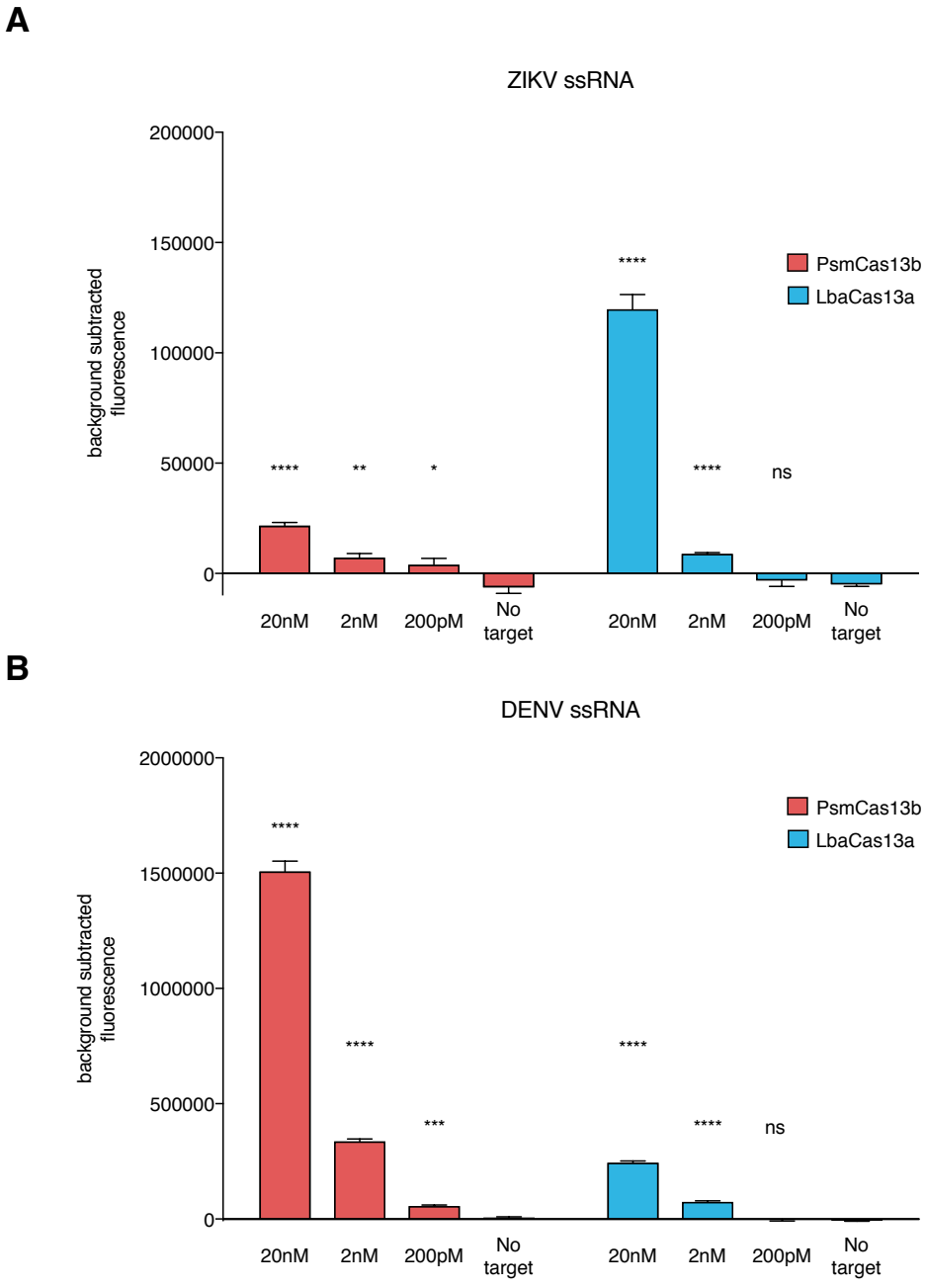

Figure S8: Comparison of cleavage activity for Cas13 orthologs with adenine cleavage preference

A) Cleavage activity of PsmCas13b and LbaCas13a incubated with respective crRNAs targeting the ZIKV ssRNA target at different concentrations (n=4 technical

replicates, two-tailed Student t-test; n.s., not significant; *, $p < 0.05$; **, $p < 0.01$; ***, $p < 0.001$; ****, $p<0.0001$; bars represent mean ± s.e.m.).

B) Cleavage activity of PsmCas13b and LbaCas13a incubated with respective crRNAs targeting a synthetic DENV ssRNA target at different concentrations (n=4 technical replicates, two-tailed Student t-test; n.s., not significant; *, $p < 0.05$; **, $p < 0.01$; ***, $p < 0.001$; ****, $p<0.0001$; bars represent mean ± s.e.m.).

Figure S9

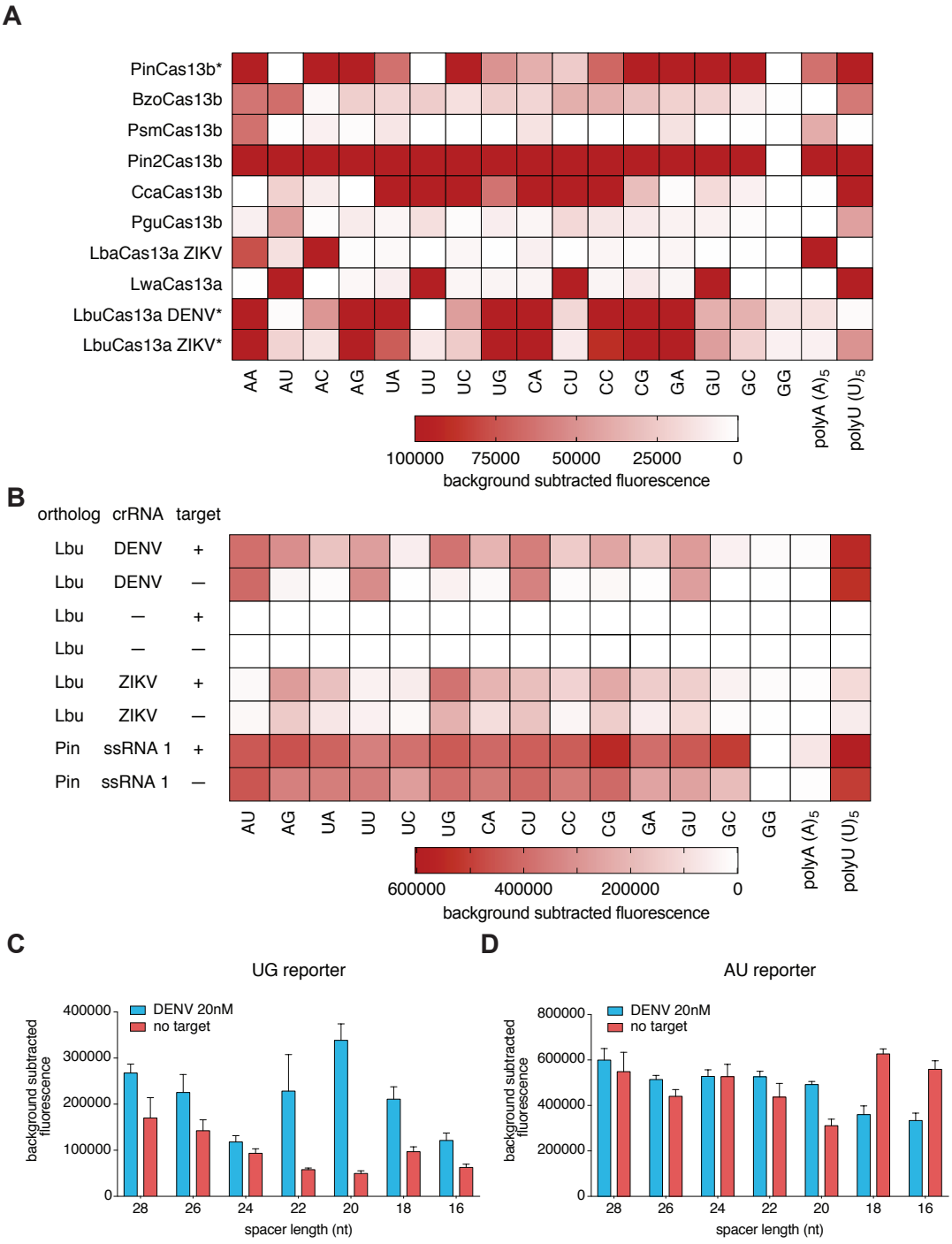

Figure S9: Di-nucleotide preferences of Cas13a/b enzymes

A) Heatmap of the di-nucleotide base preference of 10 Cas13a/b orthologs targeting ssRNA 1, unless otherwise indicated, with reporters consisting of a di-nucleotide

of A, C, G, or U RNA bases. (*) represent non-background subtracted orthologs with high background activity.

B) Heatmap of the di-nucleotide base preference of the high background activity orthologs LbuCas13a and PinCas13b tested on indicated targets.

C) Cleavage activity of LbuCas13a on AU di-nucleotide motif with and without 20nM DENV ssRNA target tested with varying spacer lengths.

D) Cleavage activity of LbuCas13a on UG di-nucleotide motif with and without 20nM DENV ssRNA target tested with varying spacer lengths.

Figure S10

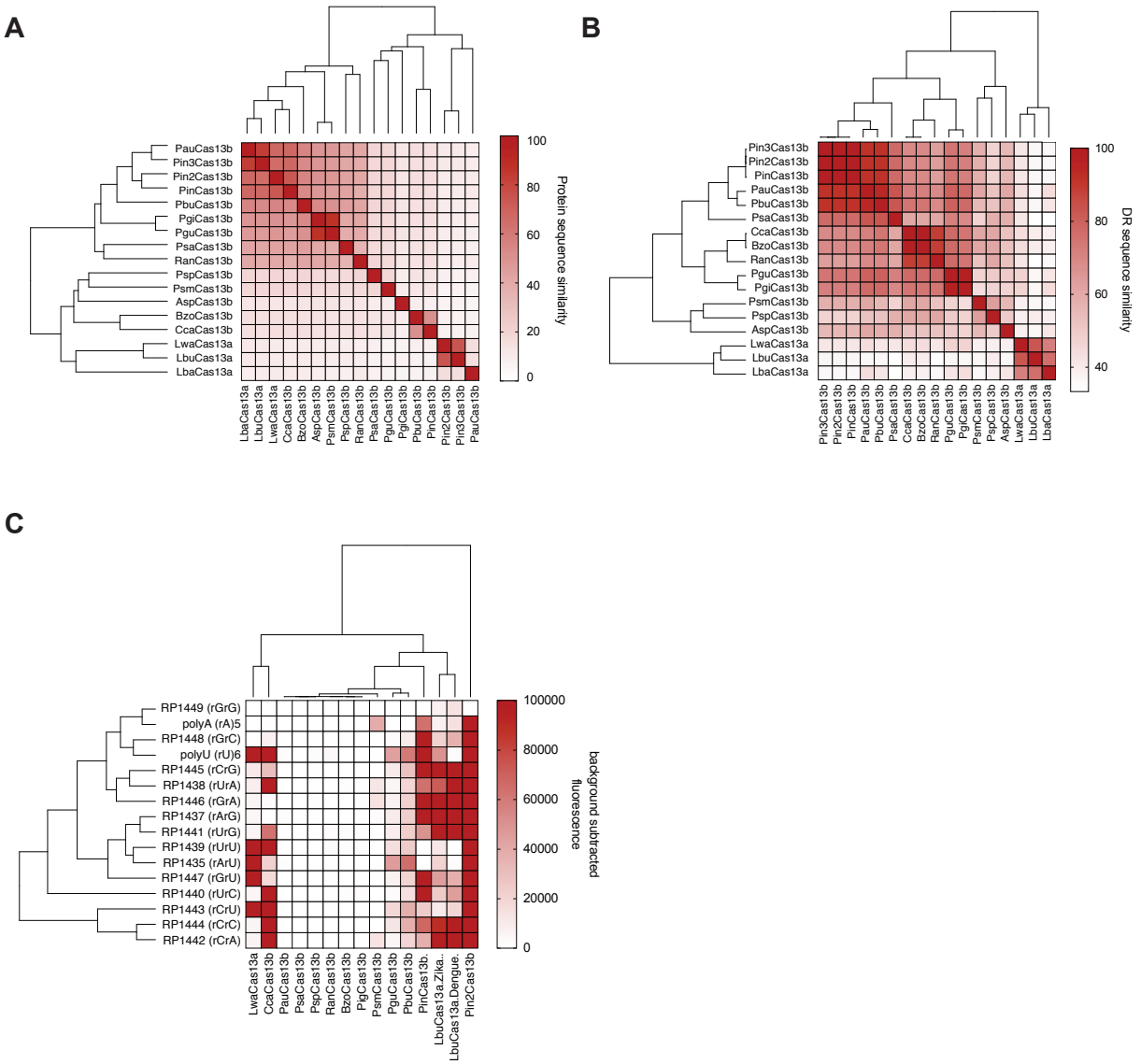

Figure S10: Relationship of Cas13 families with di-nucleotide cleavage preferences

A) Protein sequence similarity matrix based on multiple protein sequence alignment of several Cas13a and Cas13b ortholog members. Clustering is shown based on Euclidean distance.

B) Direct repeat sequence similarity matrix based on multiple sequence alignment of several Cas13a and Cas13b direct repeat sequences. Clustering is shown based on Euclidean distance

C) Clustering of the Cas13 cleavage activity base preferences of dinucleotide motif reporters.

Figure S11

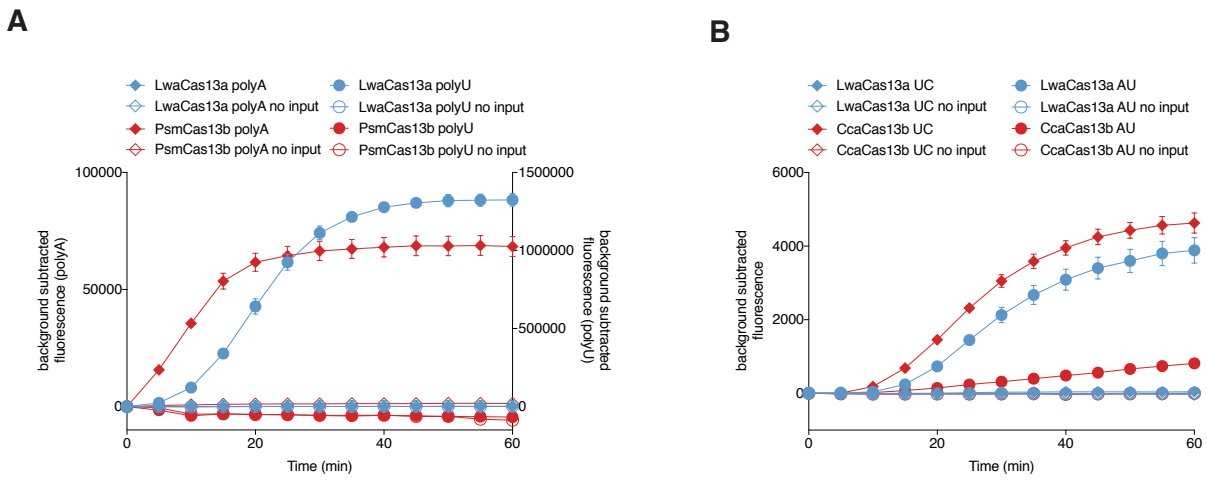

Figure S11: Kinetics of cleavage activity for Cas13 enzymes with orthogonal cleavage preferences

A) Orthogonal base preferences of PsmCas13b and LwaCas13a targeting ssRNA 1 with either a U_6 or A_6 reporter.

B) Orthogonal base preferences of CcaCas13b and LwaCas13a targeting DENV RNA with either a AU or UC reporter.

Figure S12

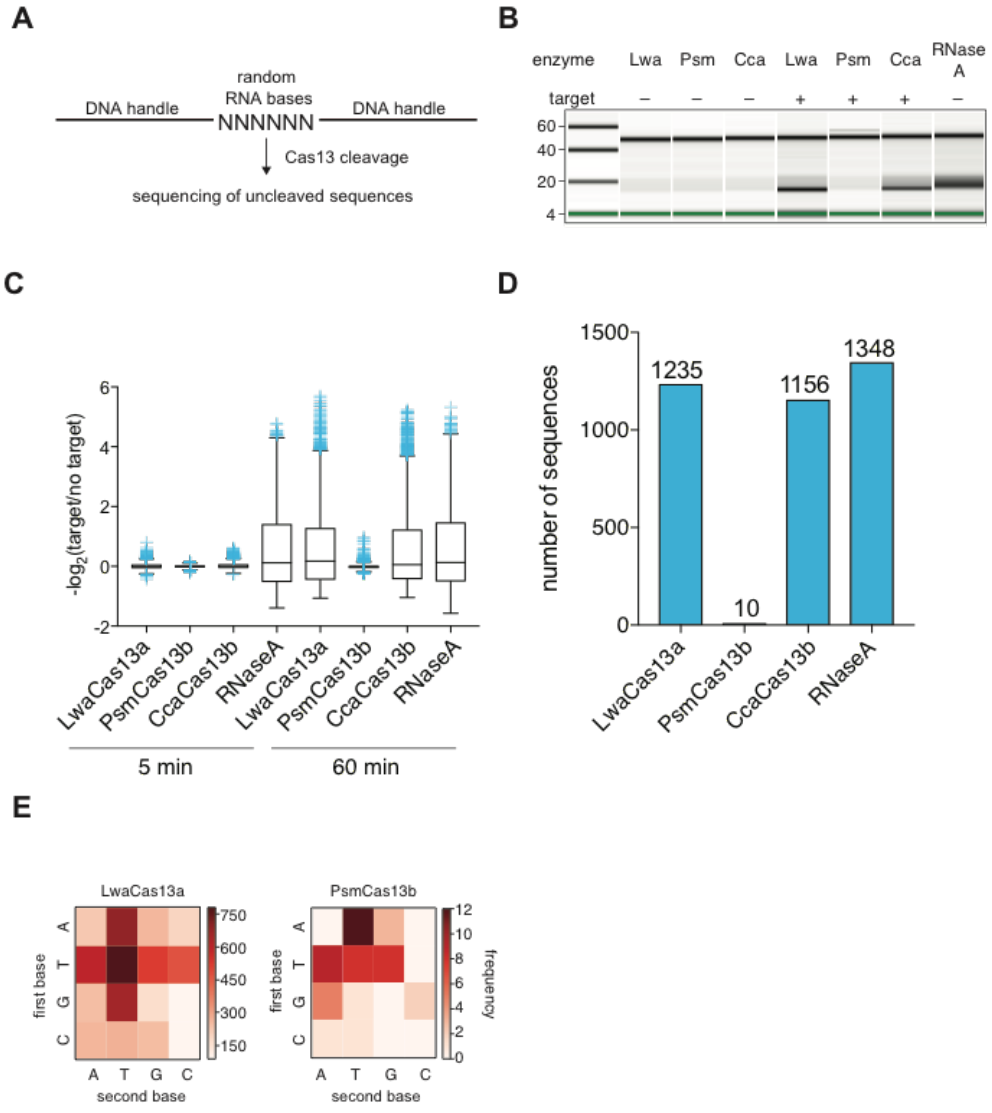

Figure S12: Random motif cleavage screen for testing Cas13 base preferences

A) Schematic of cleavage motif preference discovery screen for comparing random motif prefences.

B) Bioanalyzer traces for LwaCas13a-, PsmCas13b-, CcaCas13b-, and RNase A-treated library samples showing changes in library size after RNase activity. Cas13 orthologs are targeting DENV ssRNA and cleave the random motif-library due to collateral cleavage. Marker standards are shown in the first lane.

C) Box plots showing motif distribution of target to no-target ratios for LwaCas13a, PsmCas13b, CcaCas13b, and RNase A at 5 minute and 60 minute timepoints. RNase A ratios were compared to the average of the three Cas13 no-target conditions. Ratios are also an average of two cleavage reaction replicates.

D) Number of enriched motifs for LwaCas13a, PsmCas13b, CcaCas13b, and RNase A at the 60 minute timepoint. Enrichment motif was calculated as motifs above -$\log_2$(target/no target) thresholds of either 1 (LwaCas13a, CcaCas13b, and RNase A) or 0.5 (PsmCas13b). A threshold of 1 corresponds to at least 50% depletion while a threshold of 0.5 corresponds to at least 30% depletion.

E) Preferred two-base motifs for LwaCas13a and PsmCas13b. Values represented in the heatmap are the the counts of each two-base across all depleted motifs. Motifs are considered depleted if the -log2(target/no target) value is above 1.0 in the LwaCas13a condition or 0.5 in the PsmCas13b condition. In the -log2(target/no target) value, target and no target denote the frequency of a motif in the target and no target conditions, respectively.

Figure S13

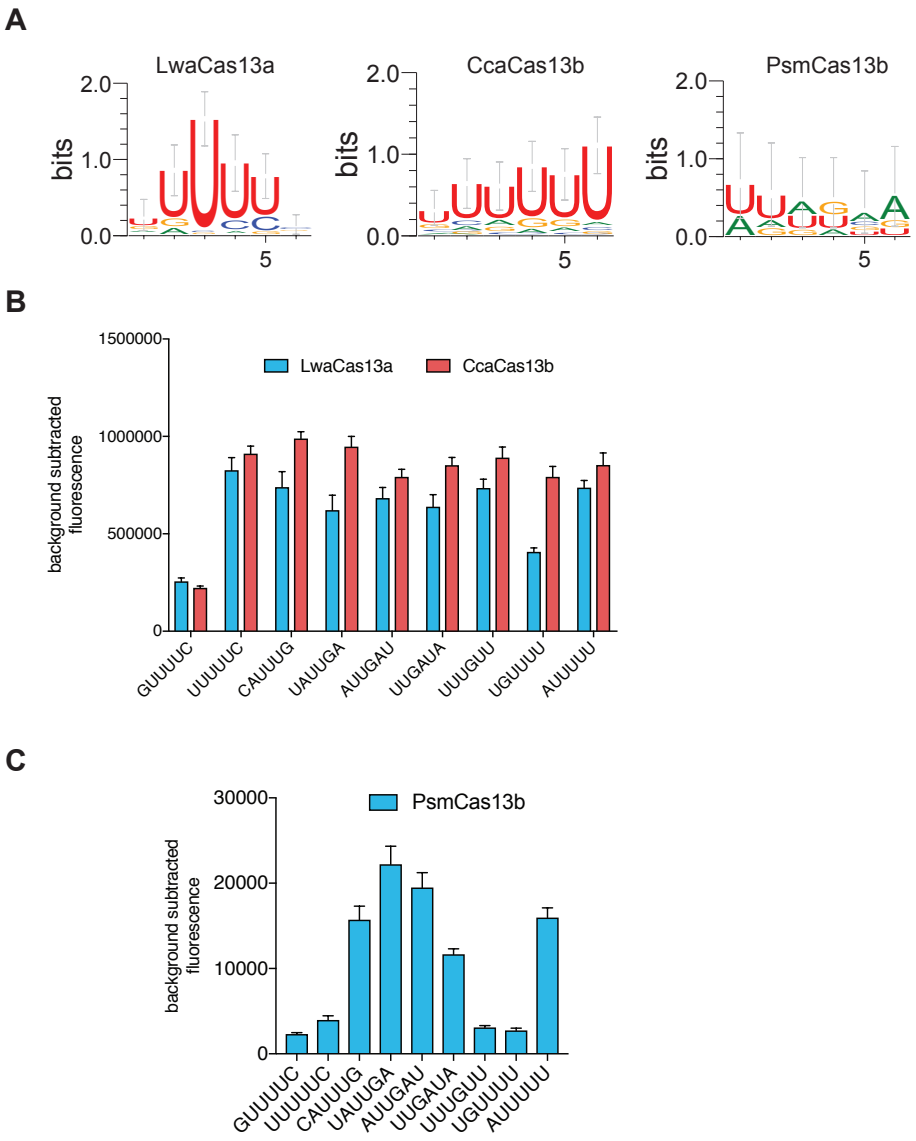

Figure S13: Motifs and orthogonal sequences from random motif cleavage screen

A) Sequence logos generated from enriched motifs for LwaCas13a, PsmCas13b, and CcaCas13b. LwaCas13a and CcaCas13b show a strong U preference as would be expected, while PsmCas13b shows a unique preference for A bases across the motif, which is consistent with homopolymer collateral activity preferences.

B) Collateral activity of LwaCas13a and CcaCas13b targeting DENV ssRNA on most depleted motifs from the RNA collateral motif screen.

C) Collateral activity of PsmCas13b targeting DENV ssRNA on most depleted motifs from the RNA collateral motif screen.

Figure S14

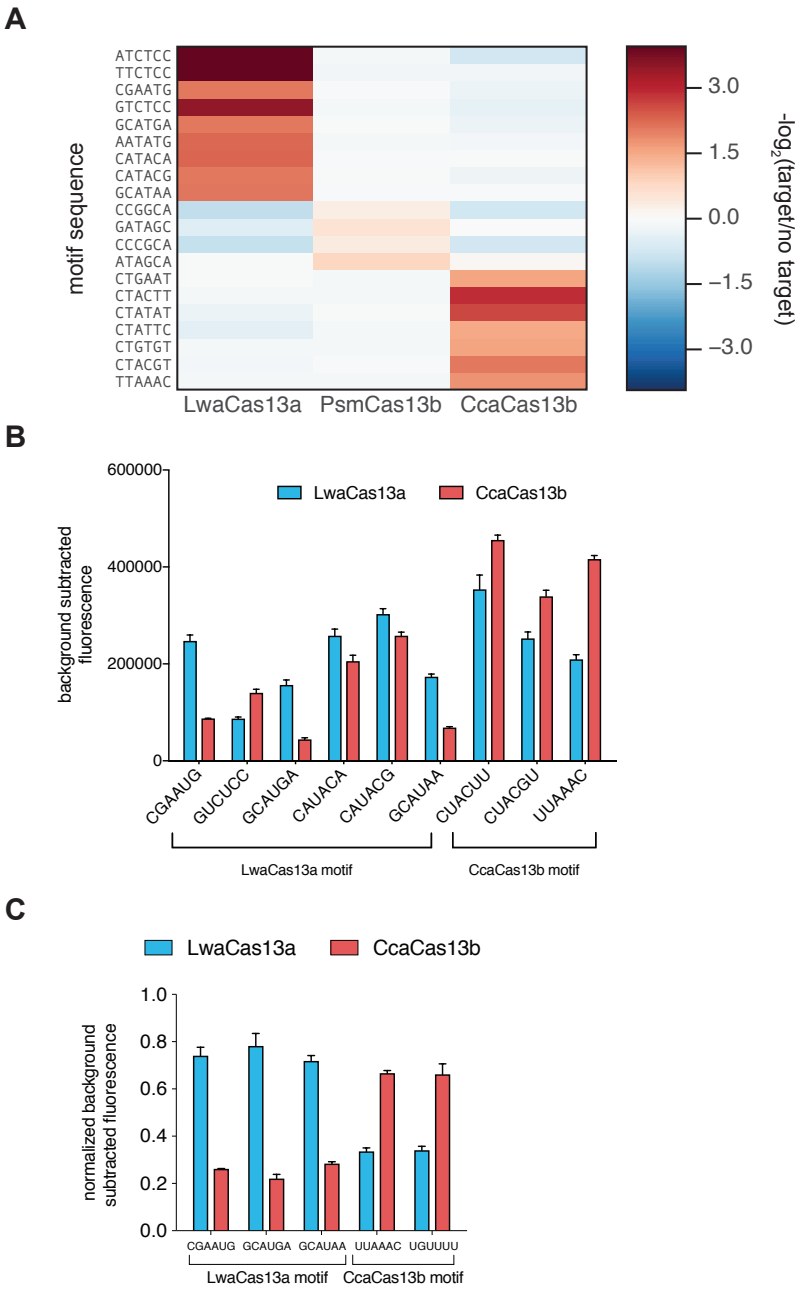

Figure S14: Comparison of top collateral activity motifs from the RNA motif collateral activity screens

A) Heatmap showing the orthogonal motif preferences of LwaCas13a, PsmCas13b, and CcaCas13b. Values represented in the heatmap are the -$\log_2$(target/no target) value of each shown motif. In the -$\log_2$(target/no target) value, target and no target denote the frequency of a motif in the target and no target conditions, respectively.

B) Cleavage activity of LwaCas13a and CcaCas13b on top orthogonal motifs derived from the motif preference discovery screen
C) Collateral activity of LwaCas13a and CcaCas13b targeting DENV ssRNA on top orthogonal RNA motifs.

Figure S15

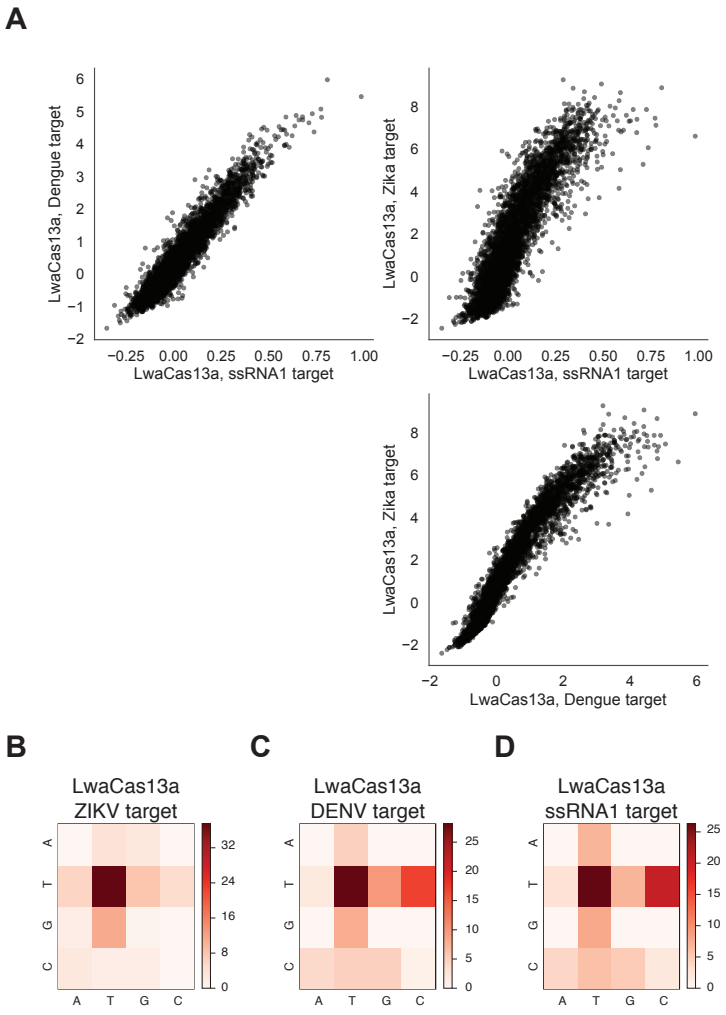

Figure S15: Comparison of random motif library screen on different targets and enzymes

A) Pair-wise comparison of enrichment scores for different activating targets with LwaCas13a.

B) Heatmaps showing two-base preference for LwaCas13a with the ZIKV ssRNA target as determined by the random motif library cleavage screen. Values represented in the heatmap are the the counts of each 2-base across all depleted motifs. Motifs are considered depleted if the $-\log_2$(target/no target) value is above 1.0.

C) Heatmaps showing two-base preference for LwaCas13a with the DENV ssRNA target as determined by the random motif library cleavage screen. Values represented in the heatmap are the the counts of each 2-base across all depleted motifs. Motifs are considered depleted if the $-\log_2$(target/no target) value is above 1.0.

D) Heatmaps showing two-base preference for LwaCas13a with the ssRNA1 target as determined by the random motif library cleavage screen. Values represented in the heatmap are the the counts of each 2-base across all depleted motifs. Motifs are considered depleted if the $-\log_2$(target/no target) value is above 1.0.

Figure S16

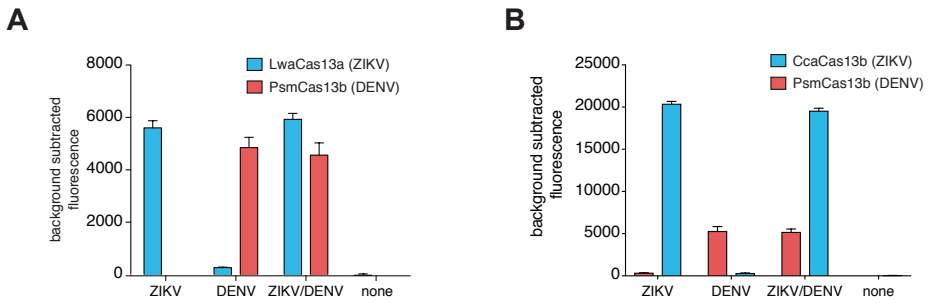

Figure S16: Multiplexed detection of ZIKV ssRNA and DENV ssRNA targets.

A) In-sample multiplexed detection of 20 nM ZIKV and DENV ssRNA targets with LwaCas13a and PsmCas13b collateral activity.

B) In-sample multiplexed detection of 20 pM ZIKV and DENV ssRNA targets with CcaCas13a and PsmCas13b collateral activity.

Figure S17

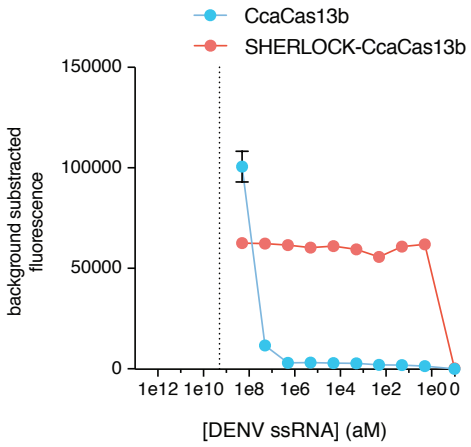

Figure S17: Attomolar detection of CcaCas13b-SHERLOCK

Comparison of collateral activity and pre-amplification enhanced collateral (SHERLOCK) of CcaCas13b.

Figure S18

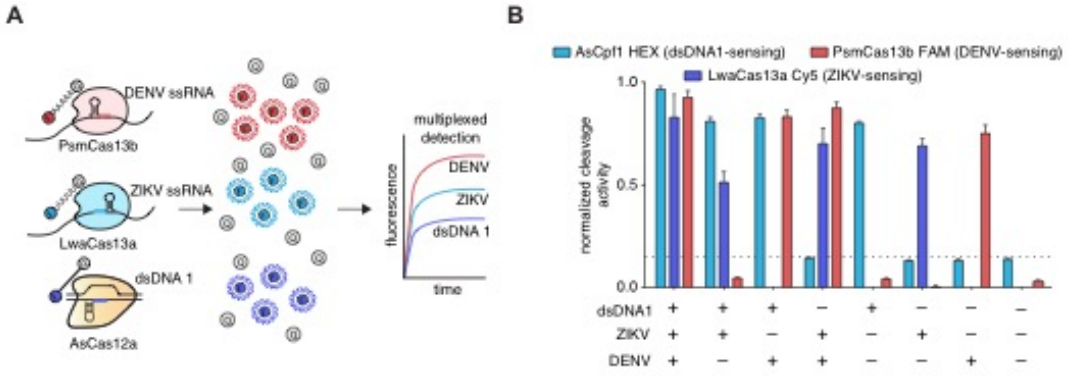

Figure S18: Triplex detection using orthogonal CRISPR enzymes

A) Schematic of in-sample 3 channel multiplexing using orthogonal Cas13 and Cas12a enzymes.

B) In-sample multiplexed detection of ZIKV ssRNA, DENV ssRNA, and dsDNA 1 with LwaCas13a, PsmCas13b, and Cas12a.

Figure S19

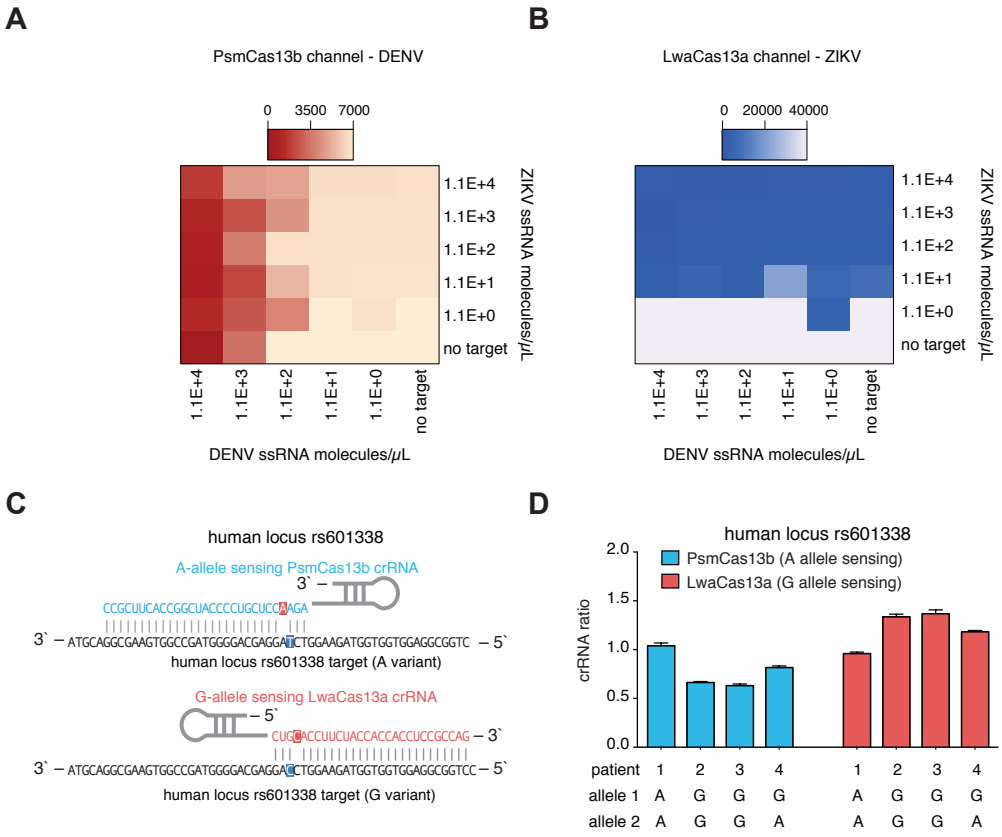

Figure S19: In-sample multiplexed RNA detection of ZIKV ssRNA and DENV ssRNA targets and human genotyping.

A) In-sample multiplexed RPA and collateral detection at decreasing concentrations of ZIKV and DENV ssRNA targets with PsmCas13b.

B) In-sample multiplexed RPA and collateral detection at decreasing concentrations of ZIKV and DENV ssRNA targets with LwaCas13a.

C) Schematic of crRNA design and target sequences for multiplexed genotyping at rs601338 with LwaCas13a and PsmCas13b.

D) Multiplexed genotyping with human samples at rs601338 with LwaCas13a and PsmCas13b.

Figure S20

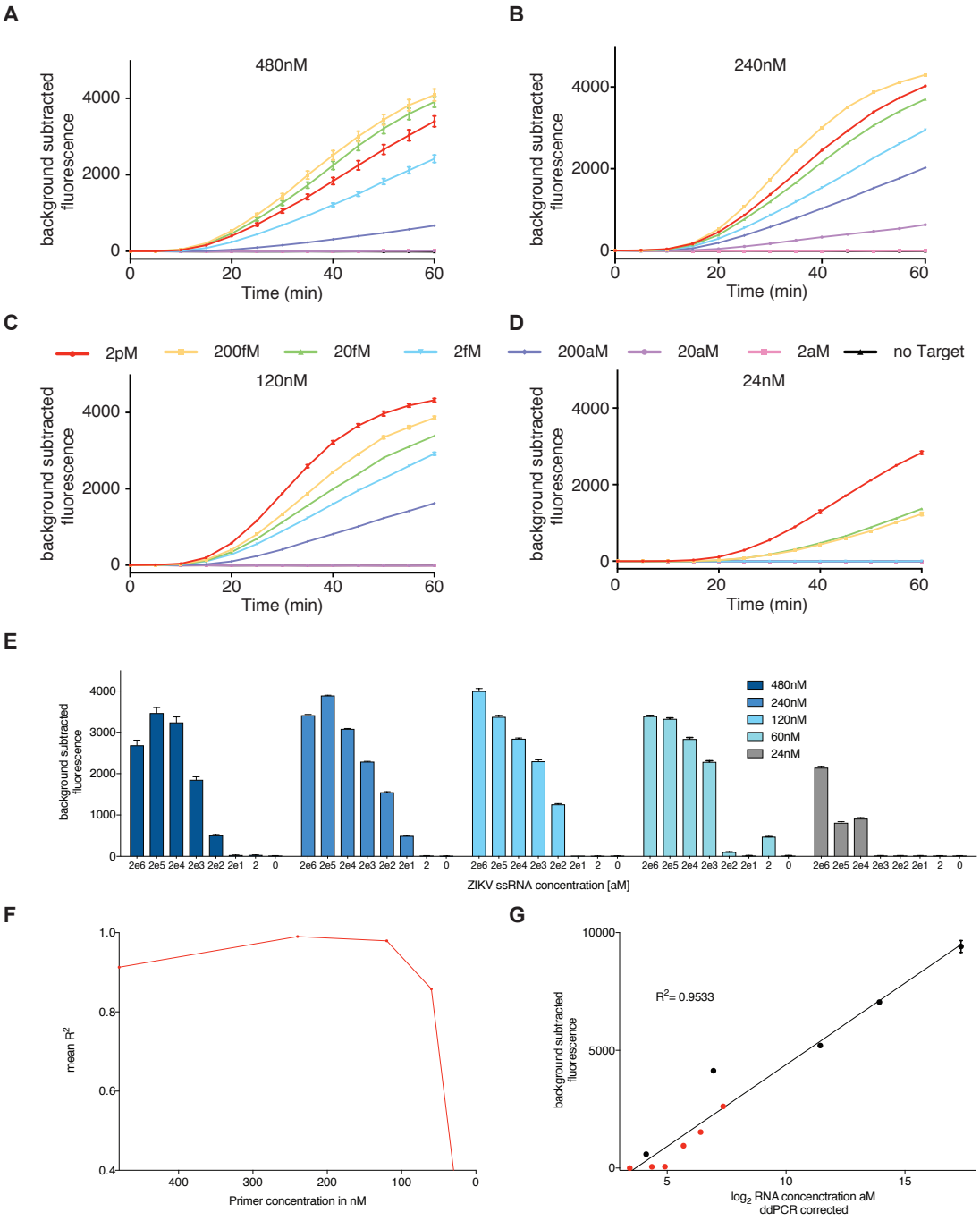

Figure S20: Optimizing primer concentration for quantitative SHERLOCK

A) SHERLOCK kinetic curves of LwaCas13a incubated with ZIKV ssRNA targets of different concentration and a complementary crRNA at an RPA primer concentration of 480nM.
B) SHERLOCK kinetic curves of LwaCas13a incubated with ZIKV ssRNA targets of different concentration and a complementary crRNA at an RPA primer concentration of 240nM.
C) SHERLOCK kinetic curves of LwaCas13a incubated with ZIKV ssRNA targets of different concentration and a complementary crRNA at an RPA primer concentration of 120nM.
D) SHERLOCK kinetic curves of LwaCas13a incubated with ZIKV ssRNA targets of different concentration and a complementary crRNA at an RPA primer concentration of 24nM.
E) SHERLOCK detection of ZIKV ssRNA of different concentrations at with four different RPA primer concentrations: 480nM, 240nM, 120nM, 60nM, and 24nM.
F) The mean R^2 correlation between background subtracted fluorescence of SHERLOCK and the ZIKV ssRNA target RNA concentration at different RPA primer concentrations.
G) Quantitative SHERLOCK detection of ZIKV ssRNA targets at different concentrations in a 10-fold dilution series (black points) and 2-fold dilution series (red points). An RPA primer concentration of 240nM was used.

Figure S21

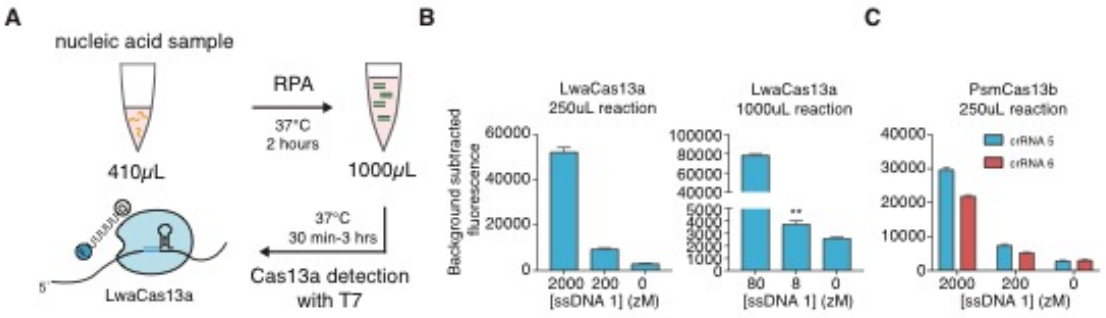

Figure S21: Large volume SHERLOCK reactions with sub-attomolar sensitivity

A) Schematic of large reactions for increased sensitivity single molecule detection.

B) Single molecule SHERLOCK detection with LwaCas13a in large reaction volumes for increased sensitivity targeting ssRNA target 1. For 250μL reaction volumes, 100μL of sample input is used and for 1000μL reaction volumes, 540μL of sample input is used.

C) Single molecule SHERLOCK detection with PsmCas13b in large reaction volumes for increased sensitivity targeting ssRNA target 1. For 250μL reaction volumes, 100μL of sample input is used.

Figure S22

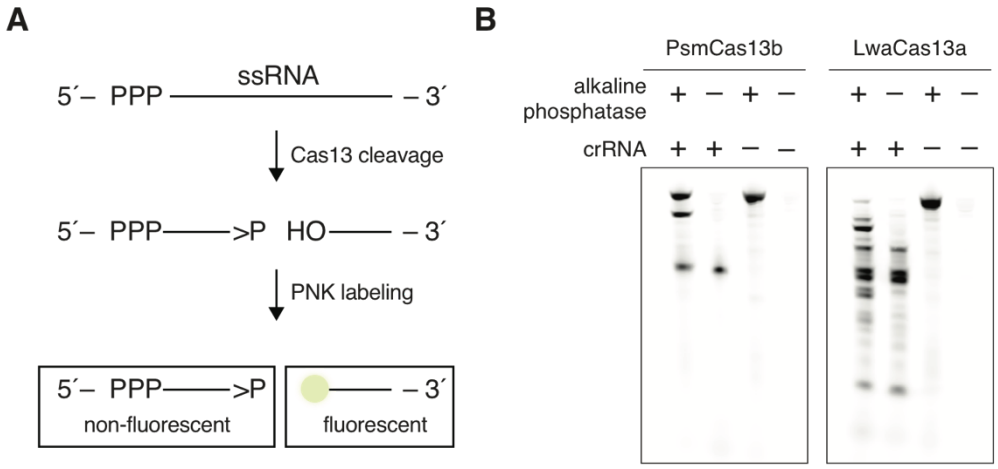

Figure S22: Profiling of cleavage ends generated by LwaCas13a and PsmCas13b

A) Schematic for detection of 2,3 cyclic phosphate ends via PNK labeling and gel electrophoresis.

B) Electrophoresis gel demonstrating 2,3 cyclic phosphate ends generated by LwaCas13a or PsmCas13b cleavage of ssRNA target 2 or 3 (homopolymer loops). The Cas13 enzyme is incubated with the appropriate crRNA targeting the ssRNA target and the cleavage products are 5' labeled with a dye IR800 with or without alkaline phosphatase treatment.

Figure S23

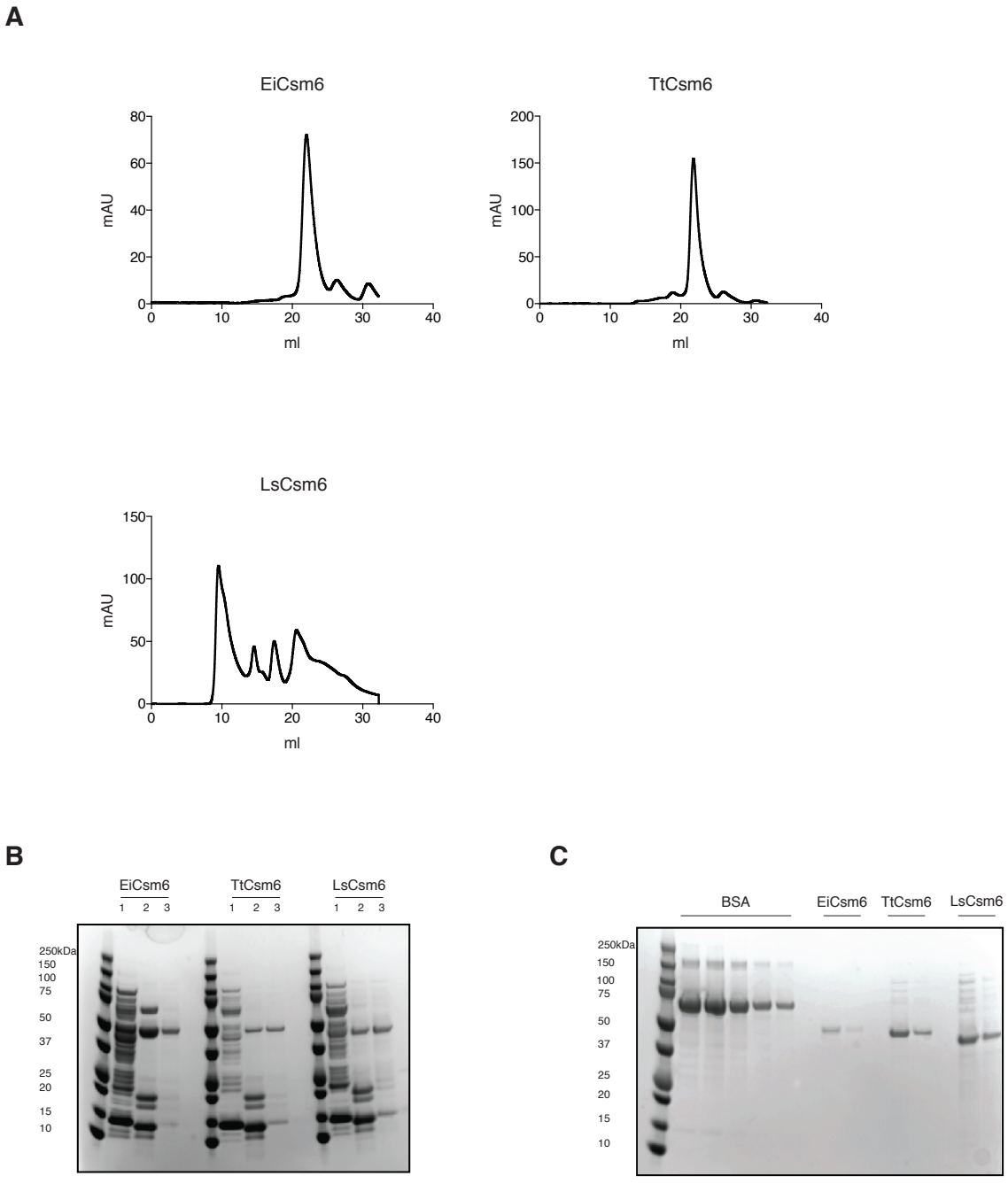

Figure S23: Protein purification of Csm6 orthologs

A) Chromatograms of size exclusion chromatography for EiCsm6, TtCsm6, LsCsm6 and SaCsm6 used in this study. Measured UV absorbance (mAU) is shown against the elution volume (ml).

B) SDS-PAGE gel of EiCsm6, TtCsm6 and LsCsm6 fractions prior to size exclusion chromatography. Fractions show the bacterial lysate supernatant (1) after streptactin incubation, streptactin resins after cleavage with SUMO protease (2), as well as released, untagged Csm6 protein (3).

C) Final SDS-PAGE of concentrated Csm6 proteins after size exclusion chromatography. BSA standard curve (left) is used to quantify Csm6 proteins (right). Five dilutions of BSA and two dilutions of EiCsm6, TtCsm6 and LsCsm6 are shown.

Figure S24

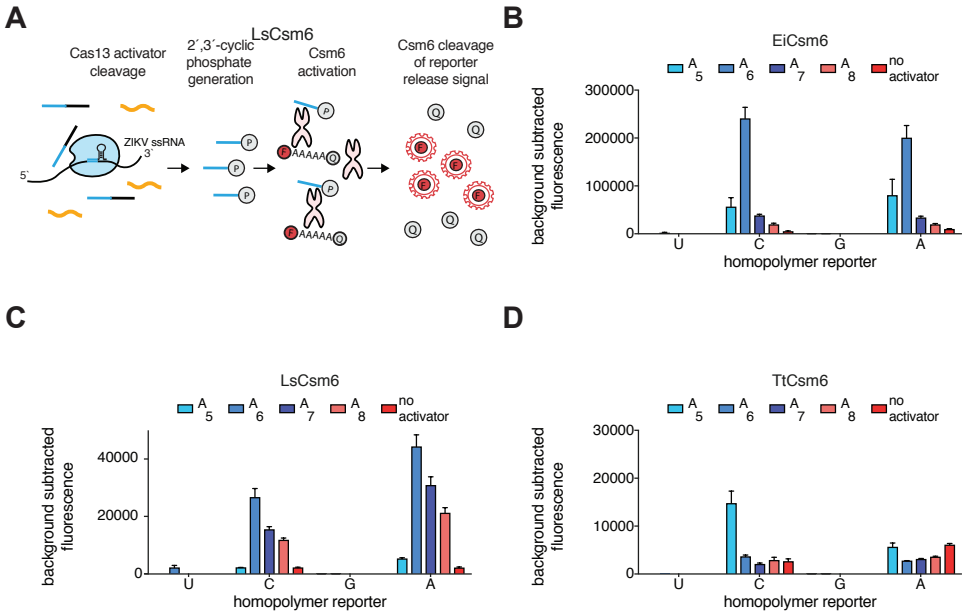

Figure S24: Base preference and activation of Csm6 orthologs

A) Schematic for Csm6-mediated positive feedback in a SHERLOCK reaction.

B) Activation of EiCsm6 by 2′,3′-cyclic phosphate-terminated adenine oligomers of different lengths. Csm6 cleavage is measured using an RNA reporter consisting of A, C, G, or U homopolymer with ends labeled with a fluorophore and quencher.

C) Base preference of LsCsm6 cleavage activated by 2′,3′-cyclic phosphate-terminated adenine oligomers.

D) Base preference of TtCsm6 cleavage activated by 2′,3′-cyclic phosphate-terminated adenine oligomers.

Figure S25

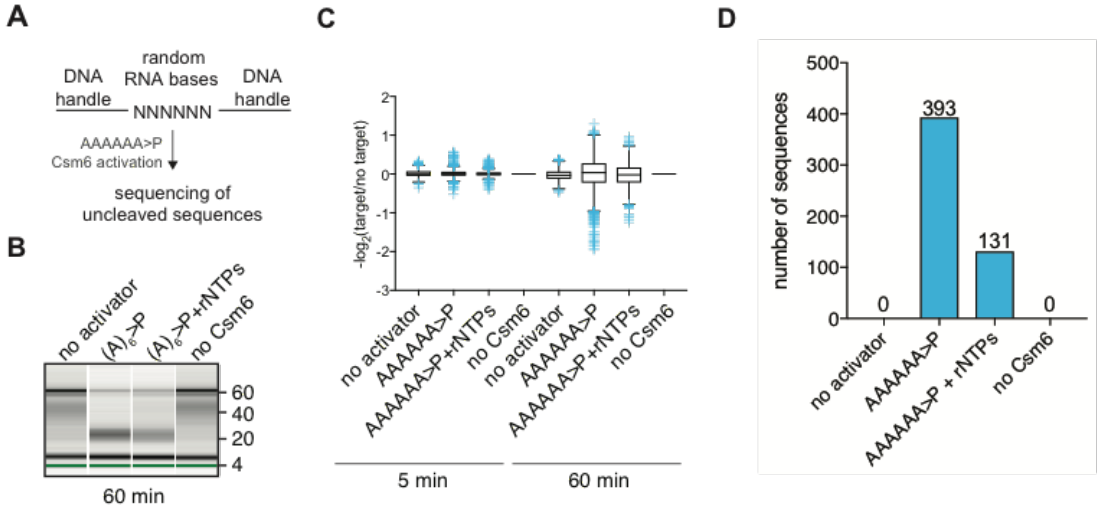

Figure S25: Size analysis and representation of various motifs after Csm6 cleavage.

A) Schematic of cleavage motif preference discovery screen for Csm6 orthologs.

B) Bioanalyzer traces for EiCsm6 samples showing changes in library size after RNase activity that is activator dependent.

C) Box plots showing motif distribution of target to non-target motif ratios for Csm6, Csm6 with activator, Csm6 with activator and rNTPs, or background library at 5 minute and 60 minute timepoints.

D) Number of depleted motifs for Csm6, Csm6 with activator, Csm6 with activator and rNTPs, or background library at the 60 minute timepoint.

Figure S26

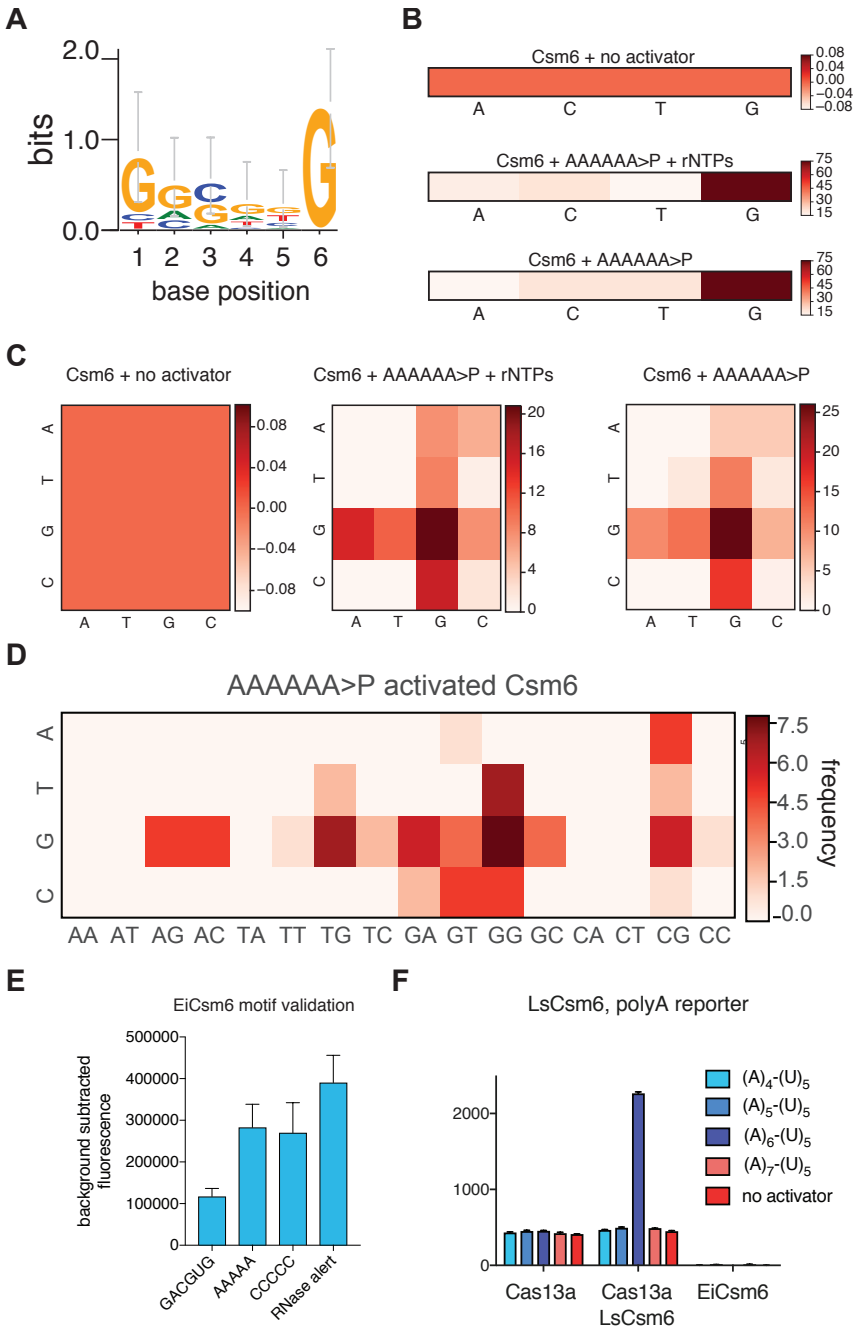

Figure S26: Single- and two-base preferences of Csm6 conditions determined by random motif library screen.

A) Sequence logo of preferred sequence motif for EiCsm6 cleavage activity.

B) Heatmaps showing single base preferences for Csm6, Csm6 with activator, and Csm6 with activator and rNTPs at the 60 minute timepoint as determined by the

random motif library cleavage screen. Values represented in the heatmap are the the counts of each single-base across all depleted motifs. Motifs are considered depleted if the $-\log_2$(target/no target) value is above 0.5. In the $-\log_2$(target/no target) value, target and no target denote the frequency of a motif in the target and no target conditions, respectively.

C) Heatmaps showing two-base preferences for Csm6, Csm6 with activator, and Csm6 with activator and rNTPs at the 60 minute timepoint as determined by the random motif library cleavage screen. Values represented in the heatmap are the the counts of each two-base across all depleted motifs. Motifs are considered depleted if the $-\log_2$(target/no target) value is above 0.5. In the $-\log_2$(target/no target) value, target and no target denote the frequency of a motif in the target and no target conditions, respectively.

D) Heatmap of preferred 3-base motifs for EiCsm6 cleavage activity. Values represented in the heatmap are the the counts of each 3-base across all depleted motifs. Motifs are considered depleted if the $-\log_2$(target/no target) value is above 0.5. In the $-\log_2$(target/no target) value, target and no target denote the frequency of a motif in the target and no target conditions, respectively.

E) Cleavage activity of EiCsm6 on top reporter sequences derived from the random motif library screen.

F) Activation of LsCsm6 by LwaCas13a cleavage of adenine-uridine activators with different length adenine tracts. LwaCas13a is targeting synthetic DENV ssRNA.

Figure S27

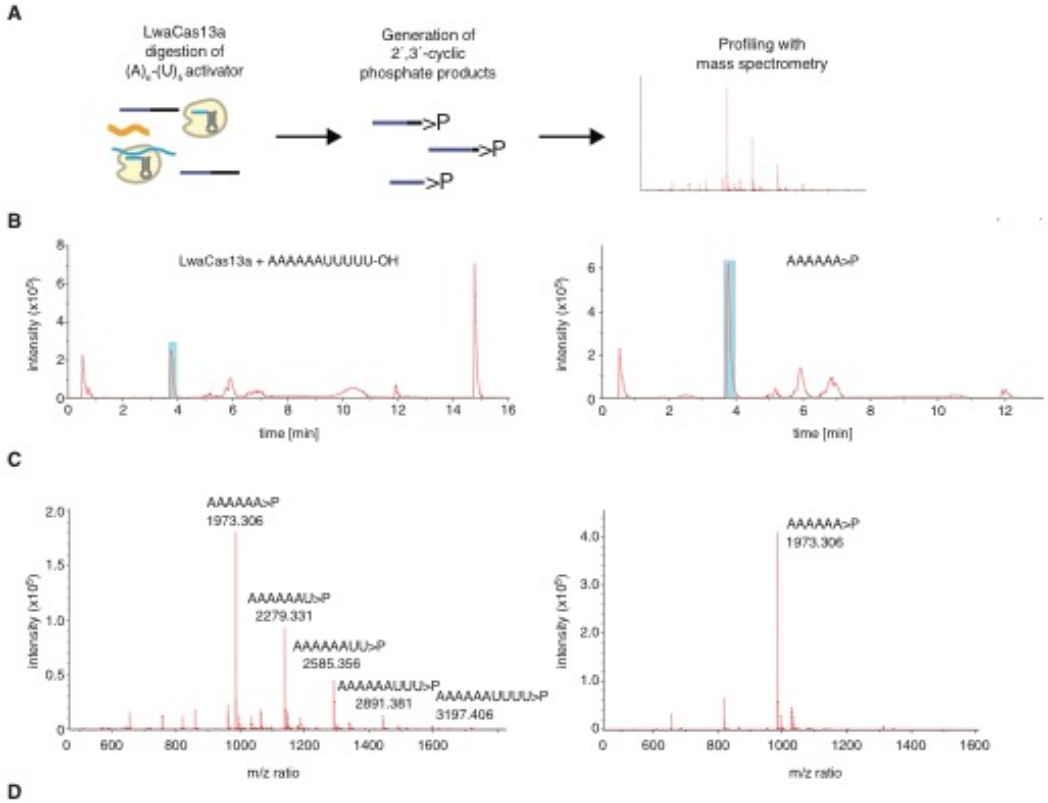

Cmpt.	Mass	Molecule	Abund.	Abd.[%]	Std.Dev.
A	1973.306	[M-H]-	196313	100	0.014056
B	2279.331	[M-H]-	107038	54.52	0.003627
C	2585.356	[M-H]-	62759	31.97	0.005015
D	2891.381	[M-H]-	32484	16.55	0.006336
E	3197.406	[M-H]-	19313	9.84	0.007767
F	3441.476	[M-H]-	14841	7.56	0.00578
G	1995.287	[M-H]-	13024	6.63	0.004689
H	1644.254	[M-H]-	11876	6.05	0.001244
I	2071.281	[M-H]-	11697	5.96	0.005988
J	2377.307	[M-H]-	10195	5.19	0.002957
K	2301.313	[M-H]-	7095	3.61	0.003839
L	2683.332	[M-H]-	7360	3.75	0.008262
M	2607.338	[M-H]-	5076	2.59	0.00323

Cmpt.	Mass	Molecule	Abund.	Abd.[%]	Std.Dev.
A	1973.306	[M-H]-	439056	100	0.003272
B	1644.254	[M-H]-	65030	14.81	0.001781
C	2063.374	[M-H]-	49525	11.28	0.003049
D	1995.287	[M-H]-	29564	6.73	0.003413
E	2071.282	[M-H]-	27554	6.28	0.003287

Figure S27: Mass spectrometry analysis of cleavage ends from LwaCas13a.

A) Schematic of LwaCas13a digestion and mass spectrometric analysis to verify cleavage products.

B) Mass spectrometry analysis of digestion products from LwaCas13a collateral cleavage (left) or 2,3 cyclic phosphate activator alone (right). Dominant peaks are labeled with mass and corresponding structure.

C) Chromatographic traces showing elution profiles for LwaCas13a-digested activator (top) or 2,3 cyclic phosphate activator (bottom). Blue highlighted peaks were analyzed for mass spectrometry in Fig. 5.

D) Table of abundances for different compounds detected by mass spectrometry in LwaCas13a-digested activator (left) or 2,3 cyclic phosphate activator (right) samples.

Figure S28

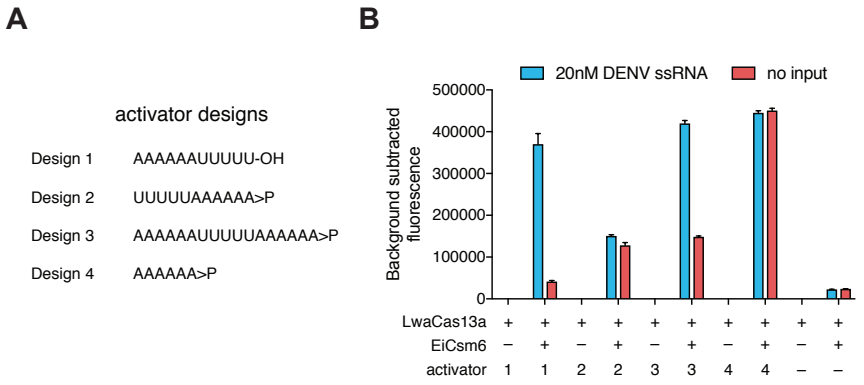

Figure S28: Effect of reporter and activator optimizations on Csm6-enhancement of LwaCas13a activity

A) Schematic of different activator designs for Csm6 enhancement of Cas13a activity.

B) Performance of EiCsm6 enhancement of LwaCas13a detection for different activator designs.

Figure S29

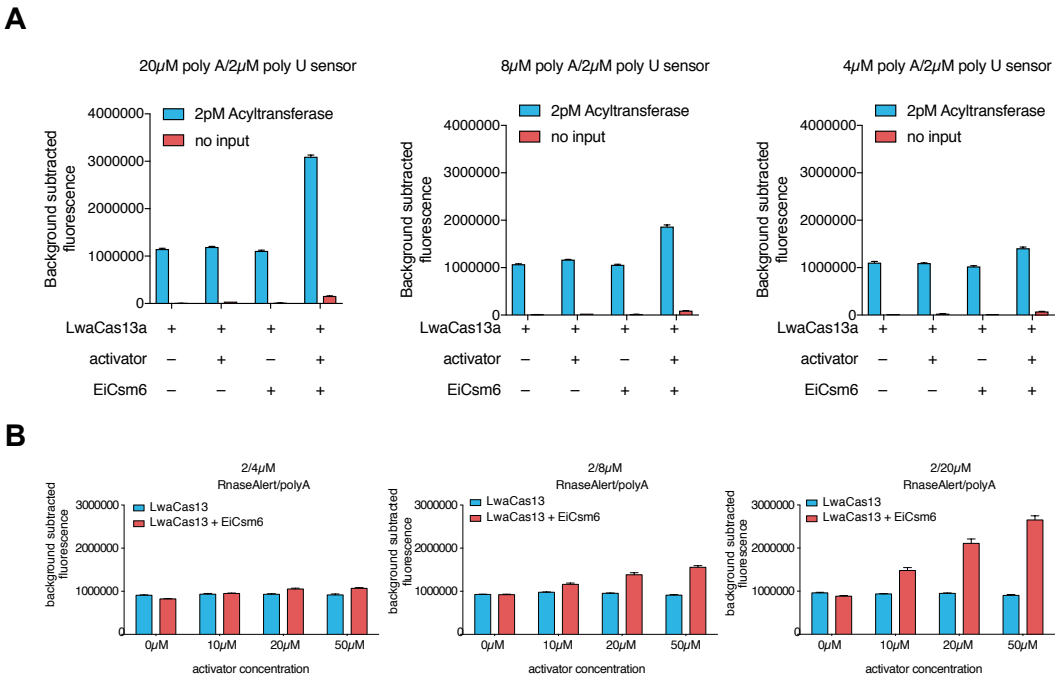

Figure S29: Effect of reporter and activator concentrations on Csm6-enhancement of LwaCas13a activity

A) EiCsm6 enhancement of LwaCas13a detection at various ratios of poly A and poly U reporters.

B) EiCsm6 enhancement of LwaCas13a detection at various concentrations of $(A)_6$-$(U)_5$ activator.

Figure S30

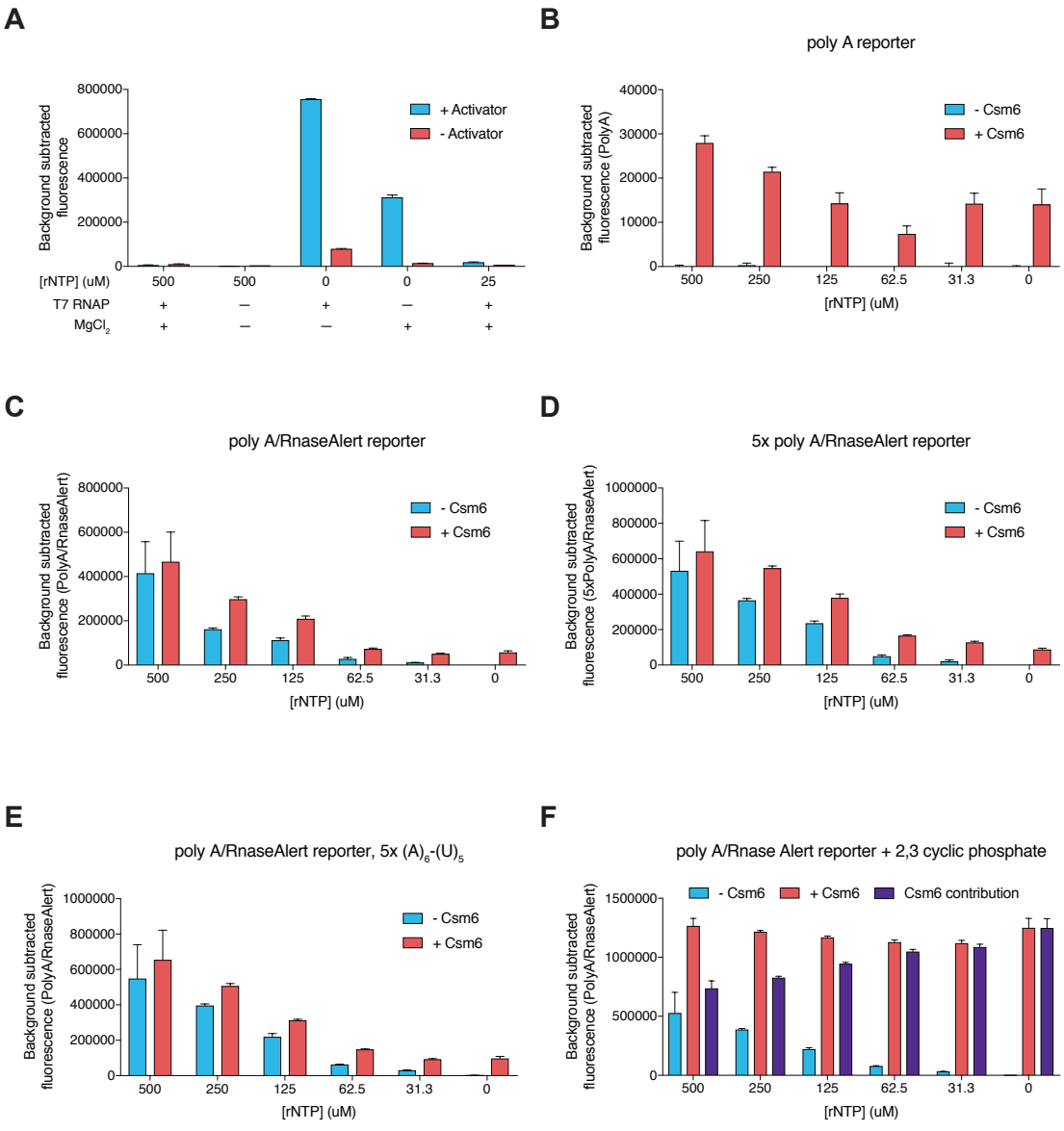

Figure S30: Effect of *in vitro* transcription components on Csm6 activity.

A) EiCsm6 activity in the presence of IVT components, with and without 2,3 cyclic phosphate activator. Components include 3mM additional MgCl2, 1mM rNTP mix, 30U T7 polymerase

B) EiCsm6 and LwaCas13a activity with $(A)_6$-$(U)_5$ activator and poly-A reporter in the presence of various concentrations of ribonucleotides

C) Combined EiCsm6 and LwaCas13a activity with $(A)_6$-$(U)_5$ activator and poly-A/RNaseAlert reporter combination in the presence of various concentrations of ribonucleotides

D) Combined EiCsm6 and LwaCas13a activity with $(A)_6$-$(U)_5$ activator and poly-A/5x RNaseAlert reporter combination in the presence of various concentrations of ribonucleotides

E) Combined EiCsm6 and LwaCas13a activity with $5x(A)_6$-$(U)_5$ activator and poly-A/RNaseAlert reporter combination in the presence of various concentrations of ribonucleotides

F) Combined EiCsm6 and LwaCas13a activity with cyclic phosphate activator and poly-A/RNaseAlert reporter combination in the presence of various concentrations of ribonucleotides

Figure S31

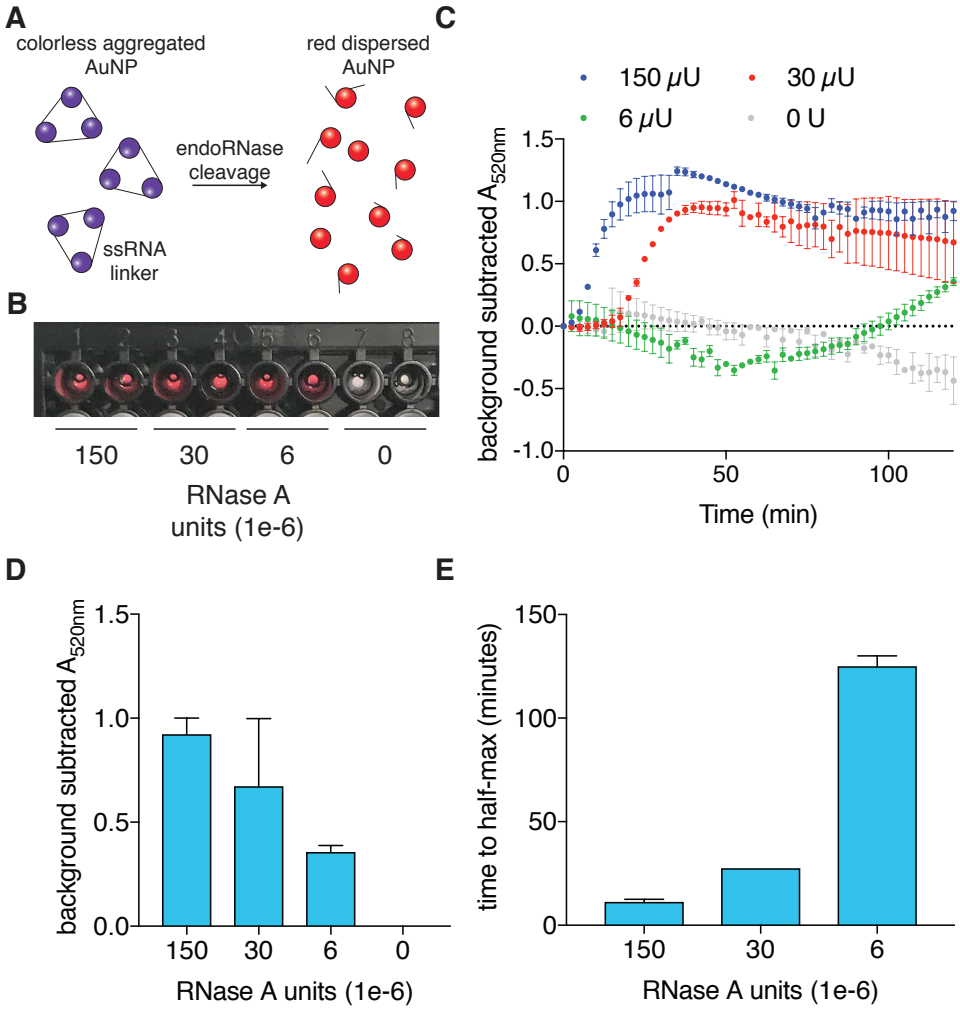

Figure S31: Colorimetric detection of RNase activity with gold nanoparticle aggregation.

A) Schematic of gold-nanoparticle based colorimetric readout for RNase activity. In the absence of RNase activity, RNA linkers aggregate gold nanoparticles, leading to loss of red color. Cleavage of RNA linkers releases nanoparticles and results in a red color change.

B) Image of colorimetric reporters after 120 minutes of RNase digestion at various units of RNase A.

C) Kinetics at 520nm absorbance of AuNP colorimetric reporters with digestion at various unit concentrations of RNase A.

D) The 520nm absorbance of AuNP colorimetric reporters after 120 minutes of digestion at various unit concentrations of RNase A.

E) Time to half-A_{520} maximum of AuNP colorimetric reporters with digestion at various unit concentrations of RNase A.

Figure S32

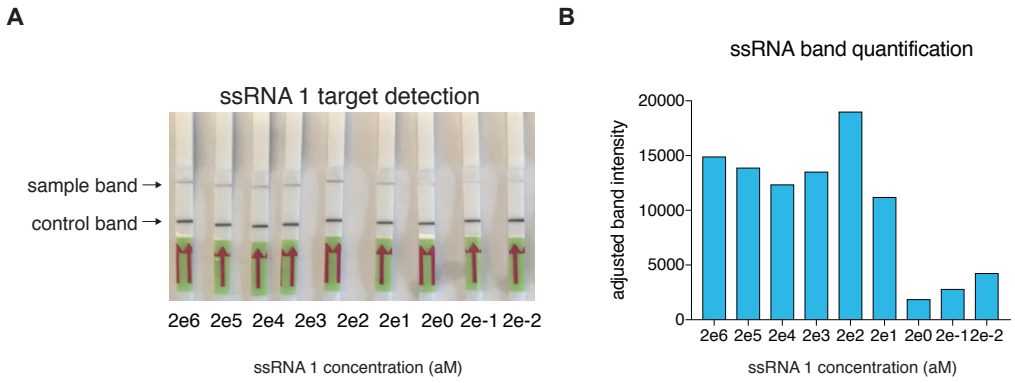

Figure S32: SHERLOCK lateral flow detection of ssRNA 1

A) Detection of ssRNA 1 using lateral flow SHERLOCK at various concentrations.

B) Quantitation of band intensity from detection in (A).

Figure S33

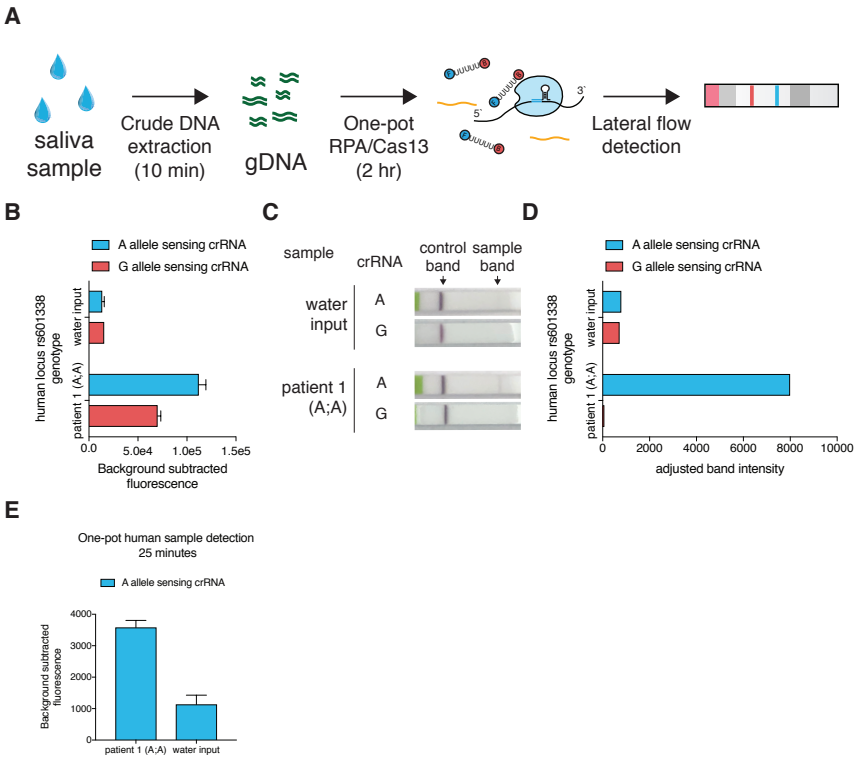

Figure S33: One-pot lateral-flow genotyping of genomic DNA from saliva

A) Schematic for rapid extraction and one-pot detection of genomic DNA from patient saliva.

B) Detection of rs601338 genotypes in from crude genomic DNA extraction compared to water input.

C) Lateral-flow detection of rs601338 genotypes in from crude genomic DNA extraction.

D) Quantitation of band intensity from detection in (C)

E) Detection of patient DNA in 25 minutes from crude saliva.

Figure S34

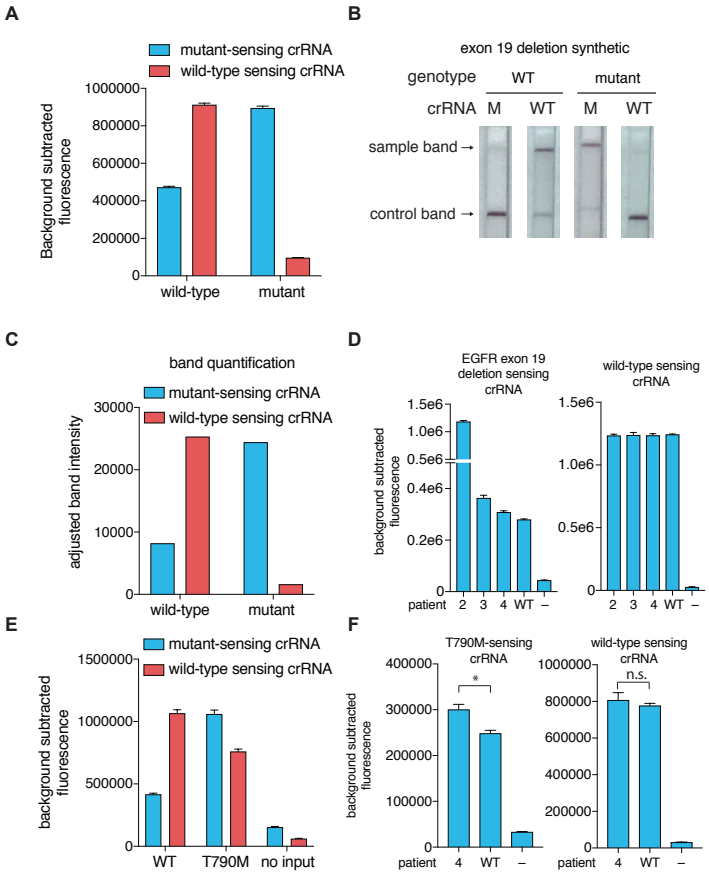

Figure S34: SHERLOCK lateral flow detection of synthetic cfDNA samples

F) Detection of EGFR exon 19 deletion mutation in synthetic DNA samples with either exon 19 deletion or WT genotype using LwaCas13a.

G) Lateral-flow detection of EGFR exon 19 deletion mutation in synthetic DNA samples with either exon 19 deletion or WT genotype using LwaCas13a.

H) Quantitation of band intensity from detection in (B).

I) Detection of EGFR exon 19 deletion mutation in 4 patient cfDNA samples with either exon 19 deletion or WT genotype using LwaCas13a.

J) Detection of EGFR T790M deletion mutation in synthetic DNA samples with either T790M or WT genotype using LwaCas13a.

K) Detection of EGFR T790M deletion mutation in patient cfDNA samples with either T790M or WT genotype using LwaCas13a. (*, $p < 0.05$; n.s., not significant; bars represent mean ± s.e.m.). In this case, patient 4's T790M allelic fraction, as verified

by targeted sequencing, was 0.6%. We were still able to see significant detection of this low allelic fraction due to the sensitivity and specificity of SHERLOCKv2, agreeing with our previous results showing that we could detect greater than 0.1% allelic fraction samples(*3*). Additionally, because the Bsu polymerase in RPA has a minimum error rate of 10^{-5} errors per base incorporated per cycle(*25*), we can expect about 0.02% of amplicons to contain an error at the mutation we are trying to sense. Because spurious signal will only be detected if the correct mutation is formed on a wild-type amplicon, then only 0.0067% of amplicons will have a mutation that causes spurious detection of the mutation. As most patients do not have below 0.01% allelic fraction of cfDNA mutations, this error rate is acceptable.

Figure S35

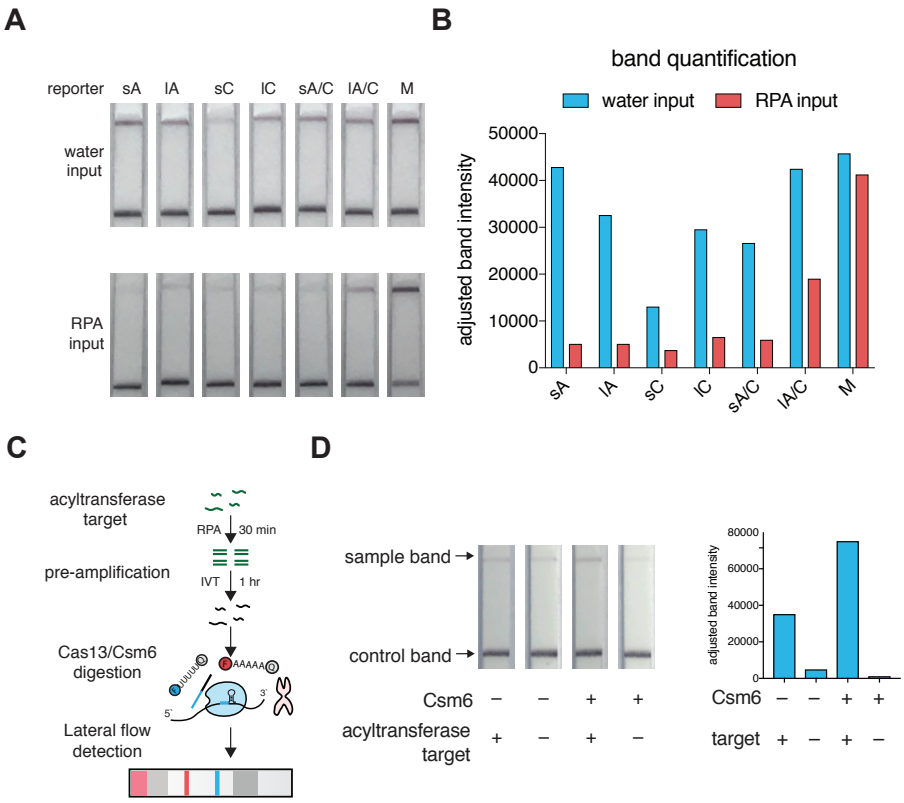

Figure S35: Lateral flow Csm6-enhanced SHERLOCK with different reporter combinations

A) Lateral-flow detection of Csm6-enhanced SHERLOCK with various reporter designs. sA: short poly-A sensor; lA: long poly A sensor; sC: short poly C sensor; lC: long poly C sensor; sA/C: short poly-A/C sensor; lA/C: long poly-A/C sensor; M: mixed RNase alert-like sensor.

B) Quantitation of band intensity from detection in (A)

C) Schematic of lateral flow readout of EiCsm6-enhanced LwaCas13a SHERLOCK detection of acyltransferase ssDNA with separate RPA and IVT steps

D) EiCsm6-enhanced lateral flow SHERLOCK of *P. aeruginosa* acyltransferase gene in combination with LwaCas13a. Band intensity quantitation is shown to the right.

Figure S36

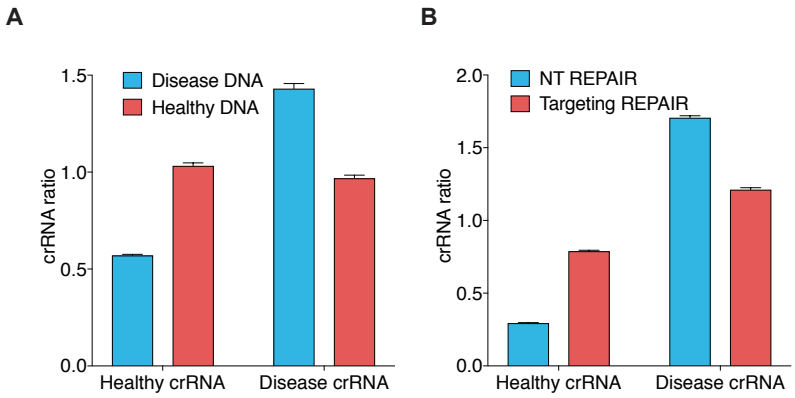

Figure S36: Non-multiplexed theranostic detection of mutations and REPAIR editing

A) Detection of *APC* alleles from healthy- and disease-simulated samples with LwaCas13a.

B) Detection with LwaCas13a of editing correction at the *APC* alleles from REPAIR targeting and non-targeting samples.

Table S1: Cas13 and Csm6 proteins purified in this study

Abbreviation	Protein name	Strain name	Benchling link	Accession number
Lwa	LwaCas13a	Leptotrichia wadei	https://benchling.com/s/seq-66CfLwu7sLMQMbcXe7Ih	WP_021746774.1
Lba	LbaCas13a	Lachnospiraceae bacterium NK4A179	https://benchling.com/s/seq-xdOysFgbmqAsTRoTiERc	WP_022785443.1
Lbu	LbuCas13a	Leptotrichia buccalis C-1013-b	https://benchling.com/s/seq-e0aUn6uEVvWXntoggf60	WP_015770004.1
Bzo	BzoCas13b	Bergeyella zoohelcum	https://benchling.com/s/seq-mA3sJ4GIi4x0JB5q7KHK	WP_002664492
Pin	PinCas13b	Prevotella intermedia	https://benchling.com/s/seq-iA58bdz9mHOZmbFLj92f	WP_036860899
Pbu	PbuCas13b	Prevotella buccae	https://benchling.com/s/seq-nNv4KSgZDFtdPX88zSS2	WP_004343973
Asp	AspCas13b	Alistipes sp. ZOR0009	https://benchling.com/s/seq-lHs6D7J5Z2NkCbbkggek	WP_047447901
Psm	PsmCas13b	Prevotella sp. MA2016	https://benchling.com/s/seq-v7Q1TzaZzAyNZIGKNnH3	WP_036929175
Ran	RanCas13b	Riemerella anatipestifer	https://benchling.com/s/seq-HIhclUZszBOQAdW5rlmW	WP_004919755
Pau	PauCas13b	Prevotella aurantiaca	https://benchling.com/s/seq-Se9MuspJQek3x4vvR1BF	WP_025000926
Psa	PsaCas13b	Prevotella saccharolytica	https://benchling.com/s/seq-NXtrOPLbhpyc9nZk1seg	WP_051522484
Pin2	Pin2Cas13b	Prevotella intermedia	https://benchling.com/s/seq-mSXhS57arjPDuvnQjZOn	WP_061868553
Cca	CcaCas13b	Capnocytophaga canimorsus	https://benchling.com/s/seq-BNVzFUQjqSnkYLARxLwE	WP_013997271
Pgu	PguCas13b	Porphyromonas gulae	https://benchling.com/s/seq-GVOv8zBVIta2utHyuTSR	WP_039434803
Psp	PspCas13b	Prevotella sp. P5-125	https://benchling.com/s/seq-XmnWQgXrpvVAwXoNtJGw	WP_044065294
Pig	PigCas13b	Porphyromonas gingivalis	https://benchling.com/s/seq-hxdDNJtJmA5axRvcxm0p	WP_053444417
Pin3	Pin3Cas13b	Prevotella intermedia	https://benchling.com/s/seq-GlaCfl5cDw4sKXz6LM11	WP_050955369
Ei	EiCsm6	Enterococcus italicus	https://benchling.com/s/seq-YrP8xiVG3rBwxYMgCUH0	WP_007208953.1
Ls	LsCsm6	Lactobacillus salivarius	https://benchling.com/s/seq-duuAaForfhsBc53zLY5z	WP_081509150.1
Tt	TtCsm6	Thermus thermophilus	https://benchling.com/s/seq-esibVH1rmHPjHYXxKWja	WP_011229148.1

Table S2: crRNA used in this study

Name	Ortholog	Complete crRNA sequence	Spacer	Direct repeat	Target	1st Fig.
ssRNA/ssDNA 1 crRNA 2	LwaCas13a	GATTTAGACTACCCCAAAA ACGAAGGGGACTAAAACCT ACCAAGTAATCCATATTTC TAGAGGATC	CTACCAAG TAATCCAT ATTTCTAG AGGATC	GATTTAGACTAC CCCAAAAACGAA GGGGACTAAAAC	ssRNA 1	Fig. 1B/fig. S3
BzoCas13b ssRNA/ssDNA crRNA 2	BzoCas13b	CTACCAAGTAATCCATATT TCTAGAGGATCGTTGGAAC TGCTCTCATTTTGGAGGGT AATCACAAC	CTACCAAG TAATCCAT ATTTCTAG AGGATC	GTTGGAACTGCT CTCATTTTGGAG GGTAATCACAAC	ssRNA 1	Fig. 1B/fig. S3
PinCas13b ssRNA/ssDNA crRNA 2	PinCas13b	CTACCAAGTAATCCATATT TCTAGAGGATCGTTGCATC TGCCTGCTGTTTGCAAGGT AAAAACAAC	CTACCAAG TAATCCAT ATTTCTAG AGGATC	GTTGCATCTGCC TGCTGTTTGCAA GGTAAAAACAAC	ssRNA 1	Fig. 1B/fig. S3
PbuCas13b ssRNA/ssDNA crRNA 2	PbuCas13b	CTACCAAGTAATCCATATT TCTAGAGGATCGTTGCATC TGCCTTCTTTTTGAAAGGT AAAAACAAC	CTACCAAG TAATCCAT ATTTCTAG AGGATC	GTTGCATCTGCC TTCTTTTTGAAA GGTAAAAACAAC	ssRNA 1	Fig. 1B/fig. S3
AspCas13b ssRNA/ssDNA crRNA 2	AspCas13b	CTACCAAGTAATCCATATT TCTAGAGGATCGCTGTTAT ATCCTTACCTTTGTAAGGG AAGTACAGC	CTACCAAG TAATCCAT ATTTCTAG AGGATC	GCTGTTATATCC TTACCTTTGTAA GGGAAGTACAGC	ssRNA 1	Fig. 1B/fig. S3
PsmCas13b ssRNA/ssDNA crRNA 2	PsmCas13b	CTACCAAGTAATCCATATT TCTAGAGGATCGTTGTAGA AGCTTATCGTTTGGATAGG TATGACAAC	CTACCAAG TAATCCAT ATTTCTAG AGGATC	GTTGTAGAAGCT TATCGTTTGGAT AGGTATGACAAC	ssRNA 1	Fig. 1B/fig. S3
RanCas13b ssRNA/ssDNA crRNA 2	RanCas13b	CTACCAAGTAATCCATATT TCTAGAGGATCGTTGGGAC TGCTCTCACTTTGAAGGGT ATTCACAAC	CTACCAAG TAATCCAT ATTTCTAG AGGATC	GTTGGGACTGCT CTCACTTTGAAG GGTATTCACAAC	ssRNA 1	Fig. 1B/fig. S3
PauCas13b ssRNA/ssDNA crRNA 2	PauCas13b	CTACCAAGTAATCCATATT TCTAGAGGATCGTTGTATC TGCCTTCTGTTTGAAAGGT AAAAACAAC	CTACCAAG TAATCCAT ATTTCTAG AGGATC	GTTGTATCTGCC TTCTGTTTGAAA GGTAAAAACAAC	ssRNA 1	Fig. 1B/fig. S3
PsaCas13b ssRNA/ssDNA crRNA 2	PsaCas13b	CTACCAAGTAATCCATATT TCTAGAGGATCGTTGTGTC TACCTCCTTTTTGAGAGGT AAAAACAGC	CTACCAAG TAATCCAT ATTTCTAG AGGATC	GTTGTGTCTACC TCCTTTTTGAGA GGTAAAAACAGC	ssRNA 1	Fig. 1B/fig. S3
Pin2Cas13b ssRNA/ssDNA crRNA 2	Pin2Cas13b	CTACCAAGTAATCCATATT TCTAGAGGATCGTTGCATC TGCCTGCTGTTTGCAAGGT AAAAACAAC	CTACCAAG TAATCCAT ATTTCTAG AGGATC	GTTGCATCTGCC TGCTGTTTGCAA GGTAAAAACAAC	ssRNA 1	Fig. 1B/fig. S3
CcaCas13b ssRNA/ssDNA crRNA 2	CcaCas13b	CTACCAAGTAATCCATATT TCTAGAGGATCGTTGGAAC TGCTCTCATTTTGGAGGGT AATCACAAC	CTACCAAG TAATCCAT ATTTCTAG AGGATC	GTTGGAACTGCT CTCATTTTGGAG GGTAATCACAAC	ssRNA 1	Fig. 1B/fig. S3
PguCas13b ssRNA/ssDNA crRNA 2	PguCas13b	CTACCAAGTAATCCATATT TCTAGAGGATCGTTGGATC TACCCTCTATTTGAAGGGT ACACACAAC	CTACCAAG TAATCCAT ATTTCTAG AGGATC	GTTGGATCTACC CTCTATTTGAAG GGTACACACAAC	ssRNA 1	Fig. 1B/fig. S3
PspCas13b ssRNA/ssDNA crRNA 2	PspCas13b	CTACCAAGTAATCCATATT TCTAGAGGATCGTTGTGGA AGGTCCAGTTTTGAGGGGC TATTACAAC	CTACCAAG TAATCCAT ATTTCTAG AGGATC	GTTGTGGAAGGT CCAGTTTTGAGG GGCTATTACAAC	ssRNA 1	Fig. 1B/fig. S3
PigCas13b ssRNA/ssDNA crRNA 2	PigCas13b	CTACCAAGTAATCCATATT TCTAGAGGATCGTTGGATC TACCCTCTATTCGAAGGGT ACACACAAC	CTACCAAG TAATCCAT ATTTCTAG AGGATC	GTTGGATCTACC CTCTATTCGAAG GGTACACACAAC	ssRNA 1	Fig. 1B/fig. S3
Pin3Cas13b ssRNA/ssDNA crRNA 2	Pin3Cas13b	CTACCAAGTAATCCATATT TCTAGAGGATCGTTGCATC TGCCTGCTGTTTGCAAGGT AAAAACAAC	CTACCAAG TAATCCAT ATTTCTAG AGGATC	GTTGCATCTGCC TGCTGTTTGCAA GGTAAAAACAAC	ssRNA 1	Fig. 1B/fig. S3
DENV crRNA LwaCas13a	LwaCas13a	GATTTAGACTACCCCAAAA ACGAAGGGGACTAAAACTG CTTCTGTCCAGTGAGCATG GTCTTCG	TGCTTCTG TCCAGTGA GCATGGTC TTCG	GATTTAGACTAC CCCAAAAACGAA GGGGACTAAAAC	DENV ssRNA	Fig. 1D
DENV crRNA PsmCas13b	PsmCas13b	TTTGCTTCTGTCCAGTGAG CATGGTCTTCGGTTGTAGA AGCTTATCGTTTGGATAGG TATGACAAC	TTTGCTTC TGTCCAGT GAGCATGG TCTTCG	GTTGTAGAAGCT TATCGTTTGGAT AGGTATGACAAC	DENV ssRNA	Fig. 1D

ssDNA 1 crRNA Cas12a	AsCas12a	TAATTTCTACTCTTGTAGA TCTGTGTTTATCCGCTCAC AA	CTGTGTTT ATCCGCTC ACAA	TAATTTCTACTC TTGTAGAT	ssDNA 1	Fig. 1D
Thermonuclease crRNA PsmCas13b	PsmCas13b	ATGCTTTGTTTCAGGTGTA TCAACCAATAAGTTGTAGA AGCTTATCGTTTGGATAGG TATGACAAC	ATGCTTTG TTTCAGGT GTATCAAC CAATAA	GTTGTAGAAGCT TATCGTTTGGAT AGGTATGACAAC	Thermon uclease ssDNA	Fig. 1H
Acyltransferase LwaCas13a crRNA	LwaCas13a	GATTTAGACTACCCCAAAA ACGAAGGGGACTAAAACAG CACGCTCACCCGCGGGTTG CCTTCGG	AGCACGCT CACCCGCG GGTTGCCT TCGG	GATTTAGACTAC CCCAAAAACGAA GGGGACTAAAAC	Acyltrans ferase ssDNA	Fig. 1H
ZIKV LwaCas13a crRNA	LwaCas13a	GATTTAGACTACCCCAAAA ACGAAGGGGACTAAAACAC TCCCTAGAACCACGACAGT TTGCCTT	ACTCCCTA GAACCACG ACAGTTTG CCTT	GATTTAGACTAC CCCAAAAACGAA GGGGACTAAAAC	ZIKV ssRNA	Fig. 3B
EGFR L858R wild-type sensing crRNA	LwaCas13a	GATTTAGACTACCCCAAAA ACGAAGGGGACTAAAACCC AGGCCAAAATCTGTGATCT TGACATG	CCAGGCCA AAATCTGT GATCTTGA CATG	GATTTAGACTAC CCCAAAAACGAA GGGGACTAAAAC	EGFR L858L WT	Fig. 3E
EGFR L858R mutant sensing crRNA	LwaCas13a	GATTTAGACTACCCCAAAA ACGAAGGGGACTAAAACCC CGGCCAAAATCTGTGATCT TGACATG	CCCGGCCA AAATCTGT GATCTTGA CATG	GATTTAGACTAC CCCAAAAACGAA GGGGACTAAAAC	EGFR L858R mutation	Fig. 3E
Exon 19 deletion mutant sensing crRNA	LwaCas13a	GATTTAGACTACCCCAAAA ACGAAGGGGACTAAAACGT TGGCTTTCGGAGATGTCTT GATAGCG	GTTGGCTT TCGGAGAT GTCTTGAT AGCG	GATTTAGACTAC CCCAAAAACGAA GGGGACTAAAAC	EGFR Exon 19 deletion	Fig. 3H
Exon 19 deletion wild-type sensing crRNA	LwaCas13a	GATTTAGACTACCCCAAAA ACGAAGGGGACTAAAACGA TGTTGCTTCTCTTAATTCC TTGATAG	GATGTTGC TTCTCTTA ATTCCTTG ATAG	GATTTAGACTAC CCCAAAAACGAA GGGGACTAAAAC	EGFR Exon 19 WT	Fig. 3H
A-allele (disease) sensing crRNA APC gene (NM_000038.5) crRNA	LwaCas13a	GATTTAGACTACCCCAAAA ACGAAGGGGACTAAAACCC TATCAGGTTTCACAGTAAG CGCGTAT	CCTATCAG GTTTCACA GTAAGCGC GTAT	GATTTAGACTAC CCCAAAAACGAA GGGGACTAAAAC	APC synthetic mutation	Fig. 5D
G-allele (healthy) sensing crRNA APC gene (NM_000038.5) crRNA	PsmCas13b	CCTGGTTCATGAGCTTCCT GCCACTGCCAAGTTGTAGA AGCTTATCGTTTGGATAGG TATGACAAC	CCTGGTTC ATGAGCTT CCTGCCAC TGCCAA	GTTGTAGAAGCT TATCGTTTGGAT AGGTATGACAAC	APC synthetic WT	Fig. 5D
DENV crRNA LbaCas13a	LbaCas13a	GTTGATGAGAAGAGCCCAA GATAGAGGGCAATAACTGC TTCTGTCCAGTGAGCATGG TCTTCG	TGCTTCTG TCCAGTGA GCATGGTC TTCG	GTTGATGAGAAG AGCCCAAGATAG AGGGCAATAAC	DENV ssRNA	fig. S6A
ZIKV crRNA PsmCas13b	PsmCas13b	TGACTCCCTAGAACCACGA CAGTTTGCCTTGTTGTAGA AGCTTATCGTTTGGATAGG TATGACAAC	TGACTCCC TAGAACCA CGACAGTT TGCCTT	GTTGTAGAAGCT TATCGTTTGGAT AGGTATGACAAC	ZIKV ssRNA	fig. S6B
ZIKV crRNA LbaCas13a	LbaCas13a	GTTGATGAGAAGAGCCCAA GATAGAGGGCAATAACACT CCCTAGAACCACGACAGTT TGCCTT	ACTCCCTA GAACCACG ACAGTTTG CCTT	GTTGATGAGAAG AGCCCAAGATAG AGGGCAATAAC	ZIKV ssRNA	fig. S6B
DENV LbuCas13a 28nt spacer	LbuCas13a	GACCACCCCAAAAATGAAG GGGACTAAAACATGCTTCT GTCCAGTGAGCATGGTCTT CG	TGCTTCTG TCCAGTGA GCATGGTC TTCG	GACCACCCCAAA AATGAAGGGGAC TAAAACA	DENV ssRNA	fig. S7A
ZIKV LbuCas13a	LbuCas13a	GACCACCCCAAAAATGAAG GGGACTAAAACAACTCCCT AGAACCACGACAGTTTGCC TT	ACTCCCTA GAACCACG ACAGTTTG CCTT	GACCACCCCAAA AATGAAGGGGAC TAAAACA	ZIKV ssRNA	fig. S7A
DENV LbuCas13a 26nt spacer	LbuCas13a	GACCACCCCAAAAATGAAG GGGACTAAAACATGCTTCT GTCCAGTGAGCATGGTCTT	TGCTTCTG TCCAGTGA GCATGGTC TT	GACCACCCCAAA AATGAAGGGGAC TAAAACA	DENV ssRNA	fig. S7C
DENV LbuCas13a 24nt spacer	LbuCas13a	GACCACCCCAAAAATGAAG GGGACTAAAACATGCTTCT GTCCAGTGAGCATGGTC	TGCTTCTG TCCAGTGA GCATGGTC	GACCACCCCAAA AATGAAGGGGAC TAAAACA	DENV ssRNA	fig. S7C

DENV LbuCas13a 22nt spacer	LbuCas13a	GACCACCCCAAAAATGAAG GGGACTAAAACATGCTTCT GTCCAGTGAGCATGG	TGCTTCTG TCCAGTGA GCATGG	GACCACCCCAAA AATGAAGGGGAC TAAAACA	DENV ssRNA	fig. S7C
DENV LbuCas13a 20nt spacer	LbuCas13a	GACCACCCCAAAAATGAAG GGGACTAAAACATGCTTCT GTCCAGTGAGCAT	TGCTTCTG TCCAGTGA GCAT	GACCACCCCAAA AATGAAGGGGAC TAAAACA	DENV ssRNA	fig. S7C
DENV LbuCas13a 18nt spacer	LbuCas13a	GACCACCCCAAAAATGAAG GGGACTAAAACATGCTTCT GTCCAGTGAGC	TGCTTCTG TCCAGTGA GC	GACCACCCCAAA AATGAAGGGGAC TAAAACA	DENV ssRNA	fig. S7C
CcaCas13b spacer test 34 nt	CcaCas13b	TGTTCTACCAAGTAATCCA TATTTCTAGAGGATCGTTG GAACTGCTCTCATTTTGGA GGGTAATCACAAC	TGTTCTAC CAAGTAAT CCATATTT CTAGAGGA TC	GTTGGAACTGCT CTCATTTTGGAG GGTAATCACAAC	ssRNA 1	fig. S10A
CcaCas13b spacer test 33 nt	CcaCas13b	GTTCTACCAAGTAATCCAT ATTTCTAGAGGATCGTTGG AACTGCTCTCATTTTGGAG GGTAATCACAAC	GTTCTACC AAGTAATC CATATTTC TAGAGGAT C	GTTGGAACTGCT CTCATTTTGGAG GGTAATCACAAC	ssRNA 1	fig. S10A
CcaCas13b spacer test 32 nt	CcaCas13b	TTCTACCAAGTAATCCATA TTTCTAGAGGATCGTTGGA ACTGCTCTCATTTTGGAGG GTAATCACAAC	TTCTACCA AGTAATCC ATATTTCT AGAGGATC	GTTGGAACTGCT CTCATTTTGGAG GGTAATCACAAC	ssRNA 1	fig. S10A
CcaCas13b spacer test 31 nt	CcaCas13b	TCTACCAAGTAATCCATAT TTCTAGAGGATCGTTGGAA CTGCTCTCATTTTGGAGGG TAATCACAAC	TCTACCAA GTAATCCA TATTTCTA GAGGATC	GTTGGAACTGCT CTCATTTTGGAG GGTAATCACAAC	ssRNA 1	fig. S10A
CcaCas13b spacer test 30 nt	CcaCas13b	CTACCAAGTAATCCATATT TCTAGAGGATCGTTGGAAC TGCTCTCATTTTGGAGGGT AATCACAAC	CTACCAAG TAATCCAT ATTTCTAG AGGATC	GTTGGAACTGCT CTCATTTTGGAG GGTAATCACAAC	ssRNA 1	fig. S10A
CcaCas13b spacer test 29 nt	CcaCas13b	TACCAAGTAATCCATATTT CTAGAGGATCGTTGGAACT GCTCTCATTTTGGAGGGTA ATCACAAC	TACCAAGT AATCCATA TTTCTAGA GGATC	GTTGGAACTGCT CTCATTTTGGAG GGTAATCACAAC	ssRNA 1	fig. S10A
CcaCas13b spacer test 28 nt	CcaCas13b	ACCAAGTAATCCATATTTC TAGAGGATCGTTGGAACTG CTCTCATTTTGGAGGGTAA TCACAAC	ACCAAGTA ATCCATAT TTCTAGAG GATC	GTTGGAACTGCT CTCATTTTGGAG GGTAATCACAAC	ssRNA 1	fig. S10A
CcaCas13b spacer test 27 nt	CcaCas13b	CCAAGTAATCCATATTTCT AGAGGATCGTTGGAACTGC TCTCATTTTGGAGGGTAAT CACAAC	CCAAGTAA TCCATATT TCTAGAGG ATC	GTTGGAACTGCT CTCATTTTGGAG GGTAATCACAAC	ssRNA 1	fig. S10A
CcaCas13b spacer test 26 nt	CcaCas13b	CAAGTAATCCATATTTCTA GAGGATCGTTGGAACTGCT CTCATTTTGGAGGGTAATC ACAAC	CAAGTAAT CCATATTT CTAGAGGA TC	GTTGGAACTGCT CTCATTTTGGAG GGTAATCACAAC	ssRNA 1	fig. S10A
CcaCas13b spacer test 25 nt	CcaCas13b	AAGTAATCCATATTTCTAG AGGATCGTTGGAACTGCTC TCATTTTGGAGGGTAATCA CAAC	AAGTAATC CATATTTC TAGAGGAT C	GTTGGAACTGCT CTCATTTTGGAG GGTAATCACAAC	ssRNA 1	fig. S10A
CcaCas13b spacer test 24 nt	CcaCas13b	AGTAATCCATATTTCTAGA GGATCGTTGGAACTGCTCT CATTTTGGAGGGTAATCAC AAC	AGTAATCC ATATTTCT AGAGGATC	GTTGGAACTGCT CTCATTTTGGAG GGTAATCACAAC	ssRNA 1	fig. S10A
CcaCas13b spacer test 23 nt	CcaCas13b	GTAATCCATATTTCTAGAG GATCGTTGGAACTGCTCTC ATTTTGGAGGGTAATCACA AC	GTAATCCA TATTTCTA GAGGATC	GTTGGAACTGCT CTCATTTTGGAG GGTAATCACAAC	ssRNA 1	fig. S10A
CcaCas13b spacer test 22 nt	CcaCas13b	TAATCCATATTTCTAGAGG ATCGTTGGAACTGCTCTCA TTTTGGAGGGTAATCACAA C	TAATCCAT ATTTCTAG AGGATC	GTTGGAACTGCT CTCATTTTGGAG GGTAATCACAAC	ssRNA 1	fig. S10A
CcaCas13b spacer test 21 nt	CcaCas13b	AATCCATATTTCTAGAGGA TCGTTGGAACTGCTCTCAT TTTGGAGGGTAATCACAAC	AATCCATA TTTCTAGA GGATC	GTTGGAACTGCT CTCATTTTGGAG GGTAATCACAAC	ssRNA 1	fig. S10A
CcaCas13b spacer test 20 nt	CcaCas13b	ATCCATATTTCTAGAGGAT CGTTGGAACTGCTCTCATT TTGGAGGGTAATCACAAC	ATCCATAT TTCTAGAG GATC	GTTGGAACTGCT CTCATTTTGGAG GGTAATCACAAC	ssRNA 1	fig. S10A
CcaCas13b spacer test 19 nt	CcaCas13b	TCCATATTTCTAGAGGATC GTTGGAACTGCTCTCATTT TGGAGGGTAATCACAAC	TCCATATT TCTAGAGG ATC	GTTGGAACTGCT CTCATTTTGGAG GGTAATCACAAC	ssRNA 1	fig. S10A
CcaCas13b spacer test 18 nt	CcaCas13b	CCATATTTCTAGAGGATCG TTGGAACTGCTCTCATTTT GGAGGGTAATCACAAC	CCATATTT CTAGAGGA TC	GTTGGAACTGCT CTCATTTTGGAG GGTAATCACAAC	ssRNA 1	fig. S10A
CcaCas13b spacer test 17 nt	CcaCas13b	CATATTTCTAGAGGATCGT TGGAACTGCTCTCATTTTG GAGGGTAATCACAAC	CATATTTC TAGAGGAT C	GTTGGAACTGCT CTCATTTTGGAG GGTAATCACAAC	ssRNA 1	fig. S10A

CcaCas13b spacer test 16 nt	CcaCas13b	ATATTTCTAGAGGATCGTT GGAACTGCTCTCATTTTGG AGGGTAATCACAAC	ATATTTCT AGAGGATC	GTTGGAACTGCT CTCATTTTGGAG GGTAATCACAAC	ssRNA 1	fig. S10A
CcaCas13b spacer test 15 nt	CcaCas13b	TATTTCTAGAGGATCGTTG GAACTGCTCTCATTTTGGA GGGTAATCACAAC	TATTTCTA GAGGATC	GTTGGAACTGCT CTCATTTTGGAG GGTAATCACAAC	ssRNA 1	fig. S10A
CcaCas13b spacer test 14 nt	CcaCas13b	ATTTCTAGAGGATCGTTGG AACTGCTCTCATTTTGGAG GGTAATCACAAC	ATTTCTAG AGGATC	GTTGGAACTGCT CTCATTTTGGAG GGTAATCACAAC	ssRNA 1	fig. S10A
CcaCas13b spacer test 13 nt	CcaCas13b	TTTCTAGAGGATCGTTGGA ACTGCTCTCATTTTGGAGG GTAATCACAAC	TTTCTAGA GGATC	GTTGGAACTGCT CTCATTTTGGAG GGTAATCACAAC	ssRNA 1	fig. S10A
CcaCas13b spacer test 12 nt	CcaCas13b	TTCTAGAGGATCGTTGGAA CTGCTCTCATTTTGGAGGG TAATCACAAC	TTCTAGAG GATC	GTTGGAACTGCT CTCATTTTGGAG GGTAATCACAAC	ssRNA 1	fig. S10A
PsmCas13b spacer test 34 nt	PsmCas13b	TGTTCTACCAAGTAATCCA TATTTCTAGAGGATCGTTG TAGAAGCTTATCGTTTGGA TAGGTATGACAAC	TGTTCTAC CAAGTAAT CCATATTT CTAGAGGA TC	GTTGTAGAAGCT TATCGTTTGGAT AGGTATGACAAC	ssRNA 1	fig. S10B
PsmCas13b spacer test 33 nt	PsmCas13b	GTTCTACCAAGTAATCCAT ATTTCTAGAGGATCGTTGT AGAAGCTTATCGTTTGGAT AGGTATGACAAC	GTTCTACC AAGTAATC CATATTTC TAGAGGAT C	GTTGTAGAAGCT TATCGTTTGGAT AGGTATGACAAC	ssRNA 1	fig. S10B
PsmCas13b spacer test 32 nt	PsmCas13b	TTCTACCAAGTAATCCATA TTTCTAGAGGATCGTTGTA GAAGCTTATCGTTTGGATA GGTATGACAAC	TTCTACCA AGTAATCC ATATTTCT AGAGGATC	GTTGTAGAAGCT TATCGTTTGGAT AGGTATGACAAC	ssRNA 1	fig. S10B
PsmCas13b spacer test 31 nt	PsmCas13b	TCTACCAAGTAATCCATAT TTCTAGAGGATCGTTGTAG AAGCTTATCGTTTGGATAG GTATGACAAC	TCTACCAA GTAATCCA TATTTCTA GAGGATC	GTTGTAGAAGCT TATCGTTTGGAT AGGTATGACAAC	ssRNA 1	fig. S10B
PsmCas13b spacer test 30 nt	PsmCas13b	CTACCAAGTAATCCATATT TCTAGAGGATCGTTGTAGA AGCTTATCGTTTGGATAGG TATGACAAC	CTACCAAG TAATCCAT ATTTCTAG AGGATC	GTTGTAGAAGCT TATCGTTTGGAT AGGTATGACAAC	ssRNA 1	fig. S10B
PsmCas13b spacer test 29 nt	PsmCas13b	TACCAAGTAATCCATATTT CTAGAGGATCGTTGTAGAA GCTTATCGTTTGGATAGGT ATGACAAC	TACCAAGT AATCCATA TTTCTAGA GGATC	GTTGTAGAAGCT TATCGTTTGGAT AGGTATGACAAC	ssRNA 1	fig. S10B
PsmCas13b spacer test 28 nt	PsmCas13b	ACCAAGTAATCCATATTTC TAGAGGATCGTTGTAGAAG CTTATCGTTTGGATAGGTA TGACAAC	ACCAAGTA ATCCATAT TTCTAGAG GATC	GTTGTAGAAGCT TATCGTTTGGAT AGGTATGACAAC	ssRNA 1	fig. S10B
PsmCas13b spacer test 27 nt	PsmCas13b	CCAAGTAATCCATATTTCT AGAGGATCGTTGTAGAAGC TTATCGTTTGGATAGGTAT GACAAC	CCAAGTAA TCCATATT TCTAGAGG ATC	GTTGTAGAAGCT TATCGTTTGGAT AGGTATGACAAC	ssRNA 1	fig. S10B
PsmCas13b spacer test 26 nt	PsmCas13b	CAAGTAATCCATATTTCTA GAGGATCGTTGTAGAAGCT TATCGTTTGGATAGGTATG ACAAC	CAAGTAAT CCATATTT CTAGAGGA TC	GTTGTAGAAGCT TATCGTTTGGAT AGGTATGACAAC	ssRNA 1	fig. S10B
PsmCas13b spacer test 25 nt	PsmCas13b	AAGTAATCCATATTTCTAG AGGATCGTTGTAGAAGCTT ATCGTTTGGATAGGTATGA CAAC	AAGTAATC CATATTTC TAGAGGAT C	GTTGTAGAAGCT TATCGTTTGGAT AGGTATGACAAC	ssRNA 1	fig. S10B
PsmCas13b spacer test 24 nt	PsmCas13b	AGTAATCCATATTTCTAGA GGATCGTTGTAGAAGCTTA TCGTTTGGATAGGTATGAC AAC	AGTAATCC ATATTTCT AGAGGATC	GTTGTAGAAGCT TATCGTTTGGAT AGGTATGACAAC	ssRNA 1	fig. S10B
PsmCas13b spacer test 23 nt	PsmCas13b	GTAATCCATATTTCTAGAG GATCGTTGTAGAAGCTTAT CGTTTGGATAGGTATGACA AC	GTAATCCA TATTTCTA GAGGATC	GTTGTAGAAGCT TATCGTTTGGAT AGGTATGACAAC	ssRNA 1	fig. S10B
PsmCas13b spacer test 22 nt	PsmCas13b	TAATCCATATTTCTAGAGG ATCGTTGTAGAAGCTTATC GTTTGGATAGGTATGACAA C	TAATCCAT ATTTCTAG AGGATC	GTTGTAGAAGCT TATCGTTTGGAT AGGTATGACAAC	ssRNA 1	fig. S10B
PsmCas13b spacer test 21 nt	PsmCas13b	AATCCATATTTCTAGAGGA TCGTTGTAGAAGCTTATCG TTTGGATAGGTATGACAAC	AATCCATA TTTCTAGA GGATC	GTTGTAGAAGCT TATCGTTTGGAT AGGTATGACAAC	ssRNA 1	fig. S10B
PsmCas13b spacer test 20 nt	PsmCas13b	ATCCATATTTCTAGAGGAT CGTTGTAGAAGCTTATCGT TTGGATAGGTATGACAAC	ATCCATAT TTCTAGAG GATC	GTTGTAGAAGCT TATCGTTTGGAT AGGTATGACAAC	ssRNA 1	fig. S10B
PsmCas13b spacer test 19 nt	PsmCas13b	TCCATATTTCTAGAGGATC GTTGTAGAAGCTTATCGTT TGGATAGGTATGACAAC	TCCATATT TCTAGAGG ATC	GTTGTAGAAGCT TATCGTTTGGAT AGGTATGACAAC	ssRNA 1	fig. S10B
PsmCas13b spacer test 18 nt	PsmCas13b	CCATATTTCTAGAGGATCG TTGTAGAAGCTTATCGTTT GGATAGGTATGACAAC	CCATATTT CTAGAGGA TC	GTTGTAGAAGCT TATCGTTTGGAT AGGTATGACAAC	ssRNA 1	fig. S10B
PsmCas13b spacer test 17 nt	PsmCas13b	CATATTTCTAGAGGATCGT TGTAGAAGCTTATCGTTTG GATAGGTATGACAAC	CATATTTC TAGAGGAT C	GTTGTAGAAGCT TATCGTTTGGAT AGGTATGACAAC	ssRNA 1	fig. S10B

PsmCas13b spacer test 16 nt	PsmCas13b	ATATTTCTAGAGGATCGTT GTAGAAGCTTATCGTTTGG ATAGGTATGACAAC	ATATTTCT AGAGGATC	GTTGTAGAAGCT TATCGTTTGGAT AGGTATGACAAC	ssRNA 1	fig. S10B
PsmCas13b spacer test 15 nt	PsmCas13b	TATTTCTAGAGGATCGTTG TAGAAGCTTATCGTTTGGA TAGGTATGACAAC	TATTTCTA GAGGATC	GTTGTAGAAGCT TATCGTTTGGAT AGGTATGACAAC	ssRNA 1	fig. S10B
PsmCas13b spacer test 14 nt	PsmCas13b	ATTTCTAGAGGATCGTTGT AGAAGCTTATCGTTTGGAT AGGTATGACAAC	ATTTCTAG AGGATC	GTTGTAGAAGCT TATCGTTTGGAT AGGTATGACAAC	ssRNA 1	fig. S10B
PsmCas13b spacer test 13 nt	PsmCas13b	TTTCTAGAGGATCGTTGTA GAAGCTTATCGTTTGGATA GGTATGACAAC	TTTCTAGA GGATC	GTTGTAGAAGCT TATCGTTTGGAT AGGTATGACAAC	ssRNA 1	fig. S10B
PsmCas13b spacer test 12 nt	PsmCas13b	TTCTAGAGGATCGTTGTAG AAGCTTATCGTTTGGATAG GTATGACAAC	TTCTAGAG GATC	GTTGTAGAAGCT TATCGTTTGGAT AGGTATGACAAC	ssRNA 1	fig. S10B
LwaCas13a tiling crRNA 1	LwaCas13a	GATTTAGACTACCCCAAAA ACGAAGGGGACTAAAACCC GGGTACCGAGCTCGAATTC ACTGGCC	CCGGGTAC CGAGCTCG AATTCACT GGCC	GATTTAGACTAC CCCAAAAACGAA GGGGACTAAAAC	ssRNA 1	fig. S11
LwaCas13a tiling crRNA 2	LwaCas13a	GATTTAGACTACCCCAAAA ACGAAGGGGACTAAAACTT TCTAGAGGATCCCCGGGTA CCGAGCT	TTTCTAGA GGATCCCC GGGTACCG AGCT	GATTTAGACTAC CCCAAAAACGAA GGGGACTAAAAC	ssRNA 1	fig. S11
LwaCas13a tiling crRNA 3	LwaCas13a	GATTTAGACTACCCCAAAA ACGAAGGGGACTAAAACCC AAGTAATCCATATTTCTAG AGGATCC	CCAAGTAA TCCATATT TCTAGAGG ATCC	GATTTAGACTAC CCCAAAAACGAA GGGGACTAAAAC	ssRNA 1	fig. S11
LwaCas13a tiling crRNA 4	LwaCas13a	GATTTAGACTACCCCAAAA ACGAAGGGGACTAAAACAG ATTGCTGTTCTACCAAGTA ATCCATA	AGATTGCT GTTCTACC AAGTAATC CATA	GATTTAGACTAC CCCAAAAACGAA GGGGACTAAAAC	ssRNA 1	fig. S11
LwaCas13a tiling crRNA 5	LwaCas13a	GATTTAGACTACCCCAAAA ACGAAGGGGACTAAAACCC TGCAGGTCGAGTAGATTGC TGTTCTA	CCTGCAGG TCGAGTAG ATTGCTGT TCTA	GATTTAGACTAC CCCAAAAACGAA GGGGACTAAAAC	ssRNA 1	fig. S11
LwaCas13a tiling crRNA 6	LwaCas13a	GATTTAGACTACCCCAAAA ACGAAGGGGACTAAAACGC CAAGCTTGCATGCCTGCAG GTCGAGT	GCCAAGCT TGCATGCC TGCAGGTC GAGT	GATTTAGACTAC CCCAAAAACGAA GGGGACTAAAAC	ssRNA 1	fig. S11
LwaCas13a tiling crRNA 7	LwaCas13a	GATTTAGACTACCCCAAAA ACGAAGGGGACTAAAACAT GACCATGATTACGCCAAGC TTGCATG	ATGACCAT GATTACGC CAAGCTTG CATG	GATTTAGACTAC CCCAAAAACGAA GGGGACTAAAAC	ssRNA 1	fig. S11
LwaCas13a tiling crRNA 8	LwaCas13a	GATTTAGACTACCCCAAAA ACGAAGGGGACTAAAACCA CAGGAAACAGCTATGACCA TGATTAC	CACAGGAA ACAGCTAT GACCATGA TTAC	GATTTAGACTAC CCCAAAAACGAA GGGGACTAAAAC	ssRNA 1	fig. S11
LwaCas13a tiling crRNA 9	LwaCas13a	GATTTAGACTACCCCAAAA ACGAAGGGGACTAAAACTG TGAGCGGATAAACACAGGA AACAGCT	TGTGAGCG GATAAACA CAGGAAAC AGCT	GATTTAGACTAC CCCAAAAACGAA GGGGACTAAAAC	ssRNA 1	fig. S11
LwaCas13a tiling crRNA 10	LwaCas13a	GATTTAGACTACCCCAAAA ACGAAGGGGACTAAAACAT GTTGTGTGGAATTGTGAGC GGATAAA	ATGTTGTG TGGAATTG TGAGCGGA TAAA	GATTTAGACTAC CCCAAAAACGAA GGGGACTAAAAC	ssRNA 1	fig. S11
LwaCas13a tiling crRNA 11	LwaCas13a	GATTTAGACTACCCCAAAA ACGAAGGGGACTAAAACTG CTTCCGGCTCGTATGTTGT GTGGAAT	TGCTTCCG GCTCGTAT GTTGTGTG GAAT	GATTTAGACTAC CCCAAAAACGAA GGGGACTAAAAC	ssRNA 1	fig. S11
CcaCas13b tiling crRNA 1	CcaCas13b	CCCCGGGTACCGAGCTCGA ATTCACTGGCCGTTGGAAC TGCTCTCATTTTGGAGGGT AATCACAAC	CCCCGGGT ACCGAGCT CGAATTCA CTGGCC	GTTGGAACTGCT CTCATTTTGGAG GGTAATCACAAC	ssRNA 1	fig. S11
CcaCas13b tiling crRNA 2	CcaCas13b	TATTTCTAGAGGATCCCCG GGTACCGAGCTGTTGGAAC TGCTCTCATTTTGGAGGGT AATCACAAC	TATTTCTA GAGGATCC CCGGGTAC CGAGCT	GTTGGAACTGCT CTCATTTTGGAG GGTAATCACAAC	ssRNA 1	fig. S11
CcaCas13b tiling crRNA 3	CcaCas13b	TACCAAGTAATCCATATTT CTAGAGGATCCGTTGGAAC TGCTCTCATTTTGGAGGGT AATCACAAC	TACCAAGT AATCCATA TTTCTAGA GGATCC	GTTGGAACTGCT CTCATTTTGGAG GGTAATCACAAC	ssRNA 1	fig. S11
CcaCas13b tiling crRNA 4	CcaCas13b	GTAGATTGCTGTTCTACCA AGTAATCCATAGTTGGAAC TGCTCTCATTTTGGAGGGT AATCACAAC	GTAGATTG CTGTTCTA CCAAGTAA TCCATA	GTTGGAACTGCT CTCATTTTGGAG GGTAATCACAAC	ssRNA 1	fig. S11
CcaCas13b tiling crRNA 5	CcaCas13b	TGCCTGCAGGTCGAGTAGA TTGCTGTTCTAGTTGGAAC TGCTCTCATTTTGGAGGGT AATCACAAC	TGCCTGCA GGTCGAGT AGATTGCT GTTCTA	GTTGGAACTGCT CTCATTTTGGAG GGTAATCACAAC	ssRNA 1	fig. S11
CcaCas13b tiling crRNA 6	CcaCas13b	ACGCCAAGCTTGCATGCCT GCAGGTCGAGTGTTGGAAC TGCTCTCATTTTGGAGGGT AATCACAAC	ACGCCAAG CTTGCATG CCTGCAGG TCGAGT	GTTGGAACTGCT CTCATTTTGGAG GGTAATCACAAC	ssRNA 1	fig. S11
CcaCas13b tiling crRNA 7	CcaCas13b	CTATGACCATGATTACGCC AAGCTTGCATGGTTGGAAC	CTATGACC ATGATTAC	GTTGGAACTGCT CTCATTTTGGAG GGTAATCACAAC	ssRNA 1	fig. S11

		TGCTCTCATTTTGGAGGGT AATCACAAC	GCCAAGCT TGCATG			
CcaCas13b tiling crRNA 8	CcaCas13b	AACACAGGAAACAGCTATG ACCATGATTACGTTGGAAC TGCTCTCATTTTGGAGGGT AATCACAAC	AACACAGG AAACAGCT ATGACCAT GATTAC	GTTGGAACTGCT CTCATTTTGGAG GGTAATCACAAC	ssRNA 1	fig. S11
CcaCas13b tiling crRNA 9	CcaCas13b	ATTGTGAGCGGATAAACAC AGGAAACAGCTGTTGGAAC TGCTCTCATTTTGGAGGGT AATCACAAC	ATTGTGAG CGGATAAA CACAGGAA ACAGCT	GTTGGAACTGCT CTCATTTTGGAG GGTAATCACAAC	ssRNA 1	fig. S11
CcaCas13b tiling crRNA 10	CcaCas13b	GTATGTTGTGTGGAATTGT GAGCGGATAAAGTTGGAAC TGCTCTCATTTTGGAGGGT AATCACAAC	GTATGTTG TGTGGAAT TGTGAGCG GATAAA	GTTGGAACTGCT CTCATTTTGGAG GGTAATCACAAC	ssRNA 1	fig. S11
CcaCas13b tiling crRNA 11	CcaCas13b	TATGCTTCCGGCTCGTATG TTGTGTGGAATGTTGGAAC TGCTCTCATTTTGGAGGGT AATCACAAC	TATGCTTC CGGCTCGT ATGTTGTG TGGAAT	GTTGGAACTGCT CTCATTTTGGAG GGTAATCACAAC	ssRNA 1	fig. S11
PsmCas13b tiling crRNA 1	PsmCas13b	CCCCGGGTACCGAGCTCGA ATTCACTGGCCGTTGTAGA AGCTTATCGTTTGGATAGG TATGACAAC	CCCCGGGT ACCGAGCT CGAATTCA CTGGCC	GTTGTAGAAGCT TATCGTTTGGAT AGGTATGACAAC	ssRNA 1	fig. S11
PsmCas13b tiling crRNA 2	PsmCas13b	TATTTCTAGAGGATCCCCG GGTACCGAGCTGTTGTAGA AGCTTATCGTTTGGATAGG TATGACAAC	TATTTCTA GAGGATCC CCGGGTAC CGAGCT	GTTGTAGAAGCT TATCGTTTGGAT AGGTATGACAAC	ssRNA 1	fig. S11
PsmCas13b tiling crRNA 3	PsmCas13b	TACCAAGTAATCCATATTT CTAGAGGATCCGTTGTAGA AGCTTATCGTTTGGATAGG TATGACAAC	TACCAAGT AATCCATA TTTCTAGA GGATCC	GTTGTAGAAGCT TATCGTTTGGAT AGGTATGACAAC	ssRNA 1	fig. S11
PsmCas13b tiling crRNA 4	PsmCas13b	GTAGATTGCTGTTCTACCA AGTAATCCATAGTTGTAGA AGCTTATCGTTTGGATAGG TATGACAAC	GTAGATTG CTGTTCTA CCAAGTAA TCCATA	GTTGTAGAAGCT TATCGTTTGGAT AGGTATGACAAC	ssRNA 1	fig. S11
PsmCas13b tiling crRNA 5	PsmCas13b	TGCCTGCAGGTCGAGTAGA TTGCTGTTCTAGTTGTAGA AGCTTATCGTTTGGATAGG TATGACAAC	TGCCTGCA GGTCGAGT AGATTGCT GTTCTA	GTTGTAGAAGCT TATCGTTTGGAT AGGTATGACAAC	ssRNA 1	fig. S11
PsmCas13b tiling crRNA 6	PsmCas13b	ACGCCAAGCTTGCATGCCT GCAGGTCGAGTGTTGTAGA AGCTTATCGTTTGGATAGG TATGACAAC	ACGCCAAG CTTGCATG CCTGCAGG TCGAGT	GTTGTAGAAGCT TATCGTTTGGAT AGGTATGACAAC	ssRNA 1	fig. S11
PsmCas13b tiling crRNA 7	PsmCas13b	CTATGACCATGATTACGCC AAGCTTGCATGGTTGTAGA AGCTTATCGTTTGGATAGG TATGACAAC	CTATGACC ATGATTAC GCCAAGCT TGCATG	GTTGTAGAAGCT TATCGTTTGGAT AGGTATGACAAC	ssRNA 1	fig. S11
PsmCas13b tiling crRNA 8	PsmCas13b	AACACAGGAAACAGCTATG ACCATGATTACGTTGTAGA AGCTTATCGTTTGGATAGG TATGACAAC	AACACAGG AAACAGCT ATGACCAT GATTAC	GTTGTAGAAGCT TATCGTTTGGAT AGGTATGACAAC	ssRNA 1	fig. S11
PsmCas13b tiling crRNA 9	PsmCas13b	ATTGTGAGCGGATAAACAC AGGAAACAGCTGTTGTAGA AGCTTATCGTTTGGATAGG TATGACAAC	ATTGTGAG CGGATAAA CACAGGAA ACAGCT	GTTGTAGAAGCT TATCGTTTGGAT AGGTATGACAAC	ssRNA 1	fig. S11
PsmCas13b tiling crRNA 10	PsmCas13b	GTATGTTGTGTGGAATTGT GAGCGGATAAAGTTGTAGA AGCTTATCGTTTGGATAGG TATGACAAC	GTATGTTG TGTGGAAT TGTGAGCG GATAAA	GTTGTAGAAGCT TATCGTTTGGAT AGGTATGACAAC	ssRNA 1	fig. S11
PsmCas13b tiling crRNA 11	PsmCas13b	TATGCTTCCGGCTCGTATG TTGTGTGGAATGTTGTAGA AGCTTATCGTTTGGATAGG TATGACAAC	TATGCTTC CGGCTCGT ATGTTGTG TGGAAT	GTTGTAGAAGCT TATCGTTTGGAT AGGTATGACAAC	ssRNA 1	fig. S11
ZIKV CcaCas13b	CcaCas13b	CTTGAACTCTACCAGTGCT TCTTTGTTGTTGTTGGAAC TGCTCTCATTTTGGAGGGT AATCACAAC	CTTGAACT CTACCAGT GCTTCTTT GTTGTT	GTTGGAACTGCT CTCATTTTGGAG GGTAATCACAAC	ZIKV ssRNA	fig. S16B
DENV crRNA CcaCas13b	CcaCas13b	TTTGCTTCTGTCCAGTGAG CATGGTCTTCGGTTGGAAC TGCTCTCATTTTGGAGGGT AATCACAAC	TTTGCTTC TGTCCAGT GAGCATGG TCTTCG	GTTGGAACTGCT CTCATTTTGGAG GGTAATCACAAC	DENV ssRNA	fig. S17A
human ID rs601338 A-allele sensing PsmCas13b	PsmCas13b	CCGCTTCACCGGCTACCCC TGCTCCAAGAGTTGTAGAA GCTTATCGTTTGGATAGGT ATGACAAC	CCGCTTCA CCGGCTAC CCCTGCTC CAAGA	GTTGTAGAAGCT TATCGTTTGGAT AGGTATGACAAC	Human locus rs601338	fig. S18C
human ID rs601338 G-allele sensing LwaCas13a	LwaCas13a	GATTTAGACTACCCCAAAA ACGAAGGGGACTAAAACCT GCACCTTCTACCACCACCT CCGCCAG	CTGCACCT TCTACCAC CACCTCCG CCAG	GATTTAGACTAC CCCAAAAACGAA GGGGACTAAAAC	Human locus rs601338	fig. S18C
ssRNA/ssDNA 1 crRNA 1	LwaCas13a	GATTTAGACTACCCCAAAA ACGAAGGGGACTAAAACTA	TAGATTGC TGTTCTAC	GATTTAGACTAC CCCAAAAACGAA GGGGACTAAAAC	ssRNA 1	fig. S20

		GATTGCTGTTCTACCAAGT AATCCAT	CAAGTAAT CCAT			
T790M mutant sensing allele crRNA	LwaCas13a	GATTTAGACTACCCCAAAA ACGAAGGGGACTAAAACGC AAGATGAGCTGCACGGTGG AGGTGAG	GCAAGATG AGCTGCAC GGTGGAGG TGAG	GATTTAGACTAC CCCAAAAACGAA GGGGACTAAAAC	EGFR T790M mutant synthetic ssDNA	fig. S24
T790M wild type sensing allele crRNA	LwaCas13a	GATTTAGACTACCCCAAAA ACGAAGGGGACTAAAACGC GTCATGAGCTGCACGGTGG AGGTGAG	GCGTCATG AGCTGCAC GGTGGAGG TGAG	GATTTAGACTAC CCCAAAAACGAA GGGGACTAAAAC	EGFR T790M WT synthetic ssDNA	fig. S24
ssRNA 3 (PsmCas13b target) crRNA	PsmCas13b	TAGATTGCTGTTCTACCAA GTAATCCATATGTTGTAGA AGCTTATCGTTTGGATAGG TATGACAAC	TAGATTGC TGTTCTAC CAAGTAAT CCATAT	GTTGTAGAAGCT TATCGTTTGGAT AGGTATGACAAC	ssRNA 3	fig. S25
ssRNA 2 (LwaCas13a target) crRNA	LwaCas13a	GATTTAGACTACCCCAAAA ACGAAGGGGACTAAAACGA TTGCTGTTCTACCAAGTAA TCCATAT	GATTGCTG TTCTACCA AGTAATCC ATAT	GATTTAGACTAC CCCAAAAACGAA GGGGACTAAAAC	ssRNA 2	fig. S25

Table S3: RNA and DNA targets used in this study

Name	Sequence	Nucleic acid	1st Fig.
DENV ssRNA	AGUACAUAUUCAGGGGCCAACCUCUCAACAAUGACGAAGACCAUGCUC ACUGGACAGAAGCAAAAAUGCUGCUGGACAACAUCAACACACCAGAAG GGAUUAUACCAGCUCUCUUUGAACCAGAAAGGGAGAAGUCAGCCGCCA UAGACGGUGAAUACCGCCUGAAGGGU	RNA	Fig. 1B
ssDNA 1	GGCCAGTGAATTCGAGCTCGGTACCCGGGGATCCTCTAGAAATATGGA TTACTTGgtAGAACAGCAATCTACTCGACCTGCAGGCATGCAAGCTTG GCGTAATCATGGTCATAGCTGTTTCCTGTGTTTATCCGCTCACAATTC CACACAACATACGAGCCGGAAGCATAAAG	DNA	Fig. 1F
ZIKV ssRNA	GACACCGGAACUCCACACUGGAACAACAAAGAAGCACUGGUAGAGUUC AAGGACGCACAUGCCAAAAGGCAAACUGUCGUGGUUCUAGGGAGUCAA GAAGGAGCAGUUCACACGGCCCUUGCUGGAGCUCUGGAGGCUGAGAUG GAUGGUGCAAAGGGAAGGCUGUCCUCUGGC	RNA	Fig. 1F
Thermonuclease ssDNA	TTAATTAAAGCGATTGATGGTGATACTGTTAAATTAATGTACAAAGGT CAACCAATGACATTCAGACTATTATTGGTTGATACACCTGAAACAAAG CATCCTAAAAAAGGTGTAGAGAAATATGGTCCTGAAGCAAGTGCATTT ACGAAAAAGATGGTAGAAAATGCAAAGAAAATTGAAGTCGAGTTTG	DNA	Fig. 1H
Acyltransferase ssDNA	GGGGAGGATGTCGGGCGCGCACGTTTTCCCTTCGCTGAGCACGCTGCG CGCGTCGCCTACGTGAATGCGCTGTTCGATGCGTTGGCCGAAGGCAAC CCGCGGGTGAGCGTGCTCGACCCCTCCAGCGTGCTCTGCGATGGCCTG GATTGTTTCGCCGAACGTGATGGCTGGTCGCTGTACATGGATAACA	DNA	Fig. 1H
ssRNA 1	GGCCAGUGAAUUCGAGCUCGGUACCCGGGGAUCCUCUAGAAAUAUGGA UUACUUGgUAGAACAGCAAUCUACUCGACCUGCAGGCAUGCAAGCUUG GCGUAAUCAUGGUCAUAGCUGUUUCCUGUGUUUAUCCGCUCACAAUUC CACACAACAUACGAGCCGGAAGCAUAAAG	RNA	fig. S3
Random motif library	TTCCTGTGAAGCTAAAGAAGGAGAATGrNrNrNrNrNrNTATTGATAG CAGCTGTGGCACCTGCAC	Mixed DNA/RNA	fig. S12
EGFR Exon19 deletion mutant synthetic ssDNA	TGCCAGTTAACGTCTTCCTTCTCTCTCTGTCATAGGGACTCTGGATCC CAGAAGGTGAGAAAGTTAAAATTCCCGTCGCTATCAAGACATCTCCGA AAGCCAACAAGGAAATCCTCGATGTGAGTTTCTGCTTTGCTGTGTGGG GGTCCATGGCTCTGAACCTCAGGCCCACCTTTTCTCAT	DNA	fig. S24A
EGFR Exon19 deletion WT synthetic ssDNA	TGCCAGTTAACGTCTTCCTTCTCTCTCTGTCATAGGGACTCTGGATCC CAGAAGGTGAGAAAGTTAAAATTCCCGTCGCTATCAAGGAATTAAGAG AAGCAACATCTCCGAAAGCCAACAAGGAAATCCTCGATGTGAGTTTCT GCTTTGCTGTGTGGGGGTCCATGGCTCTGAACCTCAGGCCCACCTTTT CTCAT	DNA	fig. S24A
EGFR T790M mutant synthetic ssDNA	CCTCCCTCCAGGAAGCCTACGTGATGGCCAGCGTGGACAACCCCCACG TGTGCCGCCTGCTGGGCATCTGCCTCACCTCCACCGTGCAGCTCATCA TGCAGCTCATGCCCTTCGGCTGCCTCCTGGACTATGTCCGGGAACACA AAGACAATATTGGCTCCCAGTACCTGCTCAACTGGTGTGTGCAGATCG CA	DNA	fig. S24E
EGFR T790M WT synthetic ssDNA	CCTCCCTCCAGGAAGCCTACGTGATGGCCAGCGTGGACAACCCCCACG TGTGCCGCCTGCTGGGCATCTGCCTCACCTCCACCGTGCAGCTCATCA CGCAGCTCATGCCCTTCGGCTGCCTCCTGGACTATGTCCGGGAACACA AAGACAATATTGGCTCCCAGTACCTGCTCAACTGGTGTGTGCAGATCG CA	DNA	fig. S24E
ssRNA 2 (LwaCas13a target	UAGGUGUUCCACAGGGUAGCCAGCAGCAUCCUGCGAUGCAAAUAUGGA UUACUUGGUAGAACAGCAAUCUAAUCCGGAACAUAAUGGUGCAGGGCG CUGACUUCCGCGUUUGUUUUAAAUCAAACACGGAAACCGAAGACCAUU CAUGUUGUUGCUGCCGGAAGCAUAAAG	RNA	fig. S25B
ssRNA 3 (PsmCas13b target	UAGGUGUUCCACAGGGUAGCCAGCAGCAUCCUGCGAUGCAAAUAUGGA UUACUUGGUAGAACAGCAAUCUAAUCCGGAACAUAAUGGUGCAGGGCG	RNA	fig. S25B

	CUGACUUCCGCGUUUGAAAAAAAACAAACACGGAAACCGAAGACCAUU CAUGUUGUUGCUGCCGGAAGCAUAAAG		

Table S4: RPA primers used in this study

Target	Forward primer sequence	Forward primer sequence (with T7 RNAP promoter)	Reverse primer sequence	1st Fig.
DENV ssRNA	GTACATATTCAGGGGCCAACCTC TC	gaaattaatacgactcactatagggg GTACATATTCAGGGGCCAACCTCTC	TTTCTGGTTCAAAG AGAGCTGGTAT	Fig. 1D
Thermonuclease ssDNA	TGTACAAAGGTCAACCAATGACA TTCAG	gaaatTAATACGACTCACTATAGGG TGTACAAAGGTCAACCAATGACATT CAG	TGCACTTGCTTCAG GACCATATTTC	Fig. 1H
Acyltransferase	CTACGTGAATGCGCTGTTCGATG	gaaatTAATACGACTCACTATAGGG CTACGTGAATGCGCTGTTCGATG	GAAACAATCCAGGC CATCGCAGAG	Fig. 1H
EGFR L858R	TCTGGATCCCAGAAGGTGAGAAA GTTAAAA	gaaatTAATACGACTCACTATAGGG TCTGGATCCCAGAAGGTGAGAAAGT TAAAA	CCACACAGCAAAGC AGAAACTCACATCG AG	Fig. 3E
EGFR Exon19 deletion	TCTGGATCCCAGAAGGTGAGAAA GTTAAAA	gaaatTAATACGACTCACTATAGGG TCTGGATCCCAGAAGGTGAGAAAGT TAAAA	CCACACAGCAAAGC AGAAACTCACATCG AG	Fig. 3H
Theranostic APC target (NM_000038.5)	AGGGCCGCCACTCCACCGGCGGC ATGGATGAG	gaaatTAATACGACTCACTATAGGG AGGGCCGCCACTCCACCGGCGGCAT GGATGAG	GAAGAGTTCTTCAC CTTTACTCACggaT CCtcc	Fig. 5B
ZIKV ssRNA	CCACACTGGAACAACAAAGAAGC AC	gaaatTAATACGACTCACTATAGGG CCACACTGGAACAACAAAGAAGCAC	ACAGCCTTCCCTTT GCACCATCCATCTC AG	fig. S6
locus rs601338	ATAGTCCCCTCGGCGAACATGGA CCCCTACAA	gaaattaatacgactcactatagggg ATAGTCCCCTCGGCGAACATGGACC CCTACAA	GAGTACGTCCGCTT CACCGGCTACCCCT GCTC	fig. S18C
ssDNA/ssRNA 1	ATCCTCTAGAAATATGGATTACT TGGTAGAACAG	AATTCTAATACGACTCACTATAGGG ATCCTCTAGAAATATGGATTACTTG GTAGAACAG	GATAAACACAGGAA ACAGCTATGACCAT GATTACG	fig. S20
EGFR T790M	CCCCACGTGTGCCGCCTGCTGGG CATCTGC	gaaatTAATACGACTCACTATAGGG CCCCACGTGTGCCGCCTGCTGGGCA TCTGC	ATATTGTCTTTGTG TTCCCGGACATAGT CC	fig. S24E

Table S5: Cleavage reporters used in this study

Name	Sequence	Fluorophore	1st Fig.
poly U reporter	/56-FAM/rUrUrUrUrU/3IABkFQ/	FAM	Fig. 1
poly A reporter	/56-FAM/rArArArArA/3IABkFQ/	FAM	Fig. 1
poly U reporter for multiplexing	/5HEX/rUrUrUrUrU/3IABkFQ/	HEX	Fig. 1
rArA reporter for testing di-base preference	/56-FAM/TArArAGC/3IABkFQ/	FAM	Fig. 1 and fig. S7
rArU reporter for testing di-base preference	/56-FAM/TArArUGC/3IABkFQ/	FAM	Fig. 1 and fig. S7
rArC reporter for testing di-base preference	/56-FAM/TArArCGC/3IABkFQ/	FAM	Fig. 1 and fig. S7
rArG reporter for testing di-base preference	/56-FAM/TArArGGC/3IABkFQ/	FAM	Fig. 1 and fig. S7
rUrA reporter for testing di-base preference	/56-FAM/TArUrAGC/3IABkFQ/	FAM	Fig. 1 and fig. S7

rUrU reporter for testing di-base preference	/56-FAM/TArUrUGC/3IABkFQ/	FAM	Fig. 1 and fig. S7
rUrC reporter for testing di-base preference	/56-FAM/TArUrCGC/3IABkFQ/	FAM	Fig. 1 and fig. S7
rUrG reporter for testing di-base preference	/56-FAM/TArUrGGC/3IABkFQ/	FAM	Fig. 1 and fig. S7
rCrA reporter for testing di-base preference	/56-FAM/TArCrAGC/3IABkFQ/	FAM	Fig. 1 and fig. S7
rCrU reporter for testing di-base preference	/56-FAM/TArCrUGC/3IABkFQ/	FAM	Fig. 1 and fig. S7
rCrC reporter for testing di-base preference	/56-FAM/TArCrCGC/3IABkFQ/	FAM	Fig. 1 and fig. S7
rCrG reporter for testing di-base preference	/56-FAM/TArCrGGC/3IABkFQ/	FAM	Fig. 1 and fig. S7
rGrA reporter for testing di-base preference	/56-FAM/TArGrAGC/3IABkFQ/	FAM	Fig. 1 and fig. S7
rGrU reporter for testing di-base preference	/56-FAM/TArGrUGC/3IABkFQ/	FAM	Fig. 1 and fig. S7
rGrC reporter for testing di-base preference	/56-FAM/TArGrCGC/3IABkFQ/	FAM	Fig. 1 and fig. S7
rGrG reporter for testing di-base preference	/56-FAM/TArGrGGC/3IABkFQ/	FAM	Fig. 1 and fig. S7
poly U Cy5 for multiplexing	/5Cy5/rUrUrUrUrU/3IAbRQSp/	FAM	Fig. 1
Lateral flow reporter with FAM/Biotin	/56-FAM/mArArUrGrGrCmAmArArUrGrGrCmA/3Bio/	N/A	Fig. 3
poly C reporter	/56-FAM/rCrCrCrCrC/3IABkFQ/	FAM	fig. S3
poly G reporter	/56-FAM/rGrGrGrGrG/3IABkFQ/	FAM	fig. S3
RNA motif library for base preference screening	TTCCTGTGAAGCTAAAGAAGGAGAATGrNrNrNrNrNrNTATTGATAGCAGCTGTGGCACCTGCAC	N/A	fig. S12
LwaCas13a validation motif 1	/56-FAM/TrGrUrUrUrUrC/3IABkFQ/	FAM	fig. S13
LwaCas13a validation motif 2	/56-FAM/TrUrUrUrUrUrC/3IABkFQ/	FAM	fig. S13
LwaCas13a validation motif 3	/56-FAM/TrCrArUrUrUrG/3IABkFQ/	FAM	fig. S13
PsmCas13b validation motif 1	/56-FAM/TrUrArUrUrGrA/3IABkFQ/	FAM	fig. S13
PsmCas13b validation motif 2	/56-FAM/TrArUrUrGrArU/3IABkFQ/	FAM	fig. S13
PsmCas13b validation motif 3	/56-FAM/TrUrUrGrArUrA/3IABkFQ/	FAM	fig. S13
CcaCas13b validation motif 1	/56-FAM/TrUrUrUrGrUrU/3IABkFQ/	FAM	fig. S13
CcaCas13b validation motif 2	/56-FAM/TrUrGrUrUrUrU/3IABkFQ/	FAM	fig. S13

CcaCas13b validation motif 3	/56-FAM/TrArUrUrUrUrU/3IABkFQ/	FAM	fig. S13
Lwa orthogonal motif 1	/56-FAM/TrCrGrArArUrG/3IABkFQ/	FAM	fig. S14
Lwa orthogonal motif 2	/56-FAM/TrGrUrCrUrCrC/3IABkFQ/	FAM	fig. S14
Lwa orthogonal motif 3	/56-FAM/TrGrCrArUrGrA/3IABkFQ/	FAM	fig. S14
Lwa orthogonal motif 4	/56-FAM/TrCrArUrArCrA/3IABkFQ/	FAM	fig. S14
Lwa orthogonal motif 5	/56-FAM/TrCrArUrArCrG/3IABkFQ/	FAM	fig. S14
Lwa orthogonal motif 6	/56-FAM/TrGrCrArUrArA/3IABkFQ/	FAM	fig. S14
CcaCas13b orthogonal motif 1	/56-FAM/TrCrUrArCrUrU/3IABkFQ/	FAM	fig. S14
CcaCas13b orthogonal motif 2	/56-FAM/TrCrUrArCrGrU/3IABkFQ/	FAM	fig. S14
CcaCas13b orthogonal motif 3	/56-FAM/TrUrUrArArArC/3IABkFQ/	FAM	fig. S14
gold nanoparticle linker	/5ThioMC6-D/rCrUrCrCrCrUrArArUrArArCrArArUrUrUrArUrArArCrUrArUrUrCrCrUrArCrCrCrUrUrUrCrCrCrArArArArArArArA/3ThioMC3-D/	N/A	fig. S21
magnetic bead conjugate oligo	/5AmMC12/AGAGCATCACCATGATCCTGrUrUrUrUrUrUrUTG/iBiodT/CTCGGATATCTCGACTA/36-FAM/	N/A	fig. S22
EiCsm6 validation motif 1	/56-FAM/TrGrArCrGrUrG/3IABkFQ/	N/A	fig. S29
short poly A for lateral flow	/FamCE/rArArArArArA/BioBB/	N/A	fig. S34A
long poly A for lateral flow	/FamCE/rArArArArArArArArArArArA/BioBB/	N/A	fig. S34A
short poly C for lateral flow	/56-FAM/rCrCrCrCrCrC/3Bio/	N/A	fig. S34A
long poly C for lateral flow	/56-FAM/rCrCrCrCrCrCrCrCrCrCrC/3Bio/	N/A	fig. S34A
short poly A/C for lateral flow	/56-FAM/rArCrArCrArC/3Bio/	N/A	fig. S34A
long poly A/C for lateral flow	/56-FAM/rArCrArCrArCrArCrArCrArC/3Bio/	N/A	fig. S34A

Table S6: Csm6 activators used in this study

Name	Sequence	1st Fig.
poly A (n=5) 2',3' cyclic phosphate end	rArArArArA-(2,3-cyclic phosphate)	Fig. 4
poly A (n=6) 2',3' cyclic phosphate end	rArArArArArA-(2,3-cyclic phosphate)	Fig. 4
poly A (n=7) 2',3' cyclic phosphate end	rArArArArArArA-(2,3-cyclic phosphate)	Fig. 4
poly A (n=8) 2',3' cyclic phosphate end	rArArArArArArArA-(2,3-cyclic phosphate)	Fig. 4
Csm6 polyA polyU probes for U cutters 4 As	rArArArArUrUrUrUrU	Fig. 4

Csm6 polyA polyU probes for U cutters 5 As	rArArArArArUrUrUrUrU	Fig. 4
Csm6 polyA polyU probes for U cutters 6 As	rArArArArArArUrUrUrUrU	Fig. 4
Csm6 polyA polyU probes for U cutters 7 As	rArArArArArArArUrUrUrUrU	Fig. 4
5' poly U / polyA 6A probe 2,3 cyclic phosphate	rUrUrUrUrUrArArArArArArA-(2,3-cyclic phosphate)	fig. S31
5'poly A/ poly U / polyA 6A probe 2,3 cyclic phosphate	rArArArArArArUrUrUrUrUrArArArArArArA-(2,3-cyclic phosphate)	fig. S31

Table S7: Allele fractions of cfDNA samples used in this study

Patient ID	Allele fractions
Patient 1	29% L858R
Patient 2	90% exon 19 deletion
Patient 3	4% exon 19 deletion
Patient 4	2% exon 19 deletion and 0.6% T790M
Patient 5	Wild Type

Table S8: REPAIR plasmids used in this study

Plasmid Name	Description	Link to plasmid map
REPAIR plasmid (pC0039)	CMV-dPspCas13b-GS-ADAR2DD(E488Q)	https://benchling.com/s/seq-arzpsupZEzGu3ghBDhtv
APC wildtype plasmid	pCMV-mScarlett-APC WT-EGFP	https://benchling.com/s/seq-w2vU03qnxfuxK4OjSxiT
APC mutant plasmid	pCMV-mScarlett-APC mutant-EGFP	https://benchling.com/s/seq-LlmQkX8dJ4sBoZfqoxHy
REPAIR guide (in pC0043)	U6-guide-PspCas13b DR	https://benchling.com/s/seq-OLVAsGt655E7pTACczl1
REPAIR nontargeting guide (pC0052)	U6-nontargeting guide-PspCas13b DR	https://benchling.com/s/seq-U9gHnOW41C1DVUBGQypw

Table S9: Comparison of SHERLOCKv1 and SHERLOCKv2

Characteristic	SHERLOCKv1	SHERLOCKv2
Sensitivity	2aM	8zM
Specificity	Single-nucleotide	Single-nucleotide
In-sample multiplexing	Single	Up to four targets
Spatial multiplexing	Unlimited	Unlimited
Speed	2 hours	30 minutes (from crude sample to detection)
Readouts	Fluorescence	Fluorescence, visual by lateral flow
Signal amplification	None	Csm6 enhancement

Cost	<$0.60	<$0.60
Companion diagnostic	None	Paired with REPAIR for measuring RNA editing results.
Nuclease compatibility	Cas13a	Cas13a, Cas13b, Cas12a, and Csm6

References:

1. S. Shmakov *et al.*, Discovery and Functional Characterization of Diverse Class 2 CRISPR-Cas Systems. *Mol Cell* **60**, 385-397 (2015).
2. O. O. Abudayyeh *et al.*, C2c2 is a single-component programmable RNA-guided RNA-targeting CRISPR effector. *Science* **353**, aaf5573 (2016).
3. J. S. Gootenberg *et al.*, Nucleic acid detection with CRISPR-Cas13a/C2c2. *Science* **356**, 438-442 (2017).
4. A. East-Seletsky *et al.*, Two distinct RNase activities of CRISPR-C2c2 enable guide-RNA processing and RNA detection. *Nature* **538**, 270-273 (2016).
5. A. East-Seletsky, M. R. O'Connell, D. Burstein, G. J. Knott, J. A. Doudna, RNA Targeting by Functionally Orthogonal Type VI-A CRISPR-Cas Enzymes. *Mol Cell* **66**, 373-383 e373 (2017).
6. S. Shmakov *et al.*, Diversity and evolution of class 2 CRISPR-Cas systems. *Nat Rev Microbiol* **15**, 169-182 (2017).
7. A. A. Smargon *et al.*, Cas13b Is a Type VI-B CRISPR-Associated RNA-Guided RNase Differentially Regulated by Accessory Proteins Csx27 and Csx28. *Mol Cell* **65**, 618-630 e617 (2017).
8. J. S. Chen, E. Ma, L. B. Harrington, X. Tian, J. A. Doudna, CRISPR-Cas12a target binding unleashes single-stranded DNase activity. *bioRxiv*, (2017).
9. W. H. Organization, in *Guidelines for Using HIV Testing Technologies in Surveillance: Selection, Evaluation and Implementation: 2009 Update*. (Geneva, 2009).
10. J. M. Barletta, D. C. Edelman, N. T. Constantine, Lowering the detection limits of HIV-1 viral load using real-time immuno-PCR for HIV-1 p24 antigen. *Am J Clin Pathol* **122**, 20-27 (2004).
11. L. Deng, R. A. Garrett, S. A. Shah, X. Peng, Q. She, A novel interference mechanism by a type IIIB CRISPR-Cmr module in Sulfolobus. *Mol Microbiol* **87**, 1088-1099 (2013).

12. G. W. Goldberg, W. Jiang, D. Bikard, L. A. Marraffini, Conditional tolerance of temperate phages via transcription-dependent CRISPR-Cas targeting. *Nature* **514**, 633-637 (2014).
13. W. Jiang, P. Samai, L. A. Marraffini, Degradation of Phage Transcripts by CRISPR-Associated RNases Enables Type III CRISPR-Cas Immunity. *Cell* **164**, 710-721 (2016).
14. O. Niewoehner, M. Jinek, Structural basis for the endoribonuclease activity of the type III-A CRISPR-associated protein Csm6. *RNA* **22**, 318-329 (2016).
15. P. Samai *et al.*, Co-transcriptional DNA and RNA Cleavage during Type III CRISPR-Cas Immunity. *Cell* **161**, 1164-1174 (2015).
16. R. H. Staals *et al.*, RNA targeting by the type III-A CRISPR-Cas Csm complex of Thermus thermophilus. *Mol Cell* **56**, 518-530 (2014).
17. G. Tamulaitis *et al.*, Programmable RNA shredding by the type III-A CRISPR-Cas system of Streptococcus thermophilus. *Mol Cell* **56**, 506-517 (2014).
18. M. Kazlauskiene, G. Kostiuk, C. Venclovas, G. Tamulaitis, V. Siksnys, A cyclic oligonucleotide signaling pathway in type III CRISPR-Cas systems. *Science* **357**, 605-609 (2017).
19. O. Niewoehner *et al.*, Type III CRISPR-Cas systems produce cyclic oligoadenylate second messengers. *Nature* **548**, 543-548 (2017).
20. W. Zhao, M. M. Ali, S. D. Aguirre, M. A. Brook, Y. Li, Paper-based bioassays using gold nanoparticle colorimetric probes. *Anal Chem* **80**, 8431-8437 (2008).
21. W. Zhao, J. C. Lam, W. Chiuman, M. A. Brook, Y. Li, Enzymatic cleavage of nucleic acids on gold nanoparticles: a generic platform for facile colorimetric biosensors. *Small* **4**, 810-816 (2008).
22. O. O. Abudayyeh *et al.*, RNA targeting with CRISPR-Cas13. *Nature* **550**, 280-284 (2017).
23. D. B. T. Cox *et al.*, RNA editing with CRISPR-Cas13. *Science* **358**, 1019-1027 (2017).
24. S. Cottrell, D. Bicknell, L. Kaklamanis, W. F. Bodmer, Molecular analysis of APC mutations in familial adenomatous polyposis and sporadic colon carcinomas. *Lancet* **340**, 626-630 (1992).
25. C. Y. Chen, DNA polymerases drive DNA sequencing-by-synthesis technologies: both past and present. *Front Microbiol* **5**, 305 (2014).
26. G. E. Crooks, G. Hon, J. M. Chandonia, S. E. Brenner, WebLogo: a sequence logo generator. *Genome research* **14**, 1188-1190 (2004).
27. J. Ye *et al.*, Primer-BLAST: a tool to design target-specific primers for polymerase chain reaction. *BMC Bioinformatics* **13**, 134 (2012).